Investigating the Effects of Nanovibrational Stimulation on Dermal Fibroblasts

Egle Morta Antanaviciute BSc (Hons)

Submitted in fulfilment of the requirements for the
Degree of Doctor of Philosophy (PhD)

Centre for the Cellular Microenvironment
School of Molecular Biosciences
College of Medical, Veterinary and Life Sciences
University of Glasgow
Glasgow

MAY 2023

Abstract

Vibration with 1000 Hz frequency, 0.12 g acceleration and 30 nm displacement has been demonstrated to promote mesenchymal stem cell osteogenesis in 2D and 3D cultures without requiring supplementation with biochemical osteogenic fate inducers. This indicates that it could potentially be applied as an *in vivo* mechanotherapy to promote bone regeneration and treat delayed fracture unions or bone tissue disorders, such as osteoporosis. Applied to the exterior of the body, nanoscale vibrational waves would propagate through the soft tissues surrounding the target bone site, stimulating the cells within those tissues. However, these vibration parameters are highly unusual in the context of other vibrational stimulation studies, and little is known about how they may affect other cell types.

Fibroblasts are the most common cell type in the soft connective tissues, where they play a vital role in tissue repair after injury. Fibroblast behaviour during the process of wound healing is regulated by complex interactions between signalling pathways stimulated by biochemical and biomechanical factors. Applied mechanical stimulation could interfere with these pathways and potentially lead to undesirable outcomes, such as impaired wound healing or excessive matrix deposition and fibrosis. This thesis aims to investigate how fibroblasts respond to nanovibrational stimulation in 2D and 3D culture conditions and in presence and absence of pro-fibrotic growth factor transforming growth factor-β1 (TGFβ1). The features important for fibroblast function during wound healing were examined, including proliferation, contractility, synthesis of collagen I, collagen III and α-smooth muscle actin, as well as gene expression of endogenous TGFβ1 and inflammatory factors interleukin-6 and osteopontin. A liquid chromatography-mass spectrometry-based metabolomics experiment was performed to detect any alterations in fibroblast metabolome in response to nanovibrational stimulation, followed by RNA sequencing to evaluate its effects on gene transcription. Finally, levels of reactive oxygen species, apoptosis, and DNA damage, all of which play a role in the development of fibrotic diseases, were investigated using flow cytometry and alkaline comet assay.

It was discovered that fibroblasts are sensitive to nanovibrational stimulation, but the effects under the basal conditions are subtle and unlikely to cause undesirable fibroblast activity in healthy tissues. However, nanovibration had potentially negative outcomes on the fibroblast phenotype in 3D when applied in the presence of TGFβ1, increasing DNA damage and gene expression of inflammatory factor osteopontin. These outcomes were not observed in 2D cultures, where indications of anti-fibrotic effects of nanovibration were observed, suggesting that the effects of nanovibrational stimulation in pro-fibrotic conditions may depend on the mechanical properties of the matrix. Overall, this work presents the first investigation of the fibroblast response to nanovibrational stimulation and highlights the potential benefits and detriments of the treatment.

Table of Contents

List of tables

List of Figures

Acknowledgements

First and foremost, I would like to thank my supervisors Prof. Matt Dalby, Dr. Monica Tsimbouri and Prof. Manuel Salmerón-Sánchez for the opportunity to do this work and for their guidance throughout the course of it. I don't know where you get your patience, but I sure do appreciate it.

Big thanks to all friends and colleagues in the CeMi, it's been a good nearly-five years and it's all because of you. Special mention goes to Dr. Alasdair MacDonald for keeping the gears spinning in the lab. Another one to Dr. Mathis Riehle for always having funny jokes and good advice to share.

I would also like to thank Dr. Izabela Szymczak-Pajor and Prof. Agnieszka Sliwinska at the Medical University of Łódź for inviting me to contribute to their research, as well as contributing to mine with valuable training.

Thanks to my friends Monika, Dominyka and Kernius for being the best support system one could ever wish for. And my friend Adomas, for all of the 'you should be writing' texts, you'll be happy to know that some of them actually worked! I also owe a big chunk of my gratitude to my family. My mum Violeta, for providing me perspective in stressful times, and my grandma Birute, who makes me feel loved and cared for even a thousand miles away. Finally, a big thanks goes to Justas. The list of things I'm grateful for would probably require a separate chapter. I could have probably done this without you, but I wouldn't want to find out.

Author's Declaration

I declare that, except where explicit reference is made to the contribution of others, that this thesis is the result of my own work and has not been submitted for any other degree at the University of Glasgow or any other institution.

Egle Morta Antanaviciute

29 May 2023

Abbreviations

2D	Two-dimensional
3D	Three-dimensional
α-SMA	α-smooth muscle actin
BMD	Bone mineral density
Akt	Protein kinase B
ATP	Adenosine Triphosphate
CaSR	Calcium sensing receptor
COL1A1	Collagen I A1
COL3A1	Collagen III A1
CTGF	Connective tissue growth factor
DE	Differentially expressed
DNA	Deoxyribonucleic Acid
ECM	Extracellular matrix
ERK	Extracellular signal-regulated kinases
FAK	Focal adhesion kinase
FGF	Fibroblast growth factor
GLRX	Glutaredoxin
GO	Gene ontology
GSH	Glutathione
H_2O_2	Hydrogen peroxide
H-TERT	Human telomerase reverse transcriptase
IL	Interleukin
IPF	Idiopathic pulmonary fibrosis
JNK	c-Jun N-terminal kinase
KEGG	Kyoto encyclopaedia of genes and genomes
LAP	Latency associated peptide
LC-MS	Liquid chromatography-mass spectrometry
MAPK	Mitogen-activated protein kinases

MMP	Matrix metalloprotease
MSCs	Mesenchymal stem cells
NOX4	NADPH oxidase 4
OPN	Osteopontin
ORA	Overrepresentation analysis
PCA	Principal component analysis
PDGF	Plateled derived growth factor
PI	Propidium iodide
q-PCR	Quantitative-polymerase chain reaction
RNA	Ribonucleic acid
RNA-Seq	RNA-sequencing
ROCK	Rho-associated protein kinase
ROS	Reactive oxygen species
RP	Ribosomal protein
SMAD	Small mothers against decapentaplegic
SOD	Superoxide dismutase
SSc	Systemic sclerosis
TAZ	Transcriptional coactivator with a PDZ-binding domain
TBHP	Tert-butyl hydroperoxide
TGFβ1	Transforming growth factor-β1
TRP	Transient receptor potential
VEGF	Vascular endothelial growth factor
WBV	Whole Body Vibration
YAP	Yes-associated protein

Chapter 1: Introduction

1.1 Mechanical stimulation of cells

The ability of cells to sense and translate biomechanical cues from the extracellular microenvironment into intracellular signalling events is essential for many biological processes, such as development, tissue homeostasis and wound healing (Paluch et al., 2015). For this purpose, cells employ a variety of 'mechanosensors', including cell-matrix adhesions, force gated ion channels, and certain g-protein coupled receptors, which relay the mechanical signals into the interior of the cell and activate downstream signalling pathways (Goodman et al., 2023). Engaging the cellular mechanotranduction pathways with applied mechanical stimuli therefore allows to manipulate cell phenotype (Zhang and Habibovic, 2022).

A variety of mechanical stimulation strategies have been developed to direct cell behaviours (Han et al., 2020, Zhang and Habibovic, 2022). Some of these strategies involve fine-tuning the physical properties of the culture substrate to achieve desired outcomes. Mesenchymal stem cells (MSC) can be driven towards specific cell fate decisions by varying substrate stiffness to mimic the physical properties of different tissues (Akhmanova et al., 2015). On soft matrices (2.5 kPa – 5 kPa) MSCs preferentially differentiate into adipocytes, while more rigid substrates (8 kPa – 20 kPa) drive them towards myogenic phenotype. Culturing MSCs on substrates with 30 kPa and higher stiffness induces osteogenic differentiation (Akhmanova et al., 2015). Fibroblasts cultured on stiff substrates undergo activation and differentiation into myofibroblast phenotype (Huang et al., 2012). Substrate surface micro- and nanotopography can also influence stem cell fate decisions (Han et al., 2020). Furthermore, it also can affect morphology, migration, and orientation of various cell types (Kim et al., 2014, Micholt et al., 2013, Bhattacharjee et al., 2020). In 3D, in addition to stiffness and topography, scaffold porosity also plays a role in regulation of cell behaviour (Rnjak-Kovacina et al., 2011, Iturriaga et al., 2021).

Other mechanical stimulation strategies rely on application of external forces using various devices and bioreactors (Zhang and Habibovic, 2022). Cyclic stretching has been shown to affect cell proliferation, migration, and adhesion in several cell types, including MSCs, fibroblasts and keratinocytes (Nishimura et al., 2009, Cui et al., 2015, Jungbauer et al., 2015, Fang et al., 2019). Adjusting stimulation parameters, such as frequency or direction of the strain, allows to elicit different effects. For example, keratinocyte proliferation could be upregulated or downregulated depending on the cyclic stretch frequency (Nishimura et al., 2009), while the expression of smooth muscle cell markers in MSCs are differentially regulated by uniaxial and equiaxial stretch (Park et al., 2004). Stem cells from various sources can be driven towards endothelial lineage with biomimetic magnitude shear stress generated in fluid flow bioreactors (Huang et al., 2021). While the effects of shear stress have been the most extensively studied in the context of vascular biology, it also has been shown to enhance osteogenic differentiation of MSCs (Datta et al., 2006) and improve mechanical properties of tissue-engineered cartilage constructs (Salinas et al., 2020).

These mechanical stimulation modalities are useful for *in vitro* tissue engineering and discovery of novel pharmaceuticals, which target mechanotransduction pathways. However, they require direct access to the cells and therefore are difficult to translate into *in vivo* applications. A few stretch-based mechanotherapies have been developed, namely soft tissue expansion, microdeformational wound therapy and distraction osteogenesis (Huang et al., 2013). Modification of surface topography has also been explored as a method to improve antibacterial properties and osseointegration of dental and joint replacement implants (Asensio et al., 2019, Liu et al., 2020). Nevertheless, considering the wide range of mechanosensitive processes involved in disease progression and tissue regeneration, further advancements in developing innovative mechanical stimulation approaches *in vivo* are highly desirable.

1.1.2 Vibration

Vibration is a useful method for delivering mechanical stimulation *in vivo* as it does not require direct contact with the target tissue and cells within it. Vibration

propagates as a mechanical wave, causing oscillatory movement of the particles in the medium. This allows the mechanical treatment to be applied to the exterior of the body in a non-invasive manner.

The idea of using vibration to improve human health dates back to 1875, when Swedish doctor Gustav Zander invented an apparatus that would simulate the vibration experienced when horse-riding, which was thought to improve muscle gain (Singh and Varma, 2023). Today there is a number of vibration-based mechanotherapies in various stages of development. Vibration has been reported to have beneficial outcomes on nerve injury repair (Yin et al., 2022), diabetic wound healing (Syabariyah et al., 2023), attenuating hepatic steatosis (Oh et al., 2014) and alleviating negative effects of cancer treatments (Lopes-Souza et al., 2018) among other therapeutic applications. However, the most widely studied application of vibrational mechanotherapy is in stimulation of the musculoskeletal system (Singh and Varma, 2023, Cerciello et al., 2016).

Bones experience vibrations from daily movements and exercise and interpret them as anabolic signals (Cerciello et al., 2016). Simulating these signals with applied vibrational treatment can potentially reduce bone resorption and increase bone mass (Thompson et al., 2014). This makes it an attractive strategy for treatment of osteoporosis and osteoporosis related fractures (Cheung et al., 2021), as majority of pharmaceuticals target bone resorption and options for anabolic agents are lacking (Li et al., 2021). In addition, vibrational treatment has been shown to increase bone mineral density (BMD) in children with motor disabilities (Kilebrant et al., 2015) and improve fracture healing in animal models of diabetes (Campos et al., 2022). However, while many clinical trials found that vibrational treatment could increase BMD, others also reported no significant improvement and a few even observed negative effects (Cerciello et al., 2016, Singh and Varma, 2023, Marin-Puyalto et al., 2018). This highlights the importance of identifying the optimal vibration parameters to achieve the desired therapeutic outcomes.

Properties of a vibrational wave can be defined by three parameters: frequency, acceleration, and displacement (Figure 1.1). Simplest form of vibration is a pure

sine wave, in which consistent displacements occur at a single frequency and the three parameters are mathematically related to each other (van Heuvelen et al., 2021). Relationships between the parameters in more complex waveforms are much less predictable. Majority of vibrational devices available commercially and tested in clinical trials deliver sinusoidal vibrations (Fratini et al., 2016), however irregular vibrations are also being investigated for mechanotherapeutic purposes (Rogan et al., 2011, Igbokwe et al., 2022).

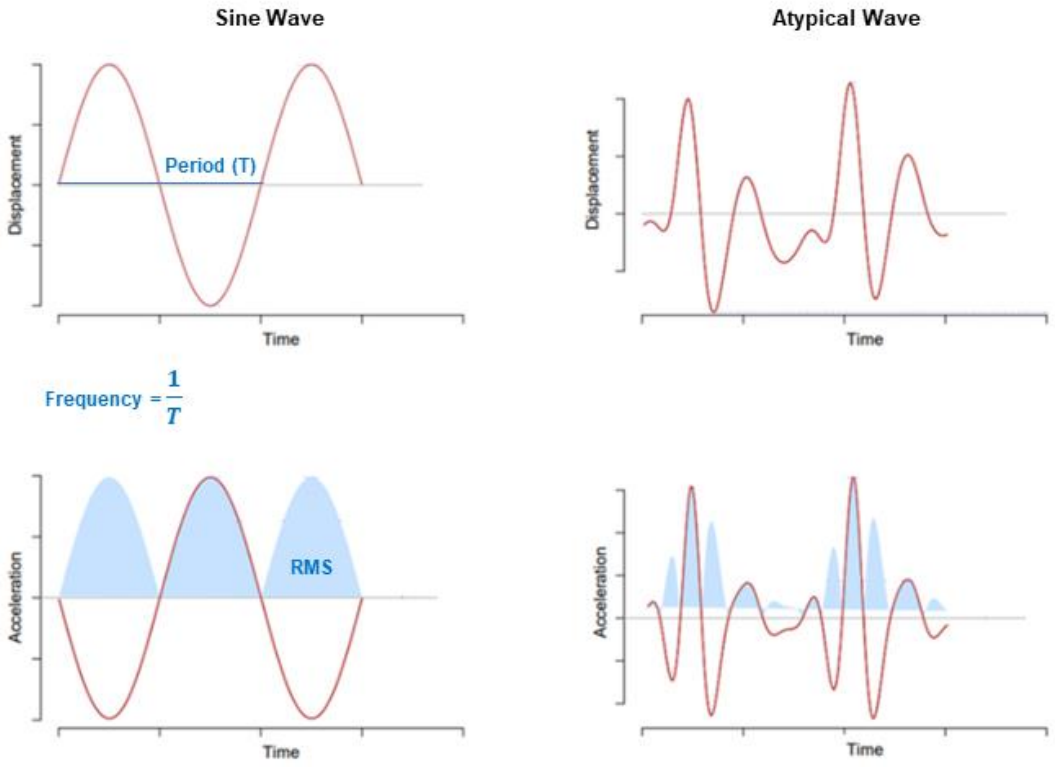

Figure 1.1 Waveforms of a sinusoidal and an atypical wave showing displacement and acceleration change over time. Acceleration can be expressed as peak acceleration or root-mean-square (RMS) shown in blue. In sine wave the relationship between displacement and acceleration is proportional, while in an irregular wave it is not. Frequency represents a number of oscillation cycles per second as is calculated from time period it takes to complete one cycle. Figure adapted from van Heuvelen et al., (2021).

The most common application method for therapeutic vibration is whole body vibration (WBV) applied from a vibrating standing platform in a vertical or horizontal direction (Singh and Varma, 2023, Marín-Cascales et al., 2018). The frequencies of WBV range from 6 Hz to 100 Hz with accelerations from 0.2 g to 8.4 g and displacements ranging from 0.3 mm to 5 mm (Singh and Varma, 2023,

Marín-Cascales et al., 2018, Fratini et al., 2016). Even though a fairly large number of studies on the effects of WBV have been carried out, the optimal stimulation parameters remain elusive. Some analyses suggested that frequencies under 20 Hz have no effect (Marín-Cascales et al., 2018), while others found them more effective than the higher frequencies in increasing BMD (Fratini et al., 2016). In terms of acceleration, over 3 g has been proposed to produce the best results (Fratini et al., 2016), but some authors recommended acceleration as high as 8 g (Marín-Cascales et al., 2018). The effects also seem to vary between different anatomical sites, with more benefits observed in the lower body (Fratini et al., 2016). And some studies reported that WBV had no positive effect on BMD at all, no matter what parameters were used (Lau et al., 2011). The mechanism through which vibration may promote bone regeneration is also unclear. Stimulation of intrinsic bone tissue piezoelectricity and improvement of muscle tone have been proposed but require further analyses to be confirmed (Fratini et al., 2016).

A number of *in vitro* studies investigating the effects of vibration on MSCs reported enhanced osteogenic differentiation after vibrational treatment with parameters comparable to those used in WBV (Steppe et al., 2020). Lu et al. (2018) found that 40 Hz vibration with acceleration of 0.3 g causing 50 μm displacements upregulated the activity of p38 signalling pathway in rat bone-marrow MSCs. In another study, vibration with the same parameters was demonstrated to promote osteogenesis through Wnt/β-catenin signalling pathway in MSCs cultured on hydroxyapatite-coated titanium scaffolds (Chen et al., 2016). Slightly lower vibration frequency of 30 Hz and 0.3 g acceleration induced production of vascular endothelial growth factor (VEGF) in MSCs in 3D, but not in 2D cultures (Kim et al., 2012). Unfortunately, similarly as in clinical trials, these effects are not fully consistent, as some studies reported no effect on MSC osteogenesis in a similar vibration parameter range (Lau et al., 2011). In addition, in the vast majority of studies, vibrational stimulation was applied in conjunction with osteogenic differentiation media (Lu et al., 2018, Kim et al., 2012) or to MSCs cultured on scaffolds with osteoinductive properties (Chen et al., 2016). Therefore, the vibration appears to enhance but not to induce MSC osteogenesis *in vitro*. Identification of vibration parameters which can promote MSC osteogenesis independent of biochemical stimulation would be greatly beneficial in treatment

of osteoporosis and other bone disorders, where biochemical environment may not favour osteogenesis (Li et al., 2015).

1.1.3 Nanovibrational stimulation

Nanovibration refers to vibration with displacement in the nanoscale (Robertson et al., 2019). Specifically, vibration with frequency of 1000 Hz causing around 30 nm displacements has been shown to be a potent pro-osteogenic signal *in vitro*, able to induce osteogenic differentiation in MSCs without the addition of biochemical fate inducers (Tsimbouri et al., 2017). This effect has been observed in 2D, in MSCs cultured on tissue culture plastic (Nikukar et al., 2013), and in 3D soft collagen gels, demonstrating that the observed effects are consistent across culture conditions and not due to the substrate stiffness (Tsimbouri et al., 2017).

The parameters of nanovibration are highly unusual compared with other vibrational stimulation studies, most of which apply vibration frequencies under 100 Hz and displacements in the micrometre – millimetre range. To apply nanovibration in a reliable manner, a custom nanovibrational bioreactor was designed and extensively characterised (Robertson et al., 2019). The bioreactor consists of a vibration plate connected to a power supply unit (Figure 1.2). The vibration plate contains an array of 13 piezoceramic actuators placed between two metal plates. The bottom plate is heavier than the top to direct the displacements upwards, where the cultureware is attached to the top plate using magnets (Robertson et al., 2019). The deformation of the piezo actuators is initiated by an electrical signal from the power supply unit. This unit includes a programmable waveform generator that produces a sinusoidal electrical signal, which is then digitally processed to eliminate any unwanted high-frequency components and passed through a series of amplifiers (Robertson et al., 2019). The amplified sinusoidal signal is then directed to the piezo array, which generates vibration of the top plate with precise parameters (Robertson et al., 2019).

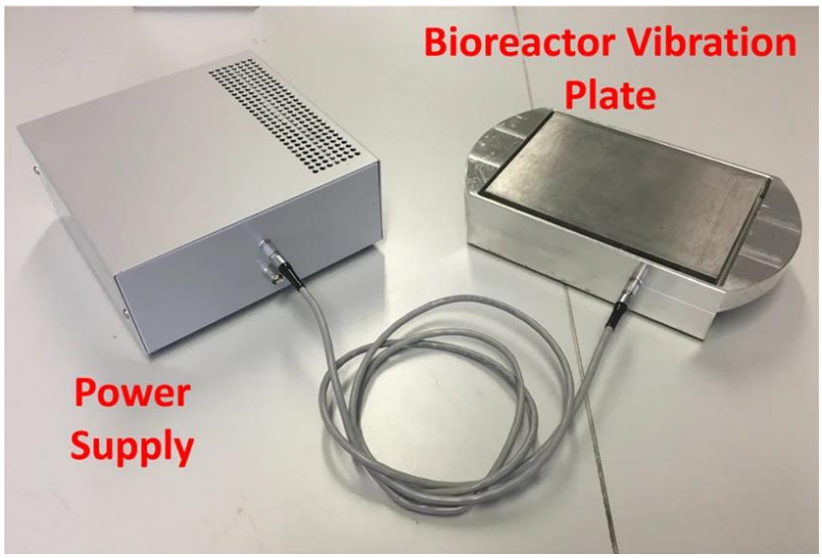

Figure 1.2 Bioreactor for application of nanovibrational stimulation, consisting of a power supply unit and a vibration plate. Adapted from Robertson et al. (2019).

The cells treated with this vibrational stimulation system at 1000 Hz experience around 30 nm displacements and 0.12 g accelerations (Tsimbouri et al., 2017, Robertson et al., 2019). In 2D, nanovobrational stimulation with these parameters was reported to cause cytoskeletal rearrangement, through the activation of Rho GTPase/Rho-associated protein kinase (Rho/ROCK) pathway and upregulate osteogenic differentiation markers runt-related transcription factor 2 (RUNX2), bone-morphogenic protein 1 (BMP2) and osteocalcin (Nikukar et al., 2013). Rho/ROCK pathway activation has been shown to be necessary for the osteogenic effects of nanovibration in 2D (Nikukar et al., 2013). In 3D, Rho/ROCK pathway also played a role in nanovibration-induced MSC osteogenesis, but it was less pronounced, and mechanosensitive ion channels were demonstrated to be the essential transducers of nanovibrational signal, potentially stimulating Wnt/ß-catenin pathway (Tsimbouri et al., 2017) (Figure 2.3).

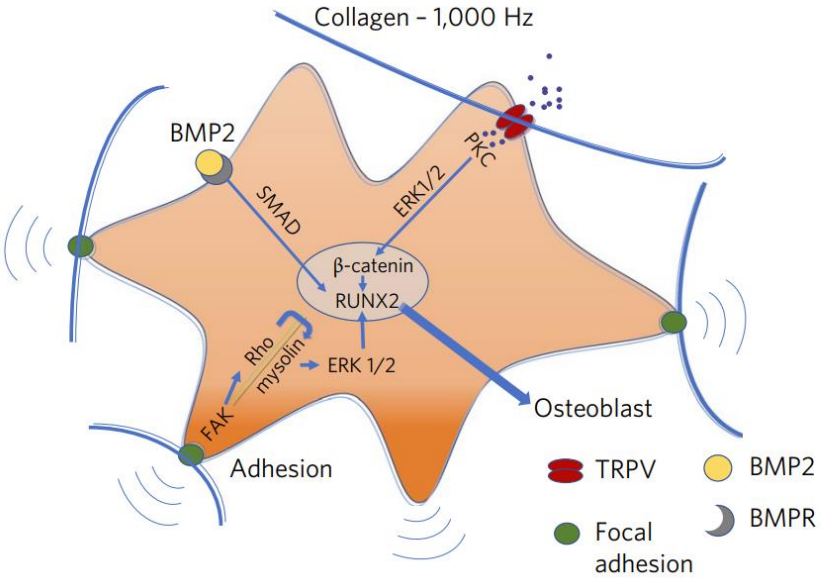

Figure 1.3 Proposed mechanisms of nanovibration induced osteogenesis in MSCs. Mechanosensation through focal adhesions and mechanosensitive TRPV ion channels as well as paracrine/autocrine BMP2 signalling have been implicated in MSCs response to nanovibrational stimulation. Adapted from Tsimbouri et al., 2017.

After 46 days of stimulation, nanovibration-treated 3D MSC cultures showed a similar Raman spectrum to cortical bone, indicating complete differentiation into osteoblasts, capable of matrix mineralisation (Tsimbouri et al., 2017). In addition, nanovibration inhibited osteoclastogenesis, suggesting that it may not only promote bone regeneration but also prevent resorption (Kennedy et al., 2021). These findings indicate that nanovibration could potentially be translated into a novel mechanotherapy for disorders associated with loss of BMD and delayed fracture union.

When applied to the exterior of the body, nanovibration would propagate through the soft tissues surrounding the bone, stimulating various cell types within those tissues. However, the effects of nanovibration have not been studied extensively outside of MSCs. Results from metabolomic experiments suggested that nanovibrational stimulation modulates the activity of extracellular signal-regulated kinase (ERK) and protein kinase B (Akt) signalling pathways (Tsimbouri et al., 2017, Kennedy et al., 2021). These pathways are involved in key biological processes, such as proliferation, survival, and apoptosis, across many different cell types (Cao et al., 2019). Different cells may sense mechanical stimuli in a

similar way but respond differently (Banes et al., 1995). Considering nearly all cell types are mechanosensitive to some degree (Banes et al., 1995), it is possible that nanovibrational stimulus might induce some kind of phenotype changes in other cells, with unpredictable and potentially negative outcomes. On the other hand, discovering of any positive effects of nanovibrational stimulation, beyond the ones observed in MSCs, could indicate further potential therapeutic applications of nanovibration.

Fibroblasts are abundant within the human body and exhibit mechanical sensitivity (Darby et al., 2014). Given their prevalence in the connective tissues, some portion of them is likely to be subjected to nanovibrational stimulation when it is applied at any anatomical site. In addition, vibration-based interventions for improvement of wound healing (Weinheimer-Haus et al., 2014) and treatment of fibrotic conditions (Maiworm et al., 2011) have been proposed. Hence, fibroblasts present an intriguing cellular model for investigating the potential effects of nanovibrational stimulation.

1.2 Fibroblasts

Fibroblasts are cells of mesenchymal origin, found in various tissues around the body (Kendall and Feghali-Bostwick, 2014). They are the most common cell type in the connective tissues, where they produce extracellular matrix (ECM) and maintain structural integrity of the tissue (Kendall and Feghali-Bostwick, 2014). Fibroblasts synthesise a wide range of ECM components, including collagen, fibronectin, laminin, elastin, proteoglycans and glycosaminoglycans in various proportions based on the tissue requirements (Karamanos et al., 2021). In addition, fibroblasts can exert forces on the surrounding matrix to maintain tissues in mechanical homeostasis (Kirk et al., 2021), secrete signalling molecules and metabolites to modulate biochemical tissue microenvironment and, in some cases, can serve as progenitors for other more specialised cell types (Plikus et al., 2021) (Figure 1.4).

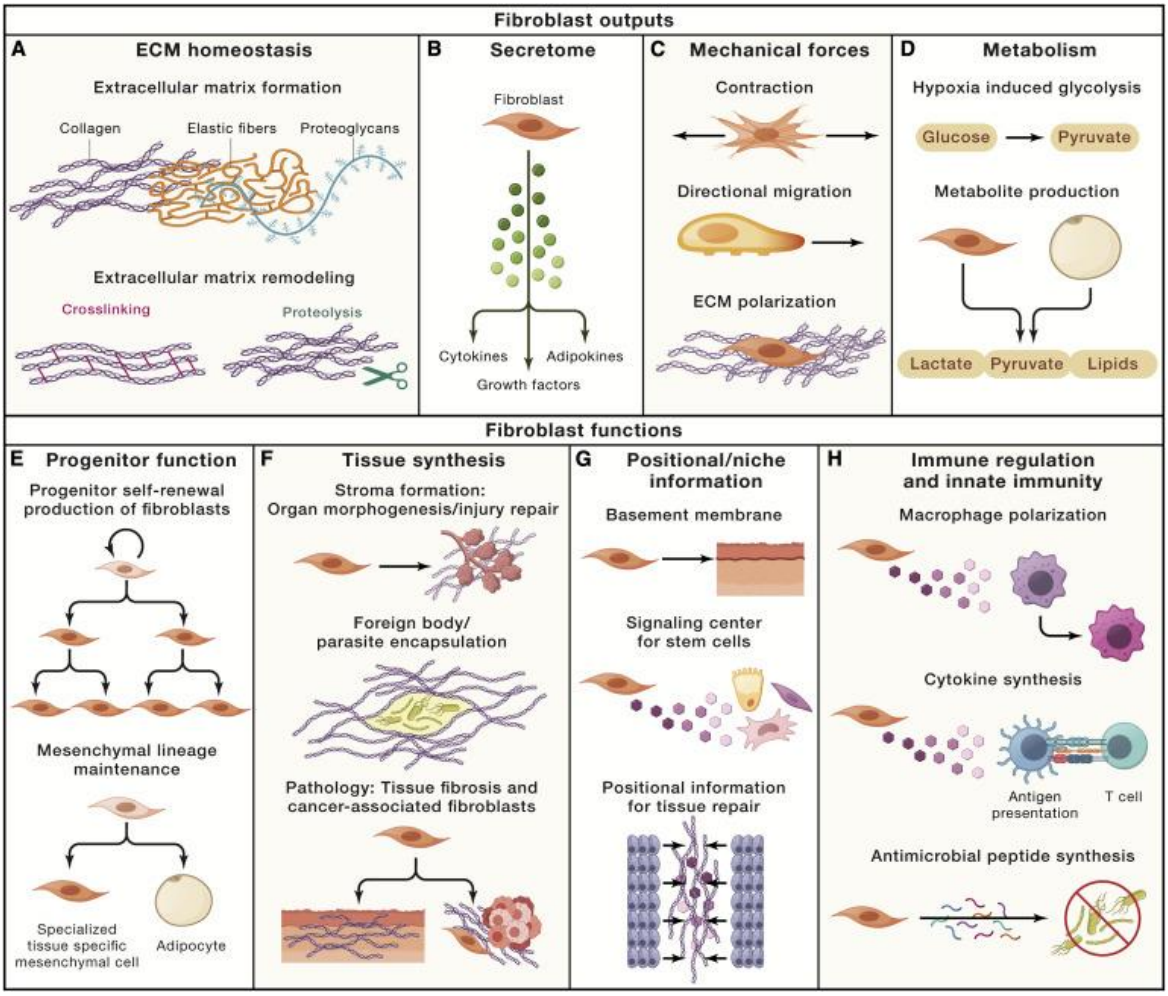

Figure 1.4. Summary of fibroblast outputs and functions. Fibroblasts produce and secrete A) ECM components and B) signalling molecules, C) generate mechanical forces and D) regulate tissue metabolism. In some tissues they can serve as E) progenitors for other cell types. Fibroblasts are essential for F) tissue development and repair, G) provide positional cues during wound healing and stem cell differentiation and H) modulate immune response. Adapted from Plikus et al., 2021.

Fibroblasts are not a well-defined cell type (Tracy et al., 2016). They lack specific markers and show distinct features and behaviours between tissues and sometimes even within the different regions of the same tissue (Tracy et al., 2016). However, despite their heterogeneity, fibroblasts are key mediators of wound healing in all tissues (Plikus et al., 2021, Kirk et al., 2021). Under homeostatic conditions fibroblasts are generally quiescent, producing moderate amounts of ECM and dividing only occasionally (Kirk et al., 2021). In response to injury, various signalling molecules released from immune cells induce fibroblast migration, proliferation and differentiation into the myofibroblast phenotype (Darby et al.,

2013). Myofibroblasts are highly contractile and produce large amounts of ECM components and remodelling factors, such as matrix metalloproteases (MMPs) (Darby et al., 2013). They also secrete inflammatory cytokines, chemokines, and growth factors. These factors stimulate the activity of other cells at the injury site, such as keratinocytes and macrophages, and contribute to angiogenesis, epithelialisation, and immune response (Arif et al., 2021). After the resolution of an injury, myofibroblasts disappear from the tissue, either by apoptosis (Darby et al., 2013) or by reverting to quiescence (Plikus et al., 2021). If myofibroblasts persist at the repair site for a prolonged period of time, it can lead to chronic inflammation, hypertrophic scarring, and tissue fibrosis (Plikus et al., 2021).

1.3 Fibroblasts and myofibroblasts in wound healing

Cutaneous wound healing is a dynamic process, in which fibroblasts play a vital role (Cialdai et al., 2022). Immediately after the injury, various factors released from the damaged cells cause activation and aggregation of platelets and formation of a fibrin network to restore the protective skin barrier and prevent further pathogen invasion (Gonzalez et al., 2016). This initiates a series of reparative events, which occur in three partially overlapping phases: inflammation, proliferation, and remodelling (Cialdai et al., 2022). Fibroblasts are active participants throughout the entire course of wound healing, responding to the evolving biochemical and biomechanical cues during each phase (Cialdai et al., 2022) (Figure 1.5).

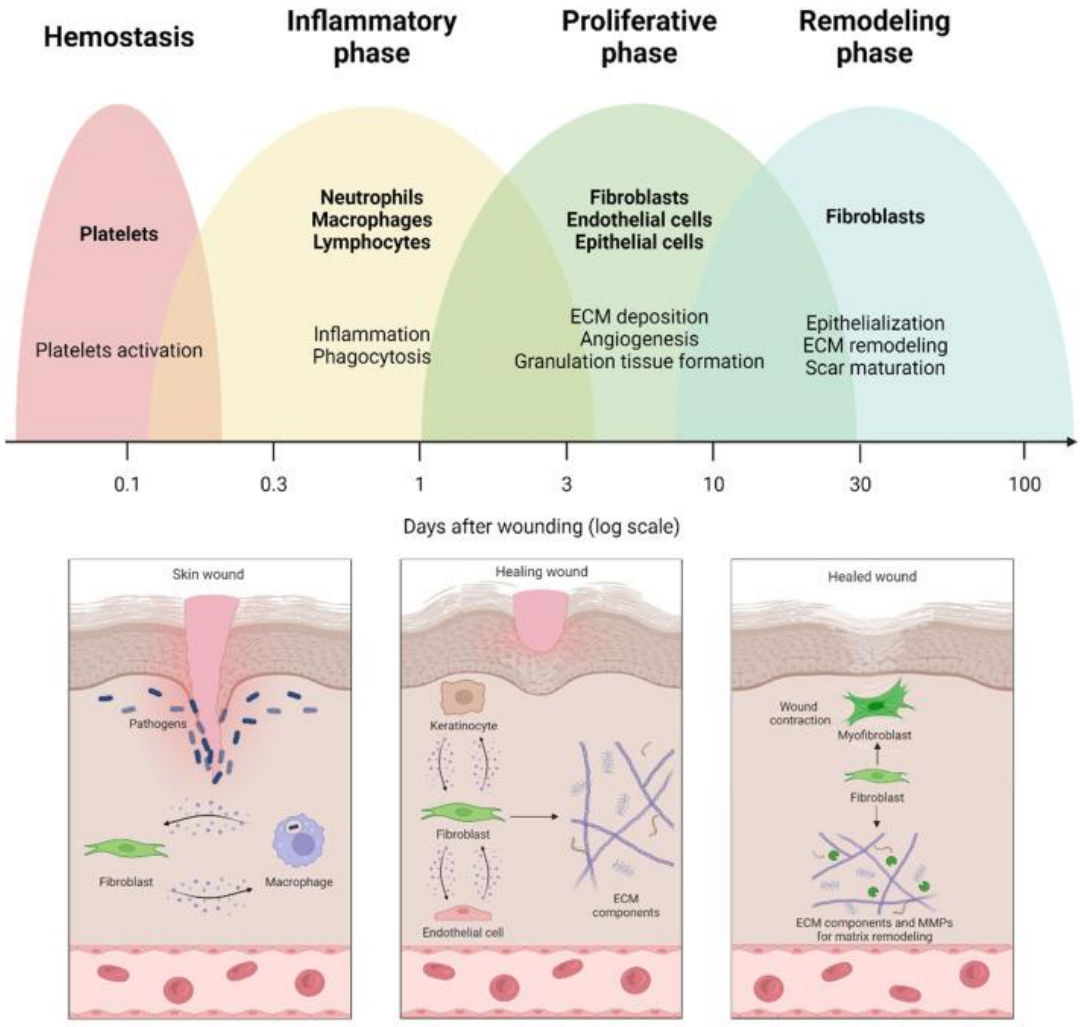

Figure 1.5 Graphic summary of wound healing phases and fibroblast role in each phase. In the inflammatory phase, fibroblasts migrate and establish reciprocal signaling with macrophages. This is followed by proliferative phase, during which fibroblasts proliferate, produce ECM components, and stimulate other cells via secreted factors. Last phase is remodeling, during which fibroblasts alter the composition of the ECM and restore mechanical homeostasis in the tissue. The graph presents a timeline consistent with rodent wound healing, while in humans the remodeling phase can take up to 2 years. Adapted from Cialdai et al., 2022.

1.3.1 Inflammatory phase

Bioactive molecules secreted from platelets in the fibrin clot recruit and stimulate macrophages at the wound site (Mescher, 2017). These signals direct macrophages into the pro-inflammatory programme and they become a major source of inflammatory cytokines, such as interleukin-11 (IL-11), interleukin-6 (IL-6) and tumour necrosis factor-α (TNF-α) (Cialdai et al., 2022). These factors stimulate fibroblast migration from the surrounding tissue into the wound site (Cialdai et al., 2022). Fibroblasts contract the fibrin matrix, enhancing further migration

(Tracy et al., 2016), and secrete MMPs, facilitating immune cell infiltration in the injury site (Cialdai et al., 2022). Contraction of the fibrin matrix has been demonstrated to sensitise fibroblasts to the transforming growth factor-β (TGFβ), which is critical for ECM synthesis during the following stages of wound healing (Tracy et al., 2016). In addition, fibroblasts themselves begin secreting various signalling molecules, which stimulate macrophages and amplify the immune response (Cialdai et al., 2022).

1.3.2 Proliferative phase

Acute inflammation subsides as macrophages gradually transition from an inflammatory to a regenerative phenotype, leading to decreased secretion of inflammatory cytokines and increased production of growth factors (Mescher, 2017). Growth factors, such as TGFβ, insulin-like growth factor-1 (IGF1), fibroblast growth factor (FGF) and platelet-derived growth factor (PDGF) induce fibroblast differentiation into the proto-myofibroblast phenotype (Darby et al., 2014, Cialdai et al., 2022). Proto-myofibroblasts produce ECM, signalling molecules and show moderately increased contractility, but lack the α-smooth muscle actin (α-SMA)-positive stress fibres, which are considered to be the defining feature of the myofibroblast phenotype (Hinz, 2007). Proto-myofibroblasts proliferate and remodel the fibrin matrix by releasing MMPs and ECM components, forming the granulation tissue (Cialdai et al., 2022, Darby et al., 2014). Collagen type III is the main ECM protein produced at this stage (Mathew-Steiner et al., 2021). Other ECM components produced by fibroblasts include fibronectin, hyaluronic acid, and proteoglycans (Cialdai et al., 2022). Newly produced ECM provides support for keratinocyte migration and contributes to the restoration of the epithelium (Moretti et al., 2022). Both fibroblasts and keratinocytes produce VEGF, cooperatively promoting angiogenesis in the granulation tissue (Kendall and Feghali-Bostwick, 2014). Formation of capillaries increases the flow of nutrients in the granulation tissue, supporting further fibroblast growth and proliferation (Darby et al., 2014).

1.3.3 Remodelling phase

As fibroblasts deposit more and more ECM proteins, stress in the ECM increases (Hinz, 2007). This, combined with TGFβ signalling, facilitates the transition from proto-myofibroblasts into mature myofibroblasts (Hinz, 2007). Incorporation of α-SMA into the stress fibres enhances cytoskeleton contractility (Darby et al., 2014) and myofibroblasts exert force on the surrounding ECM through the focal adhesions, further contracting the wound (Cialdai et al., 2022). The generated mechanical tension then sustains the myofibroblast phenotype by stimulating mechanotransduction pathways (Hinz, 2007) and by allowing the activation of latent TGFβ deposited in the ECM (Hinz, 2015). Myofibroblasts gradually remodel the matrix, degrading collagen III and replacing it with collagen I (Darby et al., 2014). Levels of hyaluronic acid and fibronectin in the ECM also decrease (Gonzales et al., 2016), while elastin increases (Darby et al., 2014). Restoration of tensional homeostasis leads to myofibroblast removal, most likely by apoptosis (Cialdai et al., 2022), although reversal to the quiescent phenotype has been suggested as well (Plikus et al., 2021). Remodelling phase is the final phase of the wound healing process and can take several months or even over a year, depending on the injury (Gonzalez et al., 2016). Apoptosis evasion and prolonged presence of myofibroblasts after the repair is thought to be a major contributor to the development of hypertrophic and keloid scars (Shih et al., 2010).

1.4 Factors modulating fibroblast phenotype

During wound healing, many different biochemical and biomechanical factors work in concert to regulate fibroblast behaviour (Cialdai et al., 2022). Abnormalities during the repair process (Cialdai et al., 2022) or exposure to these factors outside of the wound healing context, for example from tumour cells (Tao et al., 2017), can lead to sustained myofibroblast activity, excessive ECM deposition, chronic inflammation, and impaired tissue function (Kendall and Feghali-Bostwick, 2014).

1.4.1 Growth Factors

1.4.1.1 Transforming growth factor- β (TGFβ)

TGFβ growth factors are perhaps the most prominent regulators of pro-fibrotic phenotype in the fibroblasts (Frangogiannis, 2017). Elevated levels of TGFβ are found in keloid scars (Shih et al., 2010), systemic sclerosis (SSc) (Lafyatis, 2014), idiopathic pulmonary fibrosis (IPF) (Zhu et al., 2022), various tumours (Tao et al., 2017) and other disorders which involve abnormal fibroblast function (Kendall and Feghali-Bostwick, 2014).

There are three TGFβ isoforms encoded by separate genes (Wilson, 2021). Pro-fibrotic effects of TGFβ1 and TGFβ2 have been well established while the exact role of TGFβ3 in wound healing and fibrosis is not well understood (Wilson, 2021). TGFβ proteins are produced by many different cell types and deposited in the ECM as inactive homo- or heterodimers in complex with latency-associated peptide (LAP) (Shi et al., 2020). Activation of TGFβ requires release from LAP, which can be facilitated by proteases (Kubiczkova et al., 2012), mechanical forces (Hinz, 2015) or, in case of TGFβ1 specifically, reactive oxygen species (ROS) (Jobling et al., 2006).

There are three TGFβ receptors (TGFβRs), all of which can couple with any of the TGFβ isoforms (Wilson, 2021). Canonical TGFβ signalling is initiated when TGFβ dimer binds to TGFβRII, which recruits and phosphorylates TGFβRI (Shi et al., 2020). In turn, TGFβRI phosphorylates small mothers against decapentaplegic (SMAD) proteins SMAD2 and SMAD3, which form a complex with SMAD4. SMAD2/3/4 complex translocates to the nucleus and modulates the expression of TGFβ target genes (Shi et al., 2020). Non-canonical signalling pathways include activation of ERK, c-Jun N-terminal kinase (JNK), p38, Akt and Rho/ROCK signalling (Finnson et al., 2020) (Figure 1.6).

Both canonical and non-canonical TGFβ signalling pathways play an important role in fibroblast activation. SMAD2/SMAD3/SMAD4 complex regulates expression of collagens, MMPs, integrins and connective tissue growth factor (CTGF) (Walton et

al., 2017). SMAD3 but not SMAD2 is also involved in upregulation of α-SMA (Shi et al., 2020). TGFß-induced ERK pathway activation is necessary for myofibroblast differentiation in dermal fibroblasts (Carthy et al., 2015), while Akt signalling promotes fibroblast resistance to apoptosis (Kulasekaran et al., 2009), with both pathways regulated in SMAD independent way.

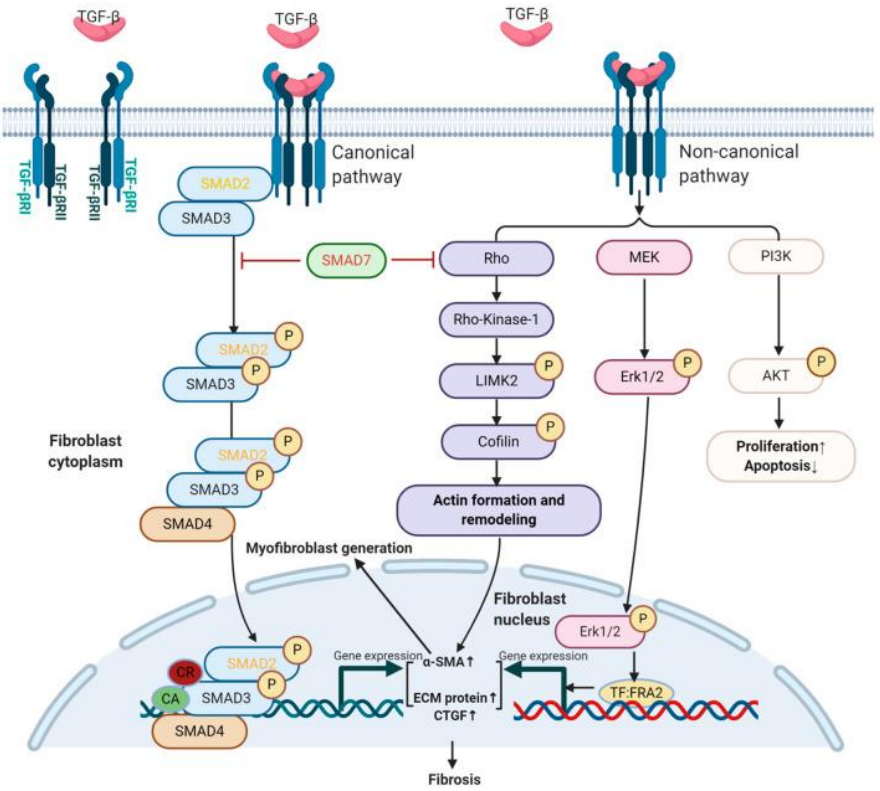

Figure 1.6. Canonical and non-canonical TGFβ signaling pathways in fibroblasts.

Canonical TGFβ signaling is occurs through phosphorylation of SMAD2/3 proteins. Non-canonical signaling is SMAD independent.

1.4.1.2 Connective tissue growth factor (CTGF)

CTGF is another potent inducer of a pro-fibrotic phenotype in fibroblasts (Lipson et al., 2012) and has been shown to be involved in renal, pulmonary, liver, and cardiac tissue fibrotic diseases (Chen et al., 2020). CTGF consists of four functional domains, which have distinct binding characteristics and can interact with a wide range of other signalling molecules (Chen et al., 2020). One of its binding partners is TGFß, which is guided to the receptors by CTGF, enhancing its signalling (Chen et al., 2020). In turn, TGFß promotes CTGF production, leading to a positive feedback loop between the two factors (van Caam et al., 2018).

Inhibition of CTGF was demonstrated to substantially reduce TGFß-induced fibroblast proliferation and fibrotic gene expression (Lipson et al., 2012). In addition, CTGF regulates cellular adhesion and migration, by interacting with integrins and directly binding fibronectin in the ECM (Chen et al., 2020).

1.4.1.3 Platelet derived growth factor (PDGF)

PDGF is another key player in wound healing and fibrosis (Kendall and Feghali-Bostwick, 2014). PDGF has been implicated in development and progression of fibrotic diseases, such as SSc (Paolini et al., 2022), both through its own signalling pathways (Juhl et al., 2020) and crosstalk with TGFß (Dadrich et al., 2016). There are four different PDGF polypeptides, which dimerise to form five different PDGF isoforms: PDGF-AA, PDGF-BB, PDGF-CC, PDGF-DD, and the only heterodimeric isoform PDGF-AB (Donovan et al., 2013). There are two PDGF receptor proteins (PDGFRs), which form heterodimeric or homodimeric receptors and have different affinities for specific PDGF ligands (Donovan et al., 2013). While the downstream effectors of different PDGFRs partially overlap (Donovan et al., 2013), some receptor specific effects also have been reported (Yamada et al., 2018). For example, both PDGFRßß and PDGFRαß were shown to induce activation of Akt and promote fibroblast migration, but the cellular localisation of the active Akt and the direction of migration were observed to be different (Yamada et al., 2018). ERK activation was found to be reduced upon inhibition of PDGFRαß but not PDGFRßß (Donovan et al., 2013). In addition to signalling via PDGFRs, PDGF ligands might engage other membrane receptors (Takamura et al., 2021). PGDF-BB has been shown to induce TGFß1 expression and subsequent ECM protein synthesis in fibroblasts independent of PDGFRs (Takamura et al., 2021).

1.4.1.4 Fibroblast growth factor (FGF)

FGFs are a family of 22 proteins, involved in a wide range of biological processes, including proliferation, cell survival and tissue repair (Farooq et al., 2021). Different FGFs can bind one or several out of 4 different FGF receptor types and regulate signalling pathways, such as ERK, Akt and JNK (Seitz and Hellerbrand, 2021). In fibroblasts, FGF1 and FGF2 have been shown to antagonise TGFß

signalling and abrogate myofibroblast differentiation (Shimbori et al., 2016, Farooq et al., 2021). FGF2 was reported to inhibit Akt signalling and induce apoptosis in granulation tissue fibroblasts stimulated with TGFβ but did not have the same effect on the untreated fibroblasts, suggesting it may play a role in myofibroblast clearance after wound repair (Akasaka et al., 2010). However, in another study, FGF2 was observed to promote proliferation but inhibit expression of pro-fibrotic genes in TGFβ treated fibroblasts (Dolivo et al., 2017). Fortier et al. (2021) observed similar results in pulmonary fibroblasts and proposed that FGF2-driven increase in fibroblast proliferation was associated with the loss of pro-fibrotic character, as cells must rearrange their cytoskeleton for division, potentially losing the stress fibres. FGF1 has also been reported to suppress TGFβ1 signalling by downregulating TGFβRI expression and promoting its degradation (Shimbori et al., 2016).

Other FGFs can also affect fibroblast phenotype but their effects are less well characterised. FGF9 downregulated basal collagen I and α-SMA levels in both healthy and fibrotic pulmonary fibroblasts, however, after stimulation with TGFβ1 the fibrotic cells resisted this effect (Joannes et al., 2016). In addition, FGF9, as well as FGF18, FGF21 and FGF10 were reported to stimulate fibroblast migration (Joannes et al., 2016, Song et al., 2016). Finally, FGF4 was found to be highly upregulated in dermal fibroblasts isolated from SSc patients, but its role in fibrosis is not yet known (Frost et al., 2019).

1.4.2 Inflammatory cytokines

1.4.2.1 Interleukins

Interleukins are a group of cytokines with a prominent role in wound healing and inflammation (Borthwick et al., 2013). They modulate immune response by stimulating immune cells and several can directly stimulate fibroblasts, promoting or repressing the pro-fibrotic phenotype (She et al., 2021).

IL-6 plays a key role in the inflammatory and the proliferative stages of wound healing (Johnson et al., 2020). It is also found upregulated in fibroblasts isolated

from SSc patients, hypertrophic and keloid scars (Johnson et al., 2020). During the wound healing process, it is first secreted by macrophages and other immune cells and promotes fibroblast migration into the wound site (Cialdai et al., 2022). IL-6 initiates fibroblast production of FGF7, also known as keratinocyte growth factor, establishing fibroblast-to-keratinocyte signalling and promoting keratinocyte migration (Johnson et al., 2020). IL-6 can also promote myofibroblast differentiation by stimulating TGFß release from macrophages, as well as by interacting with fibroblasts directly and stimulating Janus kinase (JAK)/ERK pathway activation (Johnson et al., 2020). Upon activation by TGFß, fibroblasts also start producing IL-6, which in turn potentiates TGFß signalling, leading to a positive feedback loop (Kong et al., 2018). IL-6 is potentially one of the factors contributing to myofibroblast resistance to apoptosis in fibrotic conditions, as it was reported to upregulate anti-apoptotic protein BCL-2 in IPF fibroblasts (Moodley et al., 2003). Stimulation with IL-6 can also promote collagen I synthesis in fibroblasts, however not to the same extent as TGFß or PDGF (Juhl et al., 2020).

Interleukins IL-4 and IL-13 also contribute to myofibroblast differentiation (Nguyen et al., 2020). Both were demonstrated to promote TGFß synthesis in fibroblasts and subsequent upregulation of α-SMA and ECM protein expression (Nguyen et al., 2020). IL-13 was reported to inhibit MMPs, reducing collagen degradation and leading to excessive ECM accumulation (Nguyen et al., 2020). Another interleukin IL-11 did not increase TGFß production in fibroblasts but was shown to contribute to the pro-fibrotic phenotype downstream of TGFß, potentiating non-canonical TGFß signalling pathways (Adami et al., 2020). Inhibition of IL-11 signalling partially alleviated TGFß-induced fibroblast activation in healthy and SSc dermal fibroblasts (Adami et al., 2020).

In contrast, IL-37 has anti-inflammatory properties and was found to be downregulated in a number of connective tissue disorders (Pan et al., 2020). IL-37 can interfere with TGFß signalling through interaction with SMAD3 (Mountford et al., 2021). In hepatic myofibroblasts, IL-37 was observed to downregulate production of several inflammatory factors, as well as α-SMA (Mountford et al., 2021), while in IPF fibroblasts, it inhibited TGFß signalling and reduced the

expression of collagen I and fibronectin but did not influence α-SMA levels (Kim et al., 2019).

1.4.2.2 Osteopontin (OPN)

OPN was first identified in the bone tissue, where it is involved in remodelling and mineralisation (Lund et al., 2009). However, it was soon recognised to be an important mediator of the inflammatory response (Lund et al., 2009). In normal skin tissue, OPN is present at very low levels but is highly upregulated during wound healing or in fibrotic lesions (Wu et al., 2012). OPN protein contains cell adhesion motifs, including RGD, allowing it to interact with cells through αv integrins (Lund et al., 2009) and activate intracellular signalling pathways through focal adhesion kinase (FAK) (Hunter et al., 2012). Fibroblast contractility was shown to be increased in response to OPN, potentially through FAK-mediated effects on the cytoskeleton (Hunter et al., 2012). OPN can also bind to the ECM components, such as collagens and fibronectin, therefore regulating fibroblast adhesion and migration (Takahashi et al., 2000, Fujisawa et al., 2020, Hunter et al., 2012). The exact function of OPN depends on interactions with other signalling molecules. PDGF can induce OPN production in wound fibroblasts (Mori et al., 2008) and the two factors can cooperatively promote fibroblast proliferation (Takahashi et al., 2000). OPN was also reported to increase fibroblast migration and this effect was partially dependent on induction of IL-6 expression (Fujisawa et al., 2020). And even though treatment with OPN was shown to promote proliferation and migration, it did not upregulate α-SMA in pulmonary fibroblasts (Pardo et al., 2005), suggesting that it works cooperatively with other factors to promote the full extent of myofibroblast differentiation. However, in cardiac fibroblasts, OPN has been shown to be necessary for TGFβ induced myofibroblast differentiation (Lenga et al., 2008). In addition to the direct effects on fibroblasts, OPN also promotes TGFβ production in macrophages, therefore contributing to pro-fibrotic environment (Eu et al., 2012).

1.4.3 Reactive Oxygen Species (ROS)

ROS are unstable oxygen containing molecules, which include free radicals and reactive non-radical entities (Weidinger and Kozlov, 2015). Two major sources of ROS in cells are mitochondrial respiration and NADPH oxidases (NOX) (Dunnill et al., 2017). Moderate increase in ROS is vital in wound healing process, while excessive or significantly reduced ROS generation impairs it (Sen and Roy, 2008). Extracellular ROS at the wound site serves as chemoattractant to immune cells, while intracellular ROS signalling upregulates production of inflammatory factors and other signalling molecules (Bryan et al., 2012, Sen and Roy, 2008). Extracellular ROS may also contribute to the early stages of fibroblast activation, as it has been shown to promote fibroblast migration and proliferation (Khorsandi et al., 2022). In addition, ROS can mediate release of active TGFβ1 from the ECM by oxidising LAP, upregulating pro-fibrotic signalling in the wound site (Jobling et al., 2006).

TGFβ stimulates intracellular ROS production in fibroblasts, through upregulation of cell membrane-bound enzyme NOX4 and disruption of oxidative phosphorylation chain complexes in mitochondria (Liu et al., 2015). Increased ROS generation is required for pro-fibrotic activities of TGFβ, as inhibition of NOX4 or mitochondrial ROS substantially reduces the expression of α-SMA (Murphy-Marshman et al., 2017, Jain et al., 2013). Accumulation of ROS in fibroblasts is further increased by negative regulation of antioxidant defence system components (Richter and Kietzmann, 2016). TGFβ has been shown to downregulate production of a small molecule antioxidant glutathione (GSH) and expression of glutaredoxin proteins (GRXs), which bind GSH as a cofactor and function to protect proteins from oxidative damage (Richter and Kietzmann, 2016). In addition, antioxidant enzymes superoxide dismutase (SOD) and catalase (CAT) are also downregulated in response to TGFβ (Liu et al., 2015). Treatment with exogenous antioxidants strongly reduces pro-fibrotic effects of TGFβ (Estornut et al., 2022, Marshman et al., 2017).

Reciprocal regulation between ROS and TGFβ has been implicated in development of fibrotic diseases (Spadoni et al., 2015, Liu and Desai 2015). ROS may be directly involved in TGFβ signalling pathways, as it has been reported to promote

activation of JNK and p38 and this effect was reversed by treatment with GSH (Ghosh and Vaughan, 2012). In addition, ROS can cause oxidative modifications in DNA and histone proteins, leading to epigenetic changes and altered transcription patterns (Richter and Kietzmann, 2016). Finally, ROS can cause post-translational modifications of collagens, making them more resistant to degradation, which contributes to excessive ECM accumulation and tissue stiffening (Grosche et al., 2018).

1.4.4 Mechanosensors

Various signalling molecules cooperatively orchestrate tissue repair, however the mechanical stimuli in the tissue microenvironment are just as important. During the wound healing process, ECM undergoes temporal changes in composition, architecture, and stiffness (Diller and Tabor, 2022). These topographical and mechanical cues participate in regulation of cell adhesion, migration, proliferation, and intracellular signalling (Diller and Tabor, 2022). To sense the extracellular mechanical stimuli and relay the signal into the intracellular space, fibroblasts employ multiple membrane-bound mechanosensors (Yang and Plotnikov, 2021). These include focal adhesions, mechanically gated ion channels and some g-protein coupled receptors (GPCRs) (Yang and Plotnikov, 2021) (Figure 1.7). These factors can activate downstream effectors, therefore translating the mechanical signal into a biochemical one (Yang and Plotnikov, 2021). In addition, intracellular tension is generated by the actin cytoskeleton and transmitted to the surrounding matrix via focal adhesions, thus allowing two-way mechanical communication between the cells and their environment (Yang and Plotnikov, 2021). Actin fibres also form contacts with lamin proteins within the nuclear envelope, relaying mechanical forces to the nucleus and regulating nuclear transport and chromatin arrangement through changes in the nuclear morphology (Chi et al., 2022) (Figure 1.7).

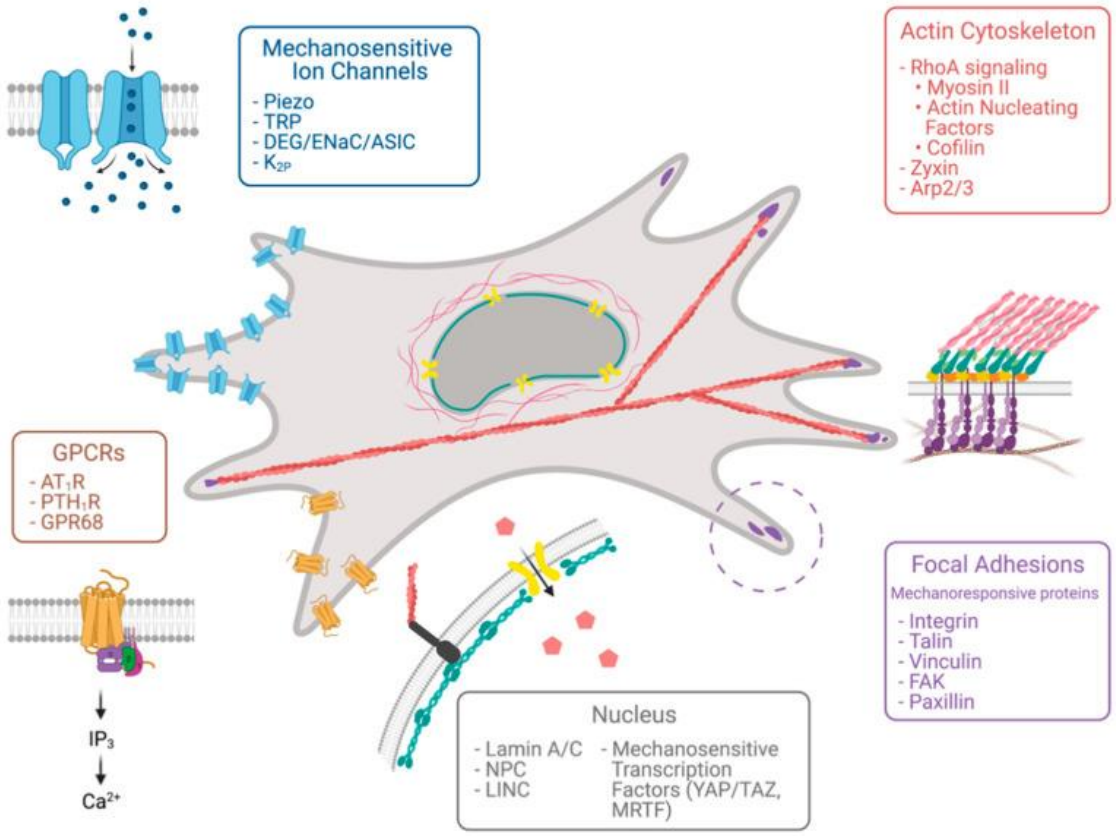

Figure 1.7 Mechanosensors in fibroblasts. Extracellular forces stimulate focal adhesions, g-protein coupled receptors and mechanosensitive ion channels, which relay mechanical information into the interior of the cell. Cells also generate intracellular tension through dynamic actin cytoskeleton. Actin cytoskeleton links the nucleus to focal adhesions, allowing force dependent nuclear deformation, which influences nuclear transport of transcription factors. Adapted from Yang and Plotnikov, 2021.

1.4.4.1 Focal adhesions

Focal adhesions are multiprotein complexes on the cell membrane, which bind the cells to the substrate (Yang and Plotnikov, 2021). The physical attachment to the substrate is mediated by transmembrane proteins integrins, which bind ECM components on the outside of the cells, and actin cytoskeleton fibres on the inside (D'Urso and Kurniawan, 2020). Integrins are inactive in folded conformation and undergo a conformational change into the extended state upon binding ECM proteins (D'Urso and Kurniawan, 2020). Integrin activation allows them to bind adaptors talin and vinculin to form a connection with the actin fibres (D'Urso and Kurniawan, 2020). This initiates integrin clustering and recruitment of other

structural and signalling components, leading to assembly of a mature focal adhesion complex (Sawant et al., 2021). Talin also serves as a mechanosensor, as its conformational state depends on the tension generated when the cytoskeleton pulls on the matrix at the adhesion site (Sawant et al., 2021). Different degrees of tension are required to unfold different binding domains of talin, therefore matrix stiffness and cytoskeletal contractility can influence adhesion composition (Goult et al., 2018).

One of the main signalling components in the focal adhesions is the focal adhesion kinase (FAK) (Zhao et al., 2016). FAK is involved in regulation of actin cytoskeleton dynamics (Iwanicki et al., 2008) and is required for growth factor-induced fibroblast migration (Zhao et al., 2016). FAK expression is upregulated in response to TGFß (Yeung et al., 2021). In turn, FAK contributes to TGFß signalling, as inhibition of FAK has been shown to reduce JNK and ERK activation and α-SMA expression in fibroblasts stimulated with TGFß (Liu et al, 2007, Wong et al., 2011). As fibroblasts remodel the ECM, increasing matrix stiffness allows formation of larger supermature focal adhesions (Hinz, 2007). Formation of the supermature focal adhesions is associated with incorporation of α-SMA into the actin cytoskeleton, leading to highly increased cytoskeleton contractility (Goffin et al., 2006). By exerting contractile forces on the surrounding matrix through the focal adhesions, fibroblasts cause release of active TGFß from LAP-TGFß complex (Buscemi et al., 2011). Paracrine signalling by TGFß then leads to constitutive activation of FAK and further amplification of fibrotic signalling (Mimura, et al., 2005).

1.4.4.2 Mechanosensitive ion channels

Mechanically gated ion channels include Piezo and some of the transient receptor potential (TRP) family members (Karska et al., 2023). Located on the cell membrane, they undergo conformational change in response to membrane deformation, allowing influx of Ca_{2+} into the cell (Karska et al., 2023). TRP family member Transient receptor potential vanilloid 4 (TRPV4) has been reported to promote myofibroblast differentiation in response to substrate stiffness and TGFß treatment, in both lung and dermal fibroblasts (Sharma et al., 2017). Inhibition of

TRPV4 had no effect on SMAD2/3 but substantially reduced activation of Akt, indicating that TRPV4 might potentiate non-canonical TGFβ signalling (Sharma et al., 2017). Actin polymerisation and nuclear localisation of myocardin-related transcription factor-A (MRTF-A), which promotes α-SMA transcription, were also lowered upon TRPV4 inhibition (Sharma et al., 2017, Rahaman et al., 2014). This indicates that TRPV4 is an important regulator of fibroblast phenotype during the wound healing, contributing both to intracellular signalling pathways and actin cytoskeleton dynamics. Two other TRP family members transient receptor potential canonical type 5 (TRPC5) and type 6 (TRPC6) have also been demonstrated to modulate cytoskeleton remodelling and differentially regulate fibroblast migration (Tian et al, 2010). TRPC5 activity was associated with the loss of stress fibres and increased cell motility, while TRPC6 promoted stress fibre formation and reduced migration (Tian et al, 2010). TRPC6 has been reported to be upregulated in response to TGFβ and was required for dermal and cardiac wound healing in mice, as well as for TGFβ-induced myofibroblast differentiation *in vitro* (Davis et al., 2012).

Piezo1 has been demonstrated to be involved in wound healing and regulate keratinocyte behaviour (Holt et al., 2021) but its role in fibroblasts is not well researched. He et al. (2021) reported that Piezo1 was highly upregulated in hypertrophic scar tissue and co-localised with α-SMA, suggesting it may be involved in promoting pro-fibrotic phenotype. Mechanical stretching applied *in vitro* upregulated the expression of Piezo1 in dermal fibroblasts and induced myofibroblast differentiation, as evidenced by increased expression of ECM proteins and α-SMA (He et al., 2021). These effects on fibroblast phenotype were Piezo1 dependent as they were substantially downregulated when Piezo1 was inhibited or knocked down (He et al., 2021). This suggests that Piezo1 may be involved in mechanosensation during aberrant wound healing but the exact mechanisms through which it mediates myofibroblast differentiation are unclear.

1.4.4.3 Mechanosensitive transcriptional coactivators

Yes-associated protein (YAP) and the transcriptional coactivator with PDZ-binding motif (TAZ) are two similar transcription regulators, which can promote expression

of collagen I, α-SMA and CTGF in fibroblasts (Noguchi et al., 2018). YAP/TAZ is phosphorylated on its serine residues by large tumor suppressor gene 1 and 2 (LATS1/2) and sequestered in the cytoplasm or targeted for proteosomal degradation (Noguchi et al., 2018). Dephosphorylation allows it to enter the nucleus and interact with other transcriptional regulators (Noguchi et al., 2018). YAP/TAZ serves as a mechanosensor, as its nuclear translocation increases with substrate stiffness (Liu et al., 2015, Scott et al., 2021). Cell and tissue mechanics influence YAP/TAZ localisation in several ways. First, active FAK in focal adhesions initiates signalling cascades that inactivate LATS1/2, reducing YAP/TAZ phosphorylation (Sabra et al., 2017, Kim et al., 2015). In addition, FAK-mediated cytoskeleton remodelling increases cell contractility, which causes nuclear deformation and changes the shape of nuclear pores, increasing YAP/TAZ import rate (Elosegui-Artola et la., 2017). YAP/TAZ potentiates TGFß-induced expression of pro-fibrotic genes (Nakamura et al., 2021) and focal adhesion components (Nardone et al., 2017), sustaining intracellular tension and myofibroblast phenotype.

MRTF-A is a transcription factor responsive to changes in actin cytoskeleton dynamics (Macarak et al., 2021). It is inactive and localised in the cytoplasm when bound to monomeric actin (Macarak et al., 2021). Increased assembly of fibrous actin through Rho/ROCK pathway reduces monomeric actin availability, releasing active MRTF-A (Velasquez et al., 2013). Active MRTF-A then translocates to the nucleus, where it binds serum response factor (SRF) and regulates transcription of various genes involved in cytoskeleton dynamics, focal adhesion assembly and induction of the myofibroblast phenotype (Macarak et al., 2021). In absence of MRTF-A, fibroblasts do not undergo stiffness-induced myofibroblast differentiation, indicating that MRTF-A is necessary for fibroblast mechanosensation (Huang et al., 2012). Pro-fibrotic gene expression induced by TGFß is also partially abrogated in fibroblasts lacking MRTF-A (Huang et la., 2012). On the other hand, constitutively active MRTF-A promotes the expression of α-SMA and formation of large focal adhesions, even on soft substrates (Huang et al., 2012).

1.4.5 2D and 3D cultures

In *in vitro* cultures, fibroblast phenotype is also affected by the culture geometry. Fibroblasts are commonly cultured as 2D monolayers on tissue culture plastic, where they adopt non-native morphology. *In vivo* or when cultured in 3D substrates, such as hydrogels or scaffolds, fibroblasts form adhesions on all sides of the cell body and display stellate shape (Baker and Chen, 2012). 2D cell culture substrates present only a single surface for the cells to adhere to. This leads to all adhesions being distributed along one side of the cell, causing cells to adopt a flattened polarised morphology (Baker and Chen, 2012). Cell morphology and spatial distribution of adhesions might influence the levels of α -SMA, integrin-β1 expression and YAP/TAZ localisation, as differences in these features were observed between fibroblasts in 2D and 3D cultures with otherwise matching mechanical properties (Smithmyer et al., 2019). In addition, on 2D surfaces the cell proliferation is not spatially restricted unless by presence of other cells (Baker and Chen, 2012). In 3D, the cells must first remodel the surrounding environment to make space for growth or movement (Baker and Chen, 2012). This leads to slower cell spreading and proliferation in 3D cultures compared to 2D (Baker and Chen, 2012, Woodley et al., 2022). Finally, fibroblasts were observed to be less sensitive to certain growth factors, such as PDGF and IL-1, when cultured in 3D compared to 2D monolayers (Woodley et al., 2022). However, common 2D substrates, such as tissue culture plastic or glass, are much more rigid than most biomaterials used for 3D cultures and their stiffness may influence fibroblast phenotype by activating mechanotransduction pathways (Baker and Chen, 2012). For this reason, the specific role of the culture dimensions on the fibroblast phenotype independent of other mechanical properties is currently not well understood (Smithmyer et al., 2019).

1.5 Fibroblast response to vibration

Biomechanical signalling plays an important role in regulating fibroblast behaviour during wound healing and development of fibrotic conditions. Applied mechanical stimuli can therefore be used to intercept the signalling pathways and influence these processes. While the response of cells to mechanical vibration has been most

extensively studied in the context of the bone tissue, a growing body of research indicates that vibration could also be used to manipulate fibroblast phenotype by modulating their migration, proliferation and ECM production (Roberts et al., 2021, Weinheimer-Haus et al., 2014).

Mohammed et al. (20D16) applied vertical vibration with frequenciesD between 100 Hz to 1600 Hz and 9 μm to sub-micrometre displacements to human lung fibroblasts and found that the treatment influenced fibroblast migration. Increased migration distance was observed at 100 Hz, while all higher frequencies decreased it, with the highest frequency resulting in the lowest migration distance (Mohammed et al., 2016). They also observed changes in the cell shape and actin cytoskeleton arrangement in vibration-treated fibroblasts, with more membrane protrusions and higher actin fibre density after the treatment. The morphological changes were frequency-dependent as frequencies up to 400 Hz promoted formation of lamellipodia, while 800 Hz showed increased filopodia and 1600 Hz had equal amount of both membrane features (Mohammed et al., 2016). Horizontal vibration of 11.4 kHz frequency was also reported to influence fibroblast migration with different effects depending on the direction and displacement (Enomoto et al., 2020). In gap closure assay, when applied parallel to the gap, displacements of 200 μm and 600 μm reduced fibroblast migration distance. However, applied orthogonally to the gap, 200 μm displacements increased migration distance, while higher displacements had no effect. Changes to nuclear morphology and orientation were also observed in the group which showed increased migration, potentially indicating cytoskeleton rearrangement in these cells (Enomoto et al., 2020).

Vibration with various parameters has also been demonstrated to influence fibroblast proliferation. Judex and Pongkitwitoon (2018) compared the effects of two vibrational devices on periodontal ligament fibroblasts, one delivering 30 Hz frequency, 0.24 g and around 148 μm vibrations and the other generating 120 Hz, 0.41 g and 12 μm vibrations. They found that treatment with both devices increased fibroblast proliferation, with the higher frequency device having a stronger effect. Higher frequency and acceleration also led to higher increase in mRNA levels of FGF2 and CTGF, while collagen I synthesis was upregulated to a

similar level by both treatments (Judex and Pongkitwitoon, 2018). Jiang et al. (2015) investigated the effects of 10-40 Hz frequency, 0.29-4.60 mm displacement horizontal vibrations with approximately 0.9 g acceleration on anterior ligament fibroblasts. They reported that 10-20 Hz vibration increased fibroblast proliferation after 4 days of treatment, while 40 Hz decreased it. After 10 days, frequencies of 20 Hz and above decreased proliferation, however metabolic activity, measured with 3-(4,5-dimethylthiazol-2-yl)-2,5-diphenyl-2H-tetrazolium bromide (MTT) assay, and cellular stress, measured by lactate dehydrogenase (LDH) assay, were increased in all vibration-treated groups (Jiang et al., 2015). Fibronectin and collagen III expression were also found upregulated in all groups after 10 days (Jiang et al., 2015). Collagen I and elastin expression showed variable results, with collagen I upregulated in all groups except 30 Hz, and elastin increased by 20 Hz and 30 Hz only (Jiang et al., 2015). Out of all parameter sets tested, 20 Hz and 1.22 mm vibration had the strongest effect on ECM protein expression (Jiang et al., 2015). Kutty and Webb (2010) observed similar results on dermal fibroblast proliferation. Fibroblasts were cultured in 3D hydrogels and treated with 100 Hz frequency and 1 mm displacement horizontal vibration. Vibrational treatment decreased cell proliferation after 5 and 10 days of treatment. However, they also found that collagen I and elastin levels were downregulated, while MMP-1 was increased in response to vibration (Kutty and Webb, 2010).

Wolchok et al. (2009) examined how 100 Hz horizontal vibration influences ECM and growth factor production in laryngeal fibroblasts. They used two different culture vessels, which affected displacement and acceleration due to their different mass. In 6-well plates the displacement was measured to be 200 μm and the acceleration was 3.4 g, while in the custom made single-well plates it was 900 μm and 15 g. After 24 h of treatment in the single wells, media levels of TGFβ1 were significantly increased compared to static controls. Gene expression was measured after 3 days of treatment in 6-well plates and showed increase in the MMP inhibitors TIMP1 and TIMP3, collagen I, collagen IX, laminin, CTGF and PDGF. In addition, increased deposition of collagen I and fibronectin was observed in fibroblasts cultured on polyurethane scaffolds and treated in the single wells for 3 days (Wolchok et al., 2009). Hortobagyi et al. (2020) also investigated how

mechanical vibration influences laryngeal fibroblast phenotype but when applied under normal and inflammatory conditions. They applied vertical variable frequency vibration ranging from 50 to 250 Hz, with average displacement of 82 μm, for 3 days. To simulate inflammatory environment, cell culture media was supplemented with 5ng/ml TGFβ1 and IL-1β. They reported that vibration had no effect on the expression of ECM proteins or TGFβ1, neither in normal nor in inflammatory conditions. However, vibration significantly downregulated inflammation-induced α-SMA and IL-11 levels, indicating that the vibrational treatment could reduce pro-fibrotic fibroblast phenotype without negatively affecting ECM protein synthesis (Hortobagyi et al., 2020).

Application of vibrational stimulation *in vivo* has been demonstrated to have parameter-dependent effects. Roberts et al. (2021) investigated the effects of different frequency and acceleration combinations on diabetic wound healing in mice. Using a vibration plate, they applied vibrations with frequencies of 45 and 90 Hz and accelerations of 0.3 and 0.6 g for 30 min every day for 7 days and examined changes in the wound area, collagen deposition and levels of growth factors FGF, VEGF, IGF-1 and PDGF in the wound tissue. Wound closure was enhanced in low frequency – low acceleration group, while both high acceleration groups had a significant negative effect. Combination of low frequency and low acceleration also increased IGF-1 levels in the wound tissue. None of the treatments significantly influenced collagen deposition or levels of other factors. Since this study did not examine individual cell types, the observed effects can not be attributed to fibroblasts specifically. However, this study illustrates the importance of thoughtful selection of the treatment parameters if vibration is to be applied *in vivo*.

1.6 Aims of the thesis

Fibroblasts integrate biochemical and biomechanical stimuli into complex signalling networks to maintain tissue homeostasis and facilitate repair. Disruptions during the wound healing process or exposure to external stimuli can

result in sustained fibroblast activation through positive feedback mechanisms, leading to the development of fibrotic disorders. Studies investigating the effects of vibrational treatment on fibroblasts have demonstrated diverse outcomes depending on various parameters, such as vibration intensity, frequency, duration, and direction of application. These studies have revealed both positive and negative effects on fibroblast migration, proliferation, ECM component synthesis, as well as the regulation of inflammatory and pro-fibrotic factors.

Nanovibrational stimulation has been shown to induce MSC osteogenesis independently of matrix rigidity or biochemical cell fate modulators. This suggests that it could potentially be translated into a mechanotherapy for bone disorders and delayed union fractures, as current treatment options are limited. However, little is known about how it may affect fibroblasts, residing in the soft tissues surrounding the bone. In MSCs, nanovibration has been demonstrated to stimulate focal adhesions and mechanosensitive ion channels, influence cytoskeleton dynamics and activate ERK and Akt signalling pathways, all of which play a role in regulating fibroblast phenotype. Therefore, to evaluate the safety and viability of potential nanovibration-based mechanotherapy, it is important to investigate the effects of nanovibrational stimulation on fibroblast behaviour. Identification of negative effects, such as highly upregulated pro-fibrotic phenotype, can help to define potential risks associated with the treatment. On the other hand, modest upregulation of fibroblast activity or suppression of growth factor induced pro-fibrotic phenotype may indicate potential benefit of nanovibrational stimulation in improving wound healing or treatment of fibrotic disorders.

Therefore, the aims of the work presented in this thesis are:

1. To determine if fibroblasts are sensitive to vertically applied mechanical nanovibration of 1000 Hz frequency, 0.12 g acceleration and 30 nm displacement.

2. To examine the effects of nanovibration on fibroblast features indicative of activation, such as proliferation, contractility, ECM component synthesis and production of inflammatory factors and compare them to the effects of biochemical stimulation with TGFβ1.
3. To compare the effects of nanovibrational stimulation in 2D monolayer and 3D collagen hydrogel cultures, to determine if the effects are consistent between the different cell culture conditions.
4. To investigate the influence of nanovibration on fibroblast metabolome and transcriptome using high-throughput techniques.
5. To identify any synergistic or antagonistic interactions between nanovibration and stimulation with TGFβ1.

Chapter 2: General Materials and Methods

2.1 Cell culture

Human telomerase reverse transcriptase (H-TERT) immortalised human dermal fibroblast cell line BJ-5ta (ATCC, #CRL-4001) was used for all experiments. Fibroblasts were cultured in Dulbecco's modified Eagle's medium (Sigma-Aldrich, #D1145) with 1% penicillin-streptomycin (Sigma-Aldrich, #P0781), 0.05% fungizone (Gibco, #15290-026), 1X non-essential amino acids solution (Sigma-Aldrich, #11140-035), 1 mM sodium pyruvate (Sigma-Aldrich, # #S8636) and 10% fetal bovine serum (FBS, Sigma-Aldrich, #F2442) and incubated at 37°C, 5% CO2.

Cells were detached from cell culture flask using 1X trypsin solution (Sigma-Aldrich, #59427C), centrifuged at 400 g for 5 min and resuspended in culture medium. Cell concentration in suspension was determined using a glass hemocytometer.

Fibroblasts were seeded in cell culture plates at the density of 1000 cells/cm2 and allowed to attach overnight before starting treatment. To induce fibrotic phenotype, 10 µg/ml TGFß-1 (Abcam, # ab50036) was added to cell culture medium.

2.2 3D culture in collagen hydrogels

For 3D experiments, the cells were cultured in bovine type I collagen hydrogels. Each 5 ml of collagen solution (6 mg/ml, Collagen Solutions) was mixed with 500 µl modified Eagle's medium (Sigma-Aldrich, #D2429) in a universal tube. The Solution was neutralised by adding 100 µl 1 M NaOH and gentle mixing until the solution was uniform pink colour. After neutralisation, cell suspension was added to yield final concentration of 40 000 cells/ml. The mixture was distributed to multi-well plates and allowed to undergo gelation at 37°C for 1 h, after which cell culture medium was added to the wells. Cells were allowed to spread overnight before commencing treatment.

2.3 Nanovibrational stimulation

Custom nanovibrational bioreactor (Tsimbouri et al., 2017) was used to stimulate cells with mechanical vibration with 1000 Hz frequency, 0.12 g acceleration and amplitude of approximately 30 nm (Figure 2.1). To couple cell culture plates with nanovibrational bioreactor surface, a magnet sheet was glued to the bottom of multi-well cell culture plates. The cells were stimulated continuously for selected period of time in a 37°C 5% CO2 incubator. Untreated controls were kept in the same incubator but not on the bioreactor.

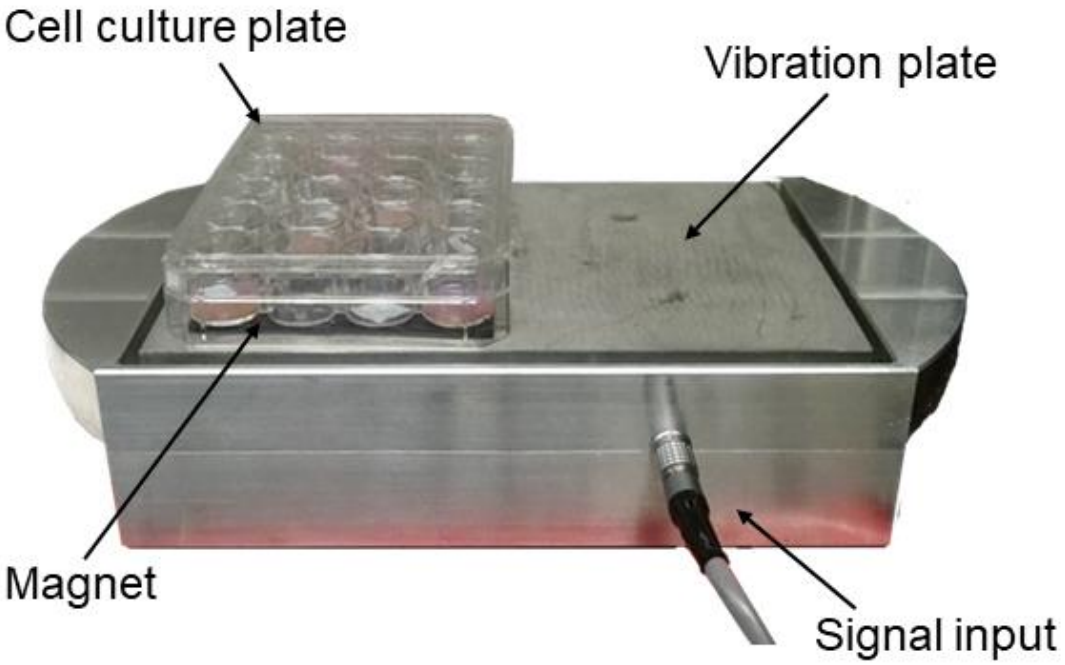

Figure 2.1 Nanovibrational bioreactor with a cell culture plate. Vibration generated by supplying electrical signal to an array of piezo actuators under the vibration plate. To ensure tight coupling between the cell culture plate and the bioreactor surface, a magnetic sheet was glued to the bottom of the well plate.

2.4 In-Cell Western

Samples were fixed using 4% formaldehyde (90ml PBS, 10ml 40% formaldehyde, 2g sucrose) solution for 15 min at 37°C, followed by permeabilization with 0.5% Triton-X (Thermo Fischer Scientific, #A16046.AE, 100 ml PBS, 0.292 g NaCl, 0.06 g MgCl2•6H2O, 0.476 g HEPES, 10.3 g sucrose, 0.5 ml Triton-X) for 4 min at 4°C.

Afterwards samples were incubated 1% milk on an orbital shaker for 1 h in room temperature. After blocking, primary antibodies diluted to working concentration (Table 2.1) in 1% milk were added to samples and samples were incubated on an orbital shaker at 4˚C overnight. After incubation primary antibody solution was removed and the samples were washed with 0.1% Tween-20 (Sigma-Aldrich, #P1379) in PBS three times for 5 min on an orbital shaker. Secondary IRdye 800CW conjugated antibodies against selected species (LI-COR) 1:800 and CellTag700 (LI-COR, #926-41090) 1:1000 were diluted in 1% milk. If investigating protein phosphorylation, 680RD conjugate was used for total protein and 800CW conjugate for phospho-protein. Samples were incubated with secondary antibodies for 1 h at room temperature on an orbital shaker and washed 3 times with 0.1% Tween-20 three times for 5 min. Plates were dried before imaging. List of primary and secondary antibodies is provided in table 2.1.

Near-infrared fluorescence readings were taken using Odyssey-SA system (LI-COR), 700 nm and 800 nm channels and ratio of readings (800 nm/700 nm) was calculated as relative fluorescence intensity indicative of protein levels in the sample.

Table 2.1 Primary and secondary antibodies used for in-cell western.

Antibody	Host species	Company (#Catalogue)	Working concentration
Anti-CaSR	Rabbit	Abcam (#ab137408)	0.94 µg/ml
Anti-Col1A1	Mouse	Cell Signalling Technology (#66948S)	0.25 µg/ml
Anti-Col3A1	Rabbit	Cell Signalling Technology (#66887)	0.5 µg/ml
Anti- αSMA	Rabbit	Abcam (#ab5694)	2 µg/ml
Anti-ERK1/2	Mouse	Cell Signalling Technology (#4696S)	2.51 µg/ml
Anti-phospho-ERK1/2	Rabbit	Cell Signalling Technology (#9101S)	1.91 µg/ml
Anti-Jnk	Rabbit	Cell Signalling Technology (#9252S)	0.41 µg/ml
Anti-phospho-Jnk	Mouse	Cell Signalling Technology (#9255S)	5.91 µg/ml
Anti-Akt	Mouse	Cell Signalling Technology (#2920S)	0.27 µg/ml
Anti-phospho-Akt	Rabbit	Cell Signalling Technology (#9271S)	0.1 µg/ml
Anti-mouse IgG 680RD	Goat	LI-COR (#926-68070)	1:800 (1.25 µg/ml)
Anti-mouse IgG 800CW	Goat	LI-COR (#926-32210)	1:800 (1.25 µg/ml)
Anti-rabbit IgG 680RD	Goat	LI-COR (#926-68071)	1:800 (1.25 µg/ml)
Anti-rabbit IgG 800CW	Goat	LI-COR (#926-32211)	1:800 (1.25 µg/ml)

2.5 RNA extraction

RNA extraction was performed using Qiagen RNeasy Micro kit (#74004). For 2D cultures, the cells were lysed by adding 350 µl of RTL lysis buffer. The lysates were stored in -80°C if not processed immediately. The extraction procedure was done according to the protocol provided by manufacturer.

For 3D samples, the gels were homogenised with a Pasteur pipette and mixed with equal volume of Trizol reagent (Thermo Fisher, #15596026). Then 0.2 ml of chloroform was added for every 1 ml of Trizol, samples were incubated for 3 min and centrifuged at 15 000 g for 15 min at 4°C. Aqueous phase was collected into a fresh 1.5 ml tube and equal volume of RTL buffer was added. The following procedure was performed using Qiagen RNeasy Micro kit according to manufacturer's protocol.

RNA concentration and purity were measured using NanoDrop 2000c (Thermo Fisher Scientific).

2.6 Statistical analysis

Statistical analysis was performed with GraphPad prism 8 software or rstatix package in R. Data collected from several independent experimental repeats was analysed using two-factor analysis of variance (ANOVA) followed by Tukey post-hoc test. When the data was collected from one experimental repeat, comparisons of more than two groups were performed using one-factor ANOVA. To determine whether the data fits ANOVA model assumptions, diagnostic plots were generated and assessed visually. Variance was assessed by plotting residuals versus fitted values and quantile-quantile (Q-Q) plots were used to assess normality. In certain cases where the data was found to be largely non-normal, it was log2 transformed and these cases are pointed out in the figure legends of the corresponding graphs. In other cases, non-normally distributed data was analysed using Kruskall-Wallis test followed by Wilcoxon pairwise rank sum test. In cases where only two groups were compared, Wilcoxon-Mann-Whitney test was used to assess significance. Details of statistical tests used to determine significance as well as the number of

samples and experimental repeats are indicated in the figure legends. Results were considered statistically significant when $p < 0.05$, unless stated otherwise. In cases where more specific statistical analysis methods were applied (e.g. RNA-Seq), details of the analysis are provided in the materials and methods section of the corresponding chapters.

Chapter 3: Indications of Fibroblast Activation in Response to Nanovibration

3.1 Introduction

Fibroblasts are the most abundant cell type in the connective tissues and play a crucial role in maintaining tissue homeostasis and remodelling based on physiological demands (Li and Wang, 2011). They are responsible for the production and maintenance of the ECM, which provides structural support to the surrounding cells (Kendall and Feghali-Bostwick, 2014). In addition, they play a vital role in the healing of injured tissues (Li and Wang, 2011, Kendall and Feghali-Bostwick, 2014). Integration of biomechanical signals from their environment is vital for this function. Therefore, fibroblasts are mechanically sensitive and have been shown to respond to matrix stiffness (El-Mohri et al., 2017), surface topography (Berry et al., 2005, Lei et al., 2020), shear stress (Lei et al., 2020, Gupta et al., 2020), static and dynamic stretching (Dai et al., 2022) and vibration (Mohammed et al., 2016, Weinheimer-Haus, 2014) among other biomechanical stimuli.

In response to injury, fibroblasts undergo differentiation into an activated phenotype, changing into myofibroblasts (Li and Wang, 2011). This activated phenotype is marked by increased proliferation (Darby et al., 2014), generation of α-SMA containing stress fibres, which confer cytoskeleton contractility (D'Urso and Kurniawan, 2020), and deposition of ECM components, such as collagen and fibronectin (Li and Wang, 2011). Fibroblast activation in the wound environment is triggered by signalling molecules, such as growth factors TGFβ1 and PDGF (Juhl et al., 2020), and inflammatory cytokines, like IL-13, IL-11 and IL-6 (Kendall and Feghali-Bostwick, 2014, Juhl et al., 2020). Exposure to these molecules induces endogenous synthesis of pro-fibrotic and pro-inflammatory molecules in fibroblasts, which then act in paracrine and autocrine manner to maintain the activated phenotype (Wei et al., 2021, Moretti et al., 2022) until the wound healing process is resolved.

While fibroblast activation is necessary for tissue repair and wound healing, excessive or prolonged activation can result in pathological conditions (Darby et al., 2014). Aberrant fibroblast proliferation, contractility and sustained pro-inflammatory signalling can result in development of fibrotic diseases, which are characterized by excessive deposition of ECM and impaired tissue function (Kendall and Feghali-Bostwick, 2014).

TGFβ1 is the most well studied pro-fibrotic growth factor and a major contributor to the activated fibroblast phenotype (Walton et al., 2017). Under the baseline conditions, TGFβ1 is produced in a complex with latency associated peptide (LAP), which prevents immediate binding to the receptors (Hinz, 2015). LAP-TGFβ1 complex is deposited by fibroblasts and other cell types into the surrounding ECM (Hinz, 2015). When a tissue injury occurs, TGFβ1 released from the immune cells drives upregulation of α-SMA and formation of contractile stress fibres in fibroblasts (D'Urso and Kurniawan, 2020). As highly contractile fibroblasts exert force on the surrounding ECM, TGFβ1 is released from the latent complex, which leads to positive feedback loop of TGFβ1 signalling (Hinz, 2015). In addition to α-SMA induction, TGFβ1 has wide ranging effects on fibroblasts, including upregulation of ECM proteins (Klingberg et al., 2014), growth factors and cytokines (Frangogiannis, 2020), induction of ROS generation (Dosoki et al., 2017) and metabolic reprogramming (Yin et al., 2019). Latent TGFβ1 activation by cell contraction illustrates how interlinked biochemical and biomechanical signals are in regulating fibroblast phenotype.

Nanovibrational stimulation has been demonstrated to be a strong inducer of osteogenic differentiation in MSCs and has potential to be applied as non-invasive mechanotherapy for osteoporosis and delayed fracture healing (Robertson et al., 2018). When applied to the body exterior, nanovibration would propagate through the soft tissues surrounding the target site and potentially stimulate cells in those tissues, including fibroblasts. Previous studies investigating the effects of mechanical vibration on fibroblasts have identified both positive and negative effects on proliferation (Jiang et al., 2014, Jones et al., 2001, Holmes et al., 2018), migration (Mohammed et al., 2016), ECM protein expression (Jiang et al., 2014, Wolchok et al., 2009) and endogenous TGFβ1 synthesis (Hortobagyi et al.,

2020, Wolchok et al., 2009). Considering a variety of vibrational devices and treatment parameters used, it is difficult to predict how nanoscale vibration of 1000 Hz and 30 nm may influence the fibroblast phenotype.

This chapter aims to examine the effect of nanovibrational stimulation on fibroblasts, specifically in terms of features indicating the activated phenotype. Cellular functions such as proliferation and contraction were investigated, as well as production of α-SMA and collagens type III and type I. In addition, mRNA levels of TGFß1, IL-6 and OPN were assessed by qPCR. After the first set of experiments, TGFß1-stimulated samples were included in the analysis to assess how nanovibration treatment compares to biochemically induced fibroblast activation. Alongside the standard 2D culture on tissue culture plastic, for some experiments the fibroblasts were cultured in 3D collagen type-I hydrogels, which more closely mimic their environment in vivo (Smithmyer et al., 2014).

3.2 Materials and Methods

3.2.1 Laser interferometry – vibrometry

To confirm vibration transmission through various plasticware and collagen gels, and to measure the vibration amplitude, laser interferometry was used. A magnetic sheet was glued to the bottom of the well plates to couple them with bioreactor surface. A small piece of reflective tape was placed on every measured material – several points on the bioreactor surface, bottom of cell culture plate wells and on the top of collagen gels. The measurements were taken using laserinterferometric vibrometer SP-S (SIOS Meßtechnik GmbH), by aiming the laser at the reflective material on the measured surface. Light interference pattern captured by the detector was processed with INFAS software (SIOS Meßtechnik GmbH) to obtain displacement readings.

3.2.2 3D culture in rat-tail collagen I

Rat-tail collagen type-I solution (2.05 mg/ml) in 0.16% acetic acid (First Link UK, #60-30-810) was aliquoted into a pre-cooled universal tube. For every 2.5 ml of

collagen solution, 1.5 ml 0.1 NaOH was added with gentle mixing. In a separate tube, x10 DMEM (Sigma-Aldrich, #D2429) and FBS (Sigma-Aldrich, #F2442) were mixed at a ratio 1:1. While keeping on ice, 500 µl of DMEM-FBS mixture were added to collagen tube and mixed gently by swirling the tube until the solution was homogenous in colour. Then, further 1.5 ml of NaOH were added to the collagen by mixing, until the solution reached pink colour indicating neutralisation. A cell pellet containing pre-counted number of cells was resuspended in the collagen to a concentration of 40 000 cells/ml. Gel mixture with cells was then divided into the well plate and placed in 37°C for 30 min to undergo gelation. After the gels were formed, cell culture medium was added on top.

3.3.3 AlamarBlue assay for cell proliferation

AlamarBlue reagent (Bio-Rad Laboratories, #BUF012B) was used to investigate cell proliferation. Cell culture medium was completely removed from testing wells. AlamarBlue reagent was mixed with filtered cell culture medium in 1:10 ratio and added to each test well and one empty well as a negative control. Samples were incubated at 37°C for 4 hours. After incubation period 100 µl was collected in duplicates from each sample and loaded into 96 well plate. Absorbance was measured using MultiscanFC absorbance reader (Thermo Scientific) at 570 nm and 600 nm. AlamarBlue reduction was calculated using the equation provided in manufacture's protocol:

$$\%\ Alamar\ reduction = \frac{(O2\ x\ A1) - (O1\ x\ A2)}{(R1\ x\ N2) - (R2\ x\ N1)}\ x\ 100$$

Where O1 and O2 are molar extinction coefficients of oxidised alamarBlue at 570 nm and 600 nm respectively, R1 and R2 are molar extinction coefficients of reduced alamarBlue at 570 nm and 600 nm, A1 and A2 are absorbance readings of test wells at 570 nm and 600 nm and N1 and N2 are absorbance readings of negative control well.

AlamarBlue assay was performed on the same samples after 3 and 7 days in culture. Difference in % alamar reduction between paired measurements was calculated, representing the change in cell number for each well between two time points.

3.3.4 Rat-tail collagen I contraction assay

Cells were cultured in T-25 flasks under basal conditions or treated with vibration or TGFß1 for 7 days. Then they were detached from the flasks using trypsin, centrifuged and re-suspended in fresh media. The cells were counted to determine cell concentration in each suspension and volumes of suspension containing 250 000 and 500 000 cells were aliquoted and centrifuged again to form a pellet. Rat-tail collagen-I was prepared as detailed in 3.3.2 and each pellet was re-suspended in 1 ml of collagen. From each suspension, 200 µl was transferred into 96-well plate four times, resulting in four replicate wells per group. Collagen without cells was also added to the plate, as a negative control. The gels were allowed to fully undergo gelation at 37°C for 30min and cell culture medium was added to each well. Images of the plate were taken every day for 7 days using LI-COR SA imaging system. Percentage of the well area covered by gel was measured using image-J.

3.3.5 Quantitative polymerase chain reaction (qPCR)

RNA was extracted as detailed in chapter 2.5. After measuring the initial concentration, RNA concentration was adjusted to 5 ng/µl with RNAse-free water. Reverse transcription was performed using QuanTiTect Reverse Transcription Kit (Qiagen, #205313) according to protocol provided by manufacturer. After reverse transcription cDNA was stored at -20°C. QPCR was performed using QuantiNova SYBR Green qPCR kit (Qiagen, #208252) in Applied Biosystems 7500 RealTime PCR System (Thermo Fisher Scientific) including a melt curve stage in the process for amplification quality control. Data was analysed using the delta-delta Ct method, using the average Ct of two housekeeping genes (GAPDH and RLP13A) for normalisation. Primer pairs used in the qPCR reactions are shown in table 3.1.

Table 3.1 Primer pair sequences used for qPCR

Target	Sequence	Binding position 5' (transcript variant)	Product length
GAPDH forward	5'- TCAAGGCTGAGAACGGGA -3'	255(1), 356(2), 347(3), 495(4), 201(7)	376 bp
GAPDH reverse	5'- TGGGTGGCAGTGATGGCA -3'	630(1), 731(2), 722(3), 722(4), 630(5), 576(7)	
RLP13A forward	5'-CTCAAAGGTGTTTGACCGCATCC-3'	325(1), 249(2)	144 bp
RLP13A reverse	5'-TACTTCCAGCCAACCTCGTGA-3'	468(1), 392(2)	
COL1A1 forward	5'- CCATGTGAAATTGTCTCCCA -3'	4635	253 bp
COL1A1 reverse	5'- GGGGCAAGACAGTGATTGAA-3'	4383	
ACTA2 forward	5'-CCCTGAAGTACCCGATAGAACA-3'	625(1), 269(2), 542(3), 700(4), 783(5), 414(6), 625(11)	95 pb
ACTA2 reverse	5'-GGCAACACGAAGCTCATTG-3'	719(1), 363(2), 636(3), 794(4), 877(5), 508(6), 719(11)	
OPN forward	5'-AGCTGGATGACCAGAGTGCT-3'	787(1), 745(2), 706(3), 664(4), 976(5)	151 bp
OPN reverse	5'-TGAAATTCATGCCTGTGGAA-3'	937(1), 856(2), 856(3), 814(4), 1126(5)	
IL-6 forward	5'-AGACAGCCACTCACCTCTTCAG-3'	193(1), 124(3)	132 bp
IL-6 reverse	5'-TTCTGCCAGTGCCTCTTTGCTG-3'	324(1), 255(3)	
TGFβ1 forward	5'-ACTACTACGCCAAGGAGGTCAC-3'	1183	73 bp
TGFβ1 reverse	5'-TGCTTGAACTTGTCATAGATTTCG-3'	1255	

3.3 Results

3.3.1 Selection of collagen hydrogel and interferometry

First, two kinds of collagen type-I hydrogels were compared in their ability to support fibroblast growth in 3D culture. Fibroblasts were cultured for 7 days in either rat-tail collagen-I or bovine collagen-I hydrogels and cell proliferation was measured as percent of alamarBlue reagent reduction on days 3 and 7. It was observed that fibroblasts in rat-tail collagen type-I proliferated faster between the two time points than those cultured in bovine collagen type-I (Figure 3.1 a). However, there was higher variation in proliferation measurements in the rat-tail

collagen group, suggesting that bovine collagen offers more replicability. Considering that bovine collagen hydrogels were easier to handle, offered more replicable results and that the difference in proliferation between the two cultures was small, bovine collagen type-I was selected for 3D fibroblast cultures for all future experiments.

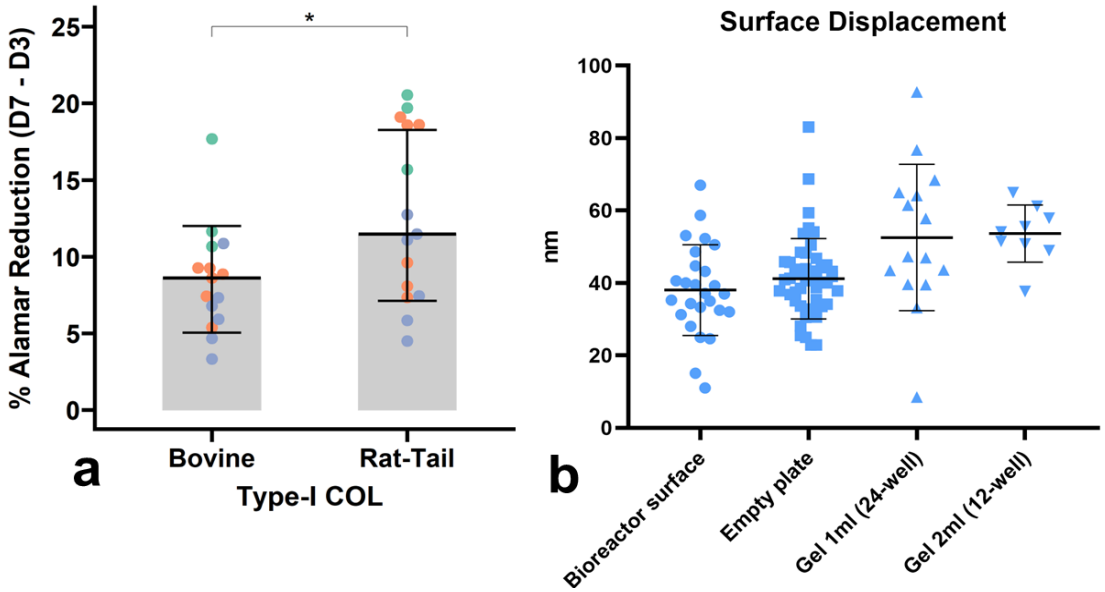

Figure 3.1 a) Comparison of alamarBlue reduction in bovine and rat-tail collagen type-I hydrogels. The cells were seeded at concentration of 40 000 cells/ml and alamarBlue reduction was measured on days 3 and 7. The difference between paired measurement values are shown as indication of cell proliferation between two time points. The bars indicate median with SD. Statistical analysis was done by Wilcoxon-Mann-Whitney test, * = $p < 0.05$. Data collected from three independent repeats, each dot representing a single sample and different repeats represented by colour, n = 15 in each group. b) Surface displacement was measured on top of bioreactor surface, empty well plate and two volumes of collagen hydrogels. Bars indicate mean with SD.

To confirm that the nanovibration from the bioreactor is efficiently transmitted to the cultureware and through the collagen hydrogels, surface displacement amplitude was measured using laser interferometry (Figure 3.1 b). Previous studies using this nanovibrational stimulation system reported that vibration of 1000 Hz frequency causes approximately 30 nm displacements (Tsimbouri et al., 2017). Measured amplitude was slightly higher on all tested surfaces, with average of 38 nm on the bioreactor surface and 42 nm on the bottom of a well-plate. Small deviations from the expected value might have been caused by the noise in the environment as the measurement system is highly sensitive. When measuring amplitude on top of the collagen hydrogels, it was observed that the amplitude increased to around 50 nm but was not dependent on the volume of collagen. This

suggests that collagen hydrogel did amplify the vibration amplitude to a small extent, however, all measurements were under 100 nm, and the average amplitude was close to the average bioreactor surface vibration amplitude, indicating that the difference is unlikely to be of practical concern.

3.3.2 The effects of nanovibration on fibroblast proliferation

Next, the effects of nanovibrational stimulation on fibroblast proliferation were investigated using alamarBlue assay. Utilising the same experimental design as in comparison of rat-tail and bovine collagen type-I hydrogels detailed above, the measurements of alamarBlue reduction were taken at days 3 and 7 and the difference between two time points was used as an indication of proliferation rate in this period. It was observed that in the 2D culture, nanovibration increased alamarBlue reduction around 5% (Figure 3.2 a) while in the 3D culture it led to a 2% decrease (Figure 3.2 b).

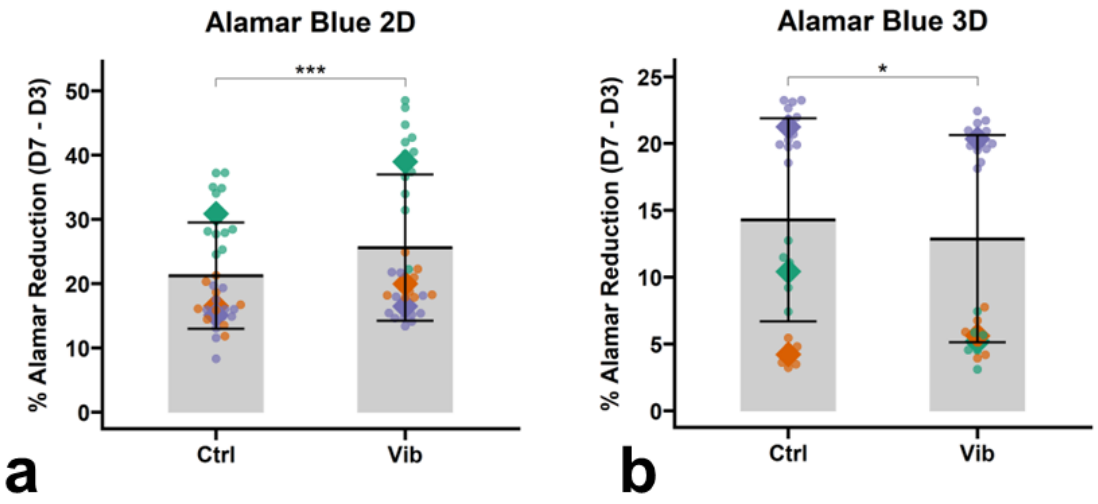

Figure 3.2 AlamarBlue reduction in 2D (a) and 3D (b) in nanovibration treated cells (vib) and untreated controls (ctrl). The cells were seeded at concentration of 40 000 cells/ml and alamarBlue reduction was measured on days 3 and 7. The difference between paired measurement values are shown as indication of cell proliferation between two time points. Data from three independent repeats, each dot representing a single sample and repeats represented by colour, with rectangles indicating mean for each repeat. Statistical analysis was done by two-factor Anova. * = $p < 0.05$, *** = $p < 0.001$. N = 33 in (a), n = 24 in (b).

Previous studies demonstrated that nanovibrational stimulation modulates the levels of membrane ion channels in MSCs (Tsimbouri et al., 2017), indicating that calcium signalling is involved in mechanosensation of nanovibration. To investigate if calcium signalling may be involved in the response to nanovibration in

fibroblasts, the levels of CaSR were measured using in-cell western. CaSR protein was upregulated in the nanovibration treated group after 7 days (Figure 3.3 a). CaSR has been previously demonstrated to activate ERK1/2 signalling pathway (Davies et al., 2006, Tomlins et al., 2005), which is a major regulator of cell growth and proliferation. The level of active phospho-ERK1/2 was measured in nanovibration-treated cells after 7 days in 2D culture and was found to be increased compared to the untreated controls (Figure 3.3 b).

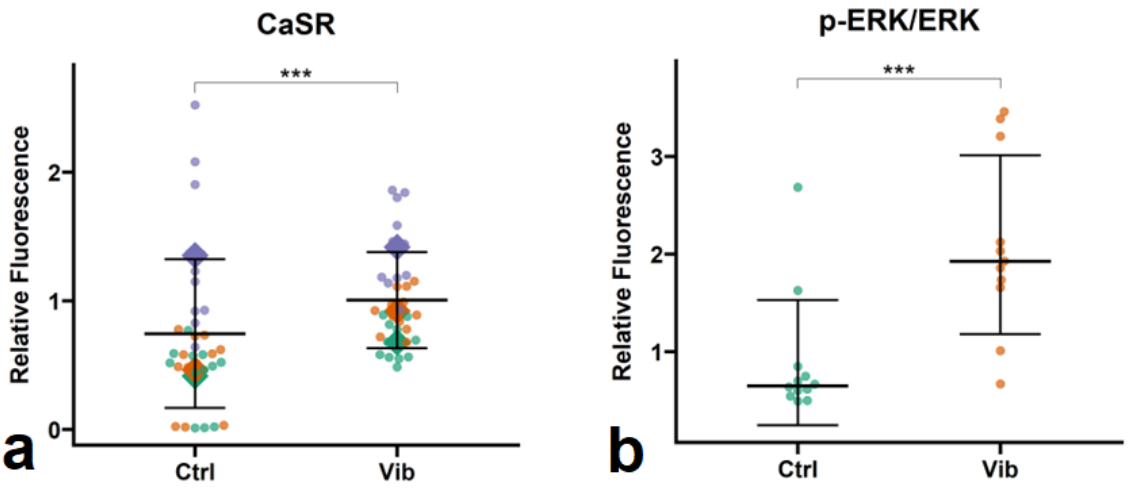

Figure 3.3 a) Levels of CaSR protein measured by in-cell western after 7 days of nanovibrational treatment in 2D cultures. b) Ratio of phosho-ERK to total ERK measured by in-cell wester after 7 days of nanovibrational treatment in 2D cultures. The bars indicate mean (a) and median (b) with SD. Statistical analysis was done by two-factor Anova (a) and Wilcoxon-Mann-Whitney test (b), *** = p < 0.001. Data from three independent repeats, each dot representing a single sample and repeats represented by colour, rectangular shape indicating group mean each repetition. N = 36 in a, n = 12 in b.

3.3.3 Collagen gel contraction

The activated fibroblast phenotype is characterized by high contractility (Li and Wang, 2011). To investigate whether nanovibrational stimulation affects fibroblast contractility, a collagen gel contraction assay was performed. To compare the effects of nanovibrational treatment with those of biochemical fibroblast activation, one group of samples was treated with TGFß1. Fibroblasts in 2D culture were subjected to nanovibrational stimulation or 10ng/ml TGFß1 for 7 days and then transferred to rat-tail collagen-I hydrogels at two cell concentrations (250 000 cells/ml and 500 000 cells/ml). Images of the well-plate were captured every day for 7 days and well area covered by collagen hydrogel was measured.

At lower cell concentration, nanovibration-treated fibroblasts contracted the gel at a similar rate as untreated controls (Figure 3.4 a). Both groups started to show decrease in the gel area by day 5 and reduced the area to 42% in the nanovibration group and 33% in the untreated group by day 7. In contrast, TGFß1-treated fibroblasts started to contract the gels by day 3 and reduced the gel area to 13% by the end of the observation period. Similar results were observed in the higher cell concentration experiment, as both nanovibration-stimulated samples and untreated controls first showed contraction on day 3, while the TGFß1 group exhibited substantial contraction on day 2 (Figure 3.4 b). These results indicate that nanovibrational treatment does not upregulate fibroblast contractility.

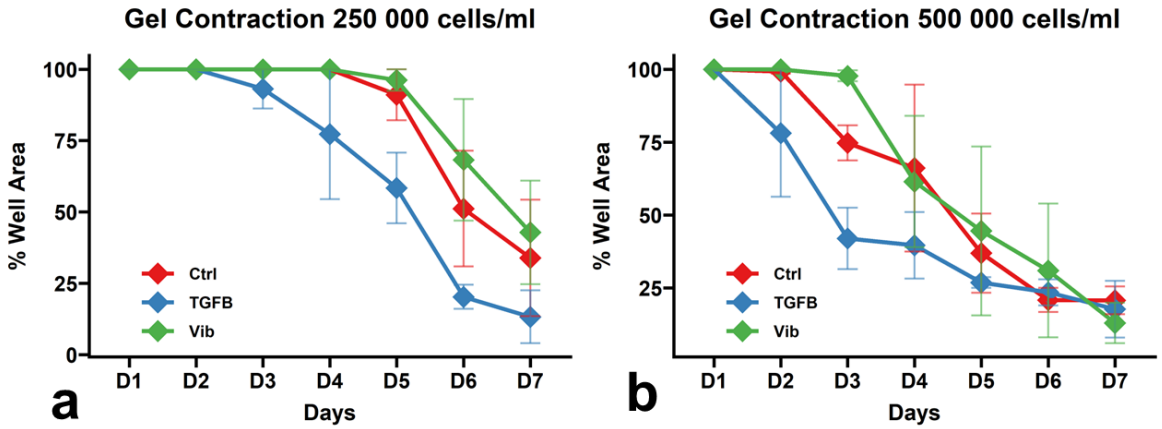

Figure 3.4 Collagen gel contraction assay. Fibroblasts were treated with nanovibrational stimulation (vib) or 10 ng/ml TGFβ1 for 7 days and transferred to rat-tail collagen-1 gels at 250 000 cells/ml (a) and 500 000 cells/ml (b). Gels were imaged every day for 7 days and well area covered by the gel was measured using imageJ. N = 3 for control (ctrl) and vib, n = 2 for TGFβ.

3.3.4 Expression of α-SMA, COL1A1 and COL3A in nanovibration treated fibroblasts

As mentioned above, increased contractility is a feature of activated fibroblast phenotype and is achieved by production and incorporation of α-SMA into the actin cytoskeleton (D'Urso and Kurniawan, 2020). Another major feature of the activated phenotype is upregulated synthesis of ECM proteins, particularly collagen type I and type III, which are critical for wound healing but can lead to fibrosis when excessive (Klingberg et al., 2014). To investigate the impact of nanovibrational stimulation on the synthesis of α-SMA, COL1A1 and COL3A1, in-cell western analysis was performed after 3, 7 and 10 days of treatment.

The results showed that α-SMA protein levels were significantly increased in the nanovibration treated groups after 3 days of stimulation, regardless of the presence of TGFβ1 (Figure 3.5 a). This effect was short-term, as all groups displayed similar α-SMA protein levels on day 7 (Figure 3.5 b). On day 10, both TGFβ1-stimulated groups showed upregulated α-SMA but the difference was not statistically significant, likely due to large variation of values in the untreated control group (Figure 3.5 c).

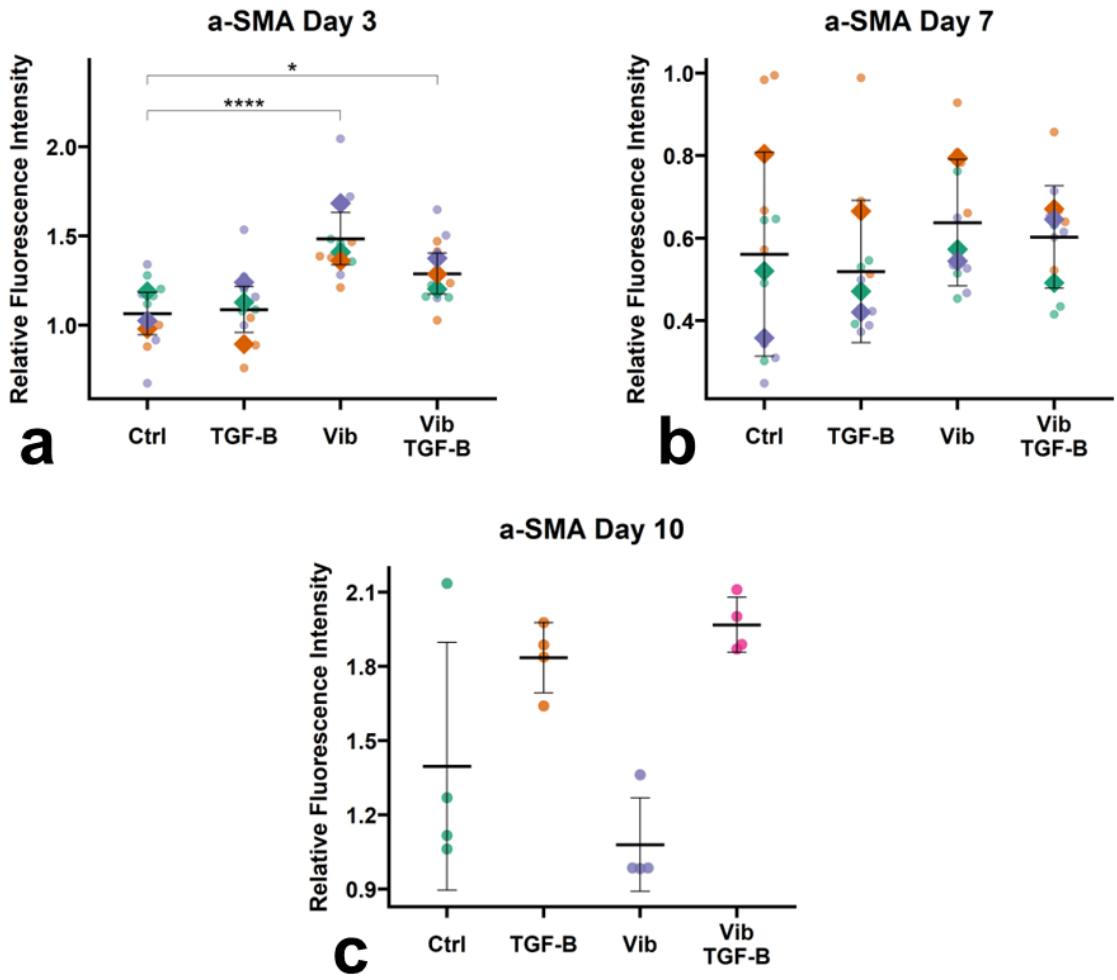

Figure 3.5 In-cell western analysis of α-SMA protein levels. Fibroblasts were treated with nanovibration, TGFβ1 or both in 2D culture for a) 3, b) 7 and c) 10 days. Bars indicate mean with SD. Statistical analysis was conducted using two-factor ANOVA followed by Tukey post-hoc test, except in c, where Kruskall-Wallis test followed by Wilcoxon pairwise rank sum test was performed. Data from 3 independent repeats represented by colour, except in c where data from one repeat is shown. Each dot represents a single sample, rectangular shapes indicate group means in each repetition. N=12 per group (a) and (b), n = 4 per group in (c). * = $p < 0.05$, *** = $p < 0.001$.

COL3A1 was consistently upregulated by TGFβ1 at all time points, regardless of nanovibrational treatment (Figure 3.6 a, b, c). COL1A1 protein levels were similar

across all groups on day 3 (Figure 3.6 d) but was upregulated in TGFß1 treated samples on days 7 and 10 (Figure 3.6 e, f). These results indicate that nanovibrational stimulation causes a short-term increase in α-SMA production, but the effect is not sustained over a longer period of time. Furthermore, the synthesis of COL3A1 and COL1A1 is not significantly affected by nanovibration in either basal or TGFß1 stimulated conditions.

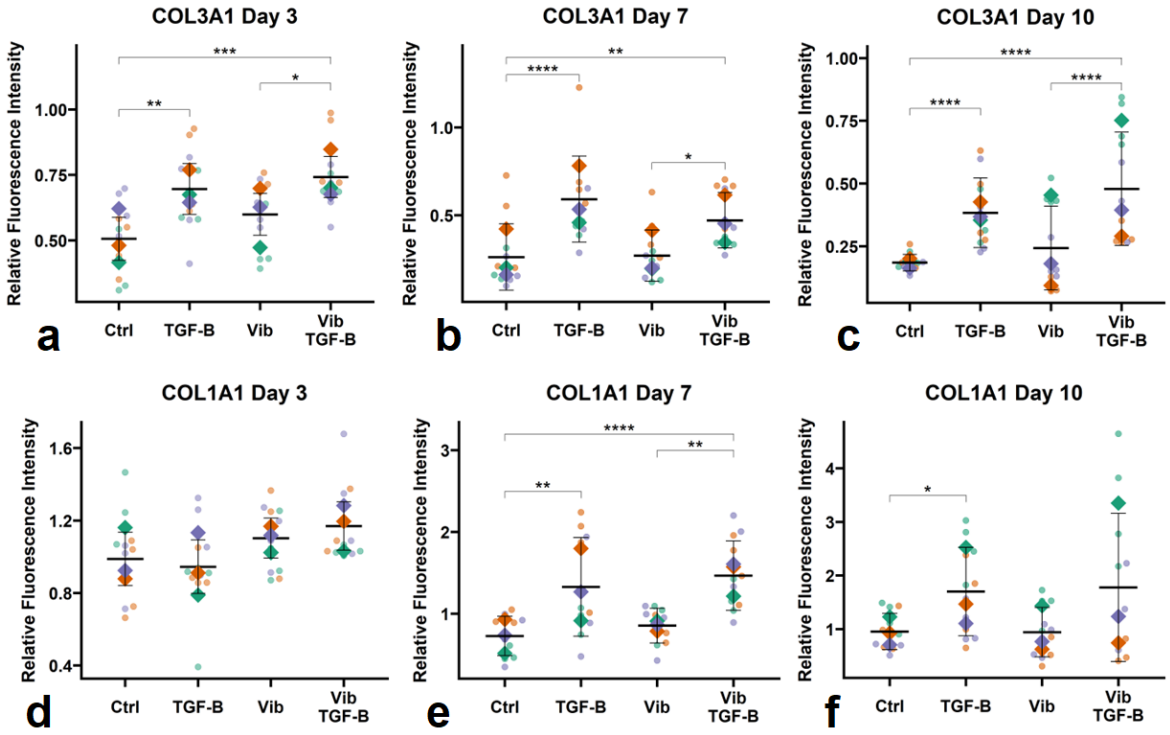

Figure 3.6 In-cell western analysis COL3A1 (a, b, c) and COL1A1 (d, e, f). Fibroblasts were treated with nanovibration, TGFβ1 or both in 2D culture for 3, 7 and 10 days. Bars indicate mean with SD. Statistical analysis was conducted using two-factor ANOVA followed by Tukey post-hoc test. In (c) and (f) statistical analysis was performed on log2 transformed data to fit ANOVA model assumptions. Data from 3 independent repeats represented by colour, each dot representing a single sample. Rectangular shape indicates group mean in each repetition. N=12 per group in all panels. * = p < 0.05, ** = p < 0.01, *** = p < 0.001.

To support the data collected from in-cell western experiments and investigate the effects of nanovibrational stimulation on gene transcription, qPCR was performed. Day 7 time point was selected for further analysis and the mRNA levels of α-SMA and COL1A1 were assessed. Gene transcript levels of α-SMA were upregulated in fibroblasts stimulated with TGFß1 but the result was only statistically significant in the group that received both TGFß1 and nanovibrational stimulation (Figure 3.7 a). This result was consistent with increased α-SMA protein

levels in both TGFß1 stimulated groups on day 10 (Figure 3.5 c), as there is a delay between gene transcription and protein accumulation.

COL1A1 mRNA increased after TGFß1 treatment, while the nanovibration-treated group showed downregulation of this gene, however neither result was statistically significant (Figure 3.7 a). Interestingly, the sample group that received both treatments showed mRNA levels comparable to the untreated controls, suggesting that nanovibration potentially abrogated the induction of COL1A1 by TGFß1. Nonetheless, it is challenging to draw conclusions since none of the changes observed in this experiment were statistically significant and the COL1A1 protein levels observed on day 10 were inconsistent between repeats for the dual treatment group (Figure 3.6 f).

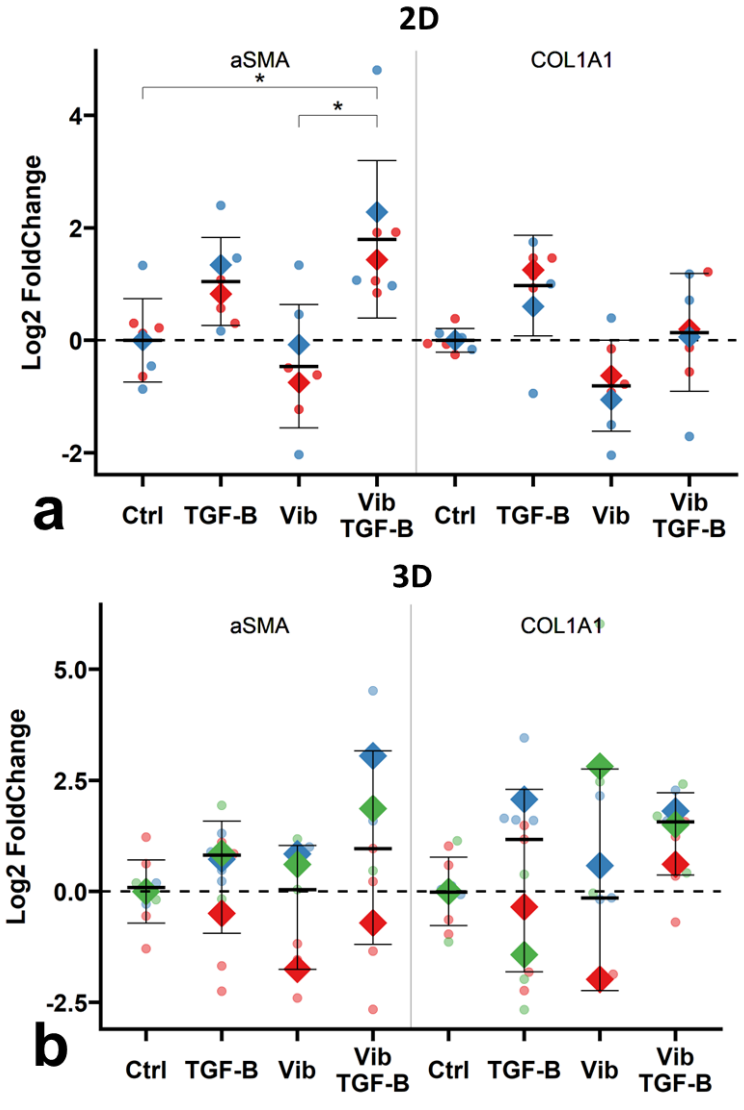

Figure 3.7 Gene expression of α-SMA and COL1A1 in fibroblasts treated with nanovibration, TGFβ1 or both for 7 days in 2D (a) and 3D (b) cultures.

Bars indicate mean with SD. Statistical analysis was conducted using two-factor ANOVA followed by Tukey post-hoc test. 2D data collected from two independent repeats with n = 7 in each group, 3D data collected from 3 independent repeats with n = 11 in each group. Different repeats indicated by colour, each dot representing a single sample and rectangles mark group mean in each repetition. * = p < 0.05

To investigate if nanovibration affects gene expression in a similar way when cultured in 3D, fibroblasts suspended in bovine collagen hydrogels were subjected to the same treatments for a period of 7 days and mRNA levels of α-SMA and COL1A1 were measured using qPCR. While none of the results were statistically significant, it was observed that there was a trend towards increased expression levels of both COL1A1 and α-SMA in the dual treatment group (Figure 3.7 b). It should be noted that there was some inconsistency in the data for α-SMA gene between the different experimental repeats in this group, as it was upregulated in two repeats and downregulated in one, therefore further analysis is necessary to clarify the results. In conclusion, these findings suggest that nanovibration might potentiate TGFβ1 signalling, inducing α-SMA gene expression in both 2D and 3D cultures, but further investigation is needed to confirm this effect. COL1A1 gene expression was not significantly affected by any of the treatments in both types of culture, however, in 2D nanovibration seemed to have a slight suppressive effect, while in 3D, it slightly and not significantly upregulated this gene when delivered in combination with TGFβ1.

3.3.5 Pro-fibrotic cytokine expression in nanovibration treated fibroblasts

Gene transcript levels of pro-fibrotic cytokines IL-6, OPN and TGFβ1 were also examined in 2D and 3D fibroblast cultures. In 2D, the results showed that TGFβ1 slightly upregulated the expression of IL-6 and OPN, however not to a statistically significant degree (Figure 3.8 a). In contrast, nanovibration suppressed the expression of both IL-6 and OPN, although the effect on IL-6 was not statistically significant when compared to the control group (Figure 3.8 a). While the amount IL-6 mRNA in the group, stimulated with both nanovibration and TGFβ1, was similar to TGFβ1-only group, expression of OPN in the combined treatment group was more comparable to the untreated controls (Figure 3.8 a), suggesting that nanovibration might supress the expression of OPN but not IL-6 in pro-fibrotic conditions. However, further experiments are needed to confirm this effect. The expression of TGFβ1 did not change significantly in any of the treated groups and there was a large variation in sample values between the two repeats.

In 3D, neither nanovibration nor TGFß1 alone had a significant impact on the expression of the genes examined (Figure 3.8 b). However, in combination these treatments upregulated mRNA levels of OPN and TGFß1. Although a slight increase in IL-6 mRNA was also observed in this group, this result was not statistically significant (Figure 3.8 b). Overall, these results indicate that nanovibration might have a negative effect on pro-fibrotic factor expression in 2D, but in 3D, it may act synergistically with TGFß1 to upregulate it.

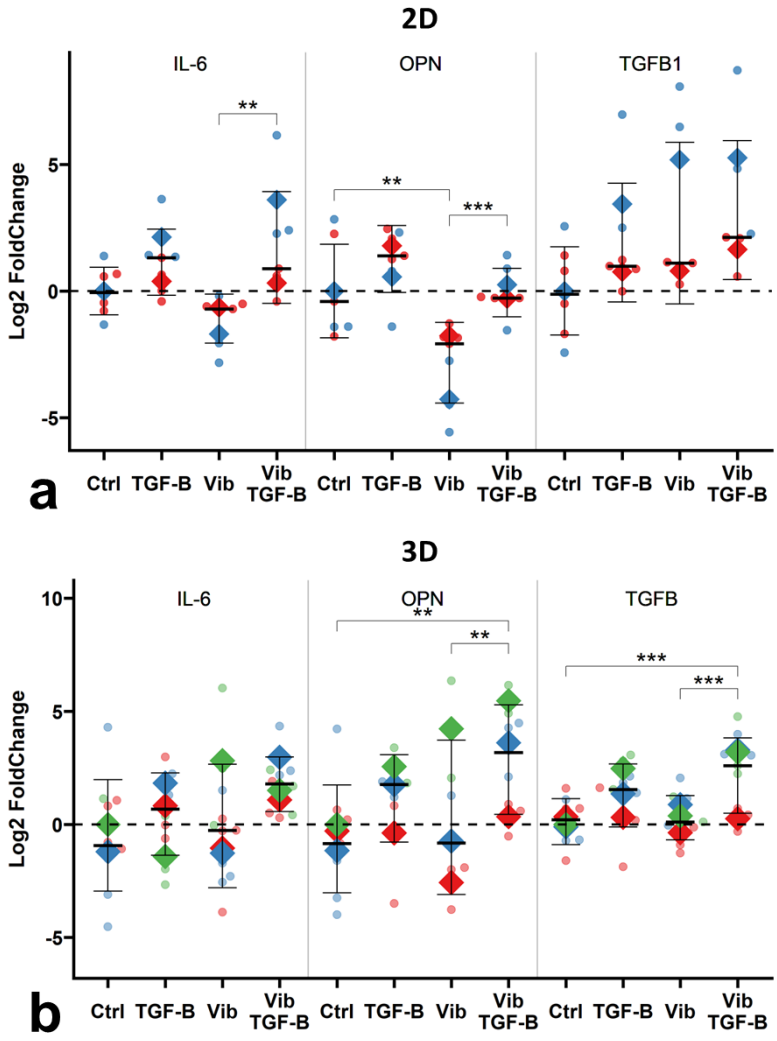

Figure 3.8 Gene expression of IL-6, OPN and TGFβ1 in fibroblasts treated with nanovibration, TGFβ1 or both for 7 days in 2D (a) and 3D (b) cultures.

Bars indicate mean with SD. Statistical analysis was conducted using two-factor ANOVA followed by Tukey post-hoc test, except in 2D TGFβ1 data, where Kruskall-Wallis test was used. 2D data collected from two independent repeats with n = 7 in each group, 3D data collected from 3 independent repeats with n = 11 in each group. Different repeats indicated by colour, each dot represents a single sample and rectangles mark group mean in each repetition. * = p < 0.05, ** = p < 0.01, *** = p < 0.001

3.4 Discussion

In this chapter, the effects of nanovibrational stimulation on fibroblast phenotype were investigated, with focus on phenotypic features associated with wound healing and fibrosis. When tissue is in a steady state, resident fibroblasts

proliferate infrequently and synthesize moderate amounts of ECM proteins (Franklin, 2021). In response to tissue injury, platelets and immune cells at the wound site secrete factors which stimulate fibroblast activation, marked by increased proliferation, migration, cell contractility and production of high levels of ECM proteins (Kimura and Tsuji, 2021).

Mechanical cues are important in regulation of activation and clearance after the resolution of the wound healing (Kollmannsberger et al., 2018). ECM architecture and rigidity are the key determinants of tissue tensile forces and have been shown to serve as signals to promote maintenance or exit from the activated state (Kollmannsberger et al., 2018, Hinz, 2015). Passive mechanical stimuli, such as substrate stiffness (Huang et al., 2012), and active mechanical stimuli, such as cyclic stretching (Walker et al., 2020), have been shown to sustain the activated phenotype even in the absence of continuous stimulation with TGFß1. Dysregulation of mechanical signalling pathways can lead to tissue stiffening, chronic inflammation and even support tumour development (Cox and Erler, 2011). Therefore, investigating how fibroblasts respond to nanovibrational stimulation is crucial to determine its viability as a non-invasive mechanotherapy for bone disorders.

Previous studies on fibroblast response to vibration revealed diverse effects on fibroblast phenotype, depending on vibrational device, stimulation parameters and treatment duration. Horizontal vibration of ligament fibroblasts at 10-40 Hz frequencies and 0.29–4.6 mm amplitudes has been shown to upregulate ECM protein synthesis and have frequency-dependent effects on proliferation (Jiang et al., 2014). Similarly, Wolchok et al. (2009) demonstrated that horizontal vibration with 100Hz frequency and amplitude of 0.2 mm applied in stimulation-rest cycles upregulated collagen type-I and pro-fibrotic cytokine synthesis in vocal fold fibroblasts. On the other hand, very high frequency (165 kHz) sub-micrometer horizontal vibration was shown to have a negative effect on fibroblast proliferation and adhesion (Holmes et al., 2018). Hortobagyi et al. (2020) applied vertical vibrational stimulation in a 50-250 Hz frequency range and average amplitude of 82 µm and found that such treatment did downregulate some inflammatory and pro-fibrotic factors but did not substantially alter ECM protein

synthesis in vocal fold fibroblasts. Mohammed et al. (2016) tested a range of frequencies from 100 Hz to 1600 Hz at 0.4 g magnitude and observed that 100 Hz promoted fibroblast migration, while higher frequencies reduced it. In their study, none of the tested frequencies significantly affected cell viability. In vivo, 45 Hz vibration at 0.3 g or 0.4 g acceleration led to faster wound healing and promoted angiogenesis in diabetic mice and rats (Weinheimer-Haus et al., 2014, Roberts et al., 2021) while 90 Hz and 0.6 g was detrimental for wound closure. These studies illustrate that different vibration parameters and stimulation regimes have different and even opposing outcomes, therefore it is hard to extrapolate their results to predict the response to nanovibrational stimulation specifically.

When applied to fibroblasts cultured in 2D, nanovibration slightly upregulated fibroblast proliferation. Consistent with increased proliferation, higher levels of phosphorylated ERK1/2 were observed in the nanovibration-treated fibroblasts. ERK1/2 is a kinase within classical MAPK signalling pathway, which is a key regulator of cell cycle progression and cell proliferation in mammalian cells (Zhang and Liu, 2002), including fibroblasts (Bentov et al., 2014). One way in which classical MAPK signalling cascade is initiated is through activation of receptor tyrosine kinases, such as epidermal growth factor receptor (EGFR), which can occur via ligand binding or transactivation by other membrane receptors (Zhang and Liu, 2002). CaSR has been demonstrated to regulate cell proliferation by transactivation of EGFR and downstream phosphorylation of ERK1/2 (Tomlins et al., 2005). It would be intriguing to see if that occurs in response to nanovibrational stimulation, as CaSR was upregulated in stimulated fibroblasts. Interestingly, cation signalling has been implicated in response to nanovibration in MSCs (Tsimbouri et al., 2017), where inhibition of TRPV1 ion channel led to downregulation of ERK1/2. Since TRPV1 is generally selective for calcium (Zhai et al., 2021), this suggests that calcium-dependent signalling plays an important role in mechanosensation and response to nanovibrational stimulus in at least two different cell types.

Nanovibration applied to 2D cultures did induce short-term upregulation of α-SMA protein, which confers cytoskeletal contractility, however, after 7 days of treatment, this effect was no longer present. This short-term upregulation did not

influence fibroblast contractile ability after 7 days of treatment, as they contracted the collagen hydrogel at a similar rate to the untreated controls, while TGFβ1-treated group showed faster contraction. Although the TGFβ1-treated group showed increased contractile ability, protein or mRNA levels of α-SMA were not significantly changed at the 7-day time point, suggesting that the contraction might have been mediated by other factors, such as secretion of MMPs (Daniels et al., 2003) or expression of specific integrins (Gutierrez et al., 2015), which were not examined in this work. Combination of TGFβ1 and nanovibration did upregulate α-SMA transcript levels after 7 days of treatment more strongly than TGFβ1 alone, but this was not reflected in the protein levels. Further experiments are needed to determine if nanovibration and TGFβ1 might be acting synergistically in upregulating α-SMA in 2D.

As expected, in TGFβ1-treated 2D cultures, COL3A1 was significantly upregulated by day 3, and COL1A1 was upregulated by day 7, which is consistent with the expression patterns in the wound healing process (Klingberg et al., 2013). Nanovibration did not seem to have an effect on the expression of these proteins, neither in basal nor in TGFβ1-stimulated conditions. Nanovibration did influence the expression of OPN and IL-6, though the latter was not statistically significant. IL-6 is an inflammatory cytokine with a proven role in fibrotic diseases (Juhl et al., 2020). Similarly, elevated OPN levels have been observed in fibrotic skin lesions in systemic sclerosis patients (Wu et al., 2012), however, its exact role in promoting fibrosis is less well understood. Mori et al. (2008) demonstrated that knockdown of OPN had a positive outcome on wound healing, leading to reduced inflammation and less scarring. Nanovibration seemed to suppress OPN, even in the presence of TGFβ1, though further investigation is needed to confirm this result as the effect was not significant.

In 3D cultures, nanovibration affected the fibroblast phenotype differently than in 2D. Proliferation was slightly reduced in vibrationally stimulated cells. None of the tested genes were significantly affected by nanovibration on its own; however, the results were quite inconsistent between the different repeats, especially for COL1A1 and OPN. Notably, the combination of TGFβ1 and nanovibration significantly increased mRNA levels of pro-fibrotic factors TGFβ and OPN. IL-6 and

COL1A1 mRNA levels were also upregulated by the combination of treatments but not significantly. This suggests that in 3D, TGFß and nanovibration could be working synergistically to upregulate inflammatory and pro-fibrotic signalling. More studies over a longer period of time are needed to clarify how this might affect the wound healing process and resolution.

3.5 Conclusions

In this chapter, fibroblast response to nanoscale vibrational stimulation of 1000 Hz frequency and approximately 30 nm displacement was examined, with the treatment delivered continuously over selected periods of time up to 10 days. The findings indicate that the effects of nanovibration on the fibroblast phenotype depend on the culture conditions. Overall, fibroblasts treated with nanovibration alone did not show signs of the activated phenotype in 2D or 3D. Cell proliferation was affected in both types of culture, however, to a small degree. In 2D cultures, nanovibration did reduce OPN mRNA synthesis but did not alter COL1A1 or COL3A1 protein expression, which may have a positive effect on wound healing by reducing inflammation while maintaining ECM synthesis. When fibroblast activation was induced using TGFß1, there were some indications of nanovibration having a synergistic effect in promoting the activated phenotype, especially in 3D cultures, where a significant upregulation of endogenous TGFß1 and OPN expression were observed. This suggests that while nanovibrational treatment is most likely safe to apply to patients with healthy soft tissues, it may not be appropriate for patients with actively healing soft tissue injuries, keloid scars, or fibrotic diseases, such as systemic sclerosis.

Chapter 4: The effects of nanovibration on the fibroblast metabolome and transcriptome

4.1 Introduction

In the previous chapter some of the features associated with fibroblast activation, such as proliferation, contractility and production of ECM proteins and cytokines, were investigated. While nanovibration on its own did not induce activation or have a strong anti-fibrotic effect, it did influence cell proliferation and expression of several factors, which indicates that fibroblasts are sensitive to nanovibrational stimulation. To capture a wider range of the effects that nanovibrational treatment may have on fibroblasts, it can be beneficial to employ high-throughput techniques, commonly referred to as 'omics'. These techniques allow for the simultaneous analysis of many cellular components, such as gene transcripts or metabolites, providing a more global view of cellular responses to a treatment (Everaet et al., 2017, Lu et al., 2018).

RNA-Sequencing (RNA-Seq) is a high-throughput technique that allows quantification of gene transcripts present in the cell, comprising the transcriptome. Unlike other techniques targeting gene transcripts, such as qPCR or microarrays, RNA-Seq does not require prior identification of genes of interest and provides unbiased view of transcriptome composition (Everaert et al., 2017). This makes RNA-Seq a good strategy to explore cellular responses to a treatment where little is known about its potential effects.

Metabolites are products of numerous enzymatic reactions occurring in the cells and are governed by a variety of factors that influence those reactions, such as enzyme abundance and activity, availability of precursors and presence of inhibitors, among others (Wishart, 2019). Because of this, the metabolome is very sensitive to environmental stimuli and intracellular events. Changes in metabolite levels reflect underlying biological processes, for example, renal fibroblasts stimulated with TGFβ1 show reduced levels of acetyl-COA and increased lactate production, which is indicative of a metabolic shift towards glycolysis (Hewitson and Smith, 2021). This not only allows faster adenosine triphosphate (ATP)

production in the activated fibroblasts (Hewitson and Smith, 2021) but also generates metabolic intermediates, which enter the glycine synthesis pathway to sustain upregulated collagen production (Nigdelioglu et al., 2016). Liquid chromatography-mass spectrometry (LC-MS) is a powerful technique that can detect and quantify numerous metabolites at once, capturing a snapshot of cellular metabolome (Lu et al., 2018) and providing information about cellular pathways affected by a treatment, such as nanovibrational stimulation.

This chapter aims to expand on the previous investigations on the effects of nanovibrational stimulation in fibroblasts by utilising LC-MS based metabolomics and RNA-Seq. Metabolite analysis examined how the effects differ when stimulation is applied for 7 and 14 days, and between 2D and 3D cultures. The group which showed the most pronounced metabolic changes after the nanovibrational treatment was then further investigated using RNA-Seq, alongside TGFβ1-treated fibroblasts for comparison.

4.2 Materials and Methods

4.2.1 Metabolite extraction

Samples were treated with nanovibration for 7 or 14 days in 2D and 3D cultures. Control samples were kept in the same incubator at 37°C but did not receive stimulation. After the treatment period, cell culture medium was removed from the sample wells, and collagen gels were homogenised using a Pasteur pipette. Pre-cooled (-20°C) metabolite extraction solution (chloroform, methanol and water ratio 1:3:1) was added to sample wells (800 µl for 2D, 1.5 ml for 3D). The plates were placed on an orbital shaker for 1h at 4°C. Afterwards, the liquid was collected into 1.5ml microcentrifuge tubes and centrifuged at 13 000 g for 10min at 4°C. Supernatant was collected into a new microcentrifuge tube. For 3D samples this procedure was repeated twice. Metabolite extracts were stored at -70°C.

4.2.2 Liquid chromatography-mass spectrometry and data analysis

Liquid chromatography-mass spectrometry was performed by Glasgow Polyomics using Dionex UltiMate 3000 RSLC liquid chromatography system (Thermo Fisher Scientific) with a ZIC-pHILIC column (150 mm × 4.6 mm, 5 µm column, Merck Sequant) and Orbitrap Fusion mass spectrometer (Thermo Fisher Scientific). Data was processed using IDEOM MS Excel interface (Creek et al., 2012). Further analysis was performed using Metaboanalyst (Xia et al., 2009), Omu (Tiffany and Baumler, 2019) package in R and Ingenuity Pathway analysis software (Qiagen). P values adjusted for multiple testing were obtained by two-sample t-test with Benjamini-Hochberg correction.

4.2.3 RNA library preparation and sequencing

RNA was extracted using QIAGEN RNeasy micro kit (#74004) following manufacturer's instructions. The experiment was repeated three times and each time three technical replicates from every group were pooled in equal proportions by drawing a volume containing 500 µg total RNA from each replicate. Protein coding mRNA was enriched using poly-A tail selection. Paired-end sequencing with read length of 100 bp and read depth of 30 million reads was performed on NextSeq2000 system (Illumina).

4.2.4 RNA Sequencing data analysis

RNA-Seq reads were aligned to human genome using HISAT2 software (Kim et al., 2019) and feature counts were obtained using Rsubread R package (Liao et al., 2013). A differential expression table was generated with DESeq2 (Love et al., 2014) R package. The initial analysis indicated presence of the batch effect, as the samples clustered together by experimental repeat rather than treatment condition (Figure 4.1 a). To eliminate the batch effect, raw counts table was processed using ComBat-seq (Zhang et al., 2020) R package prior to differential expression analysis (Figure 4.1 b). Over-representation analysis (ORA) was performed using ClusterProfiler R package (Wu et al., 2021).

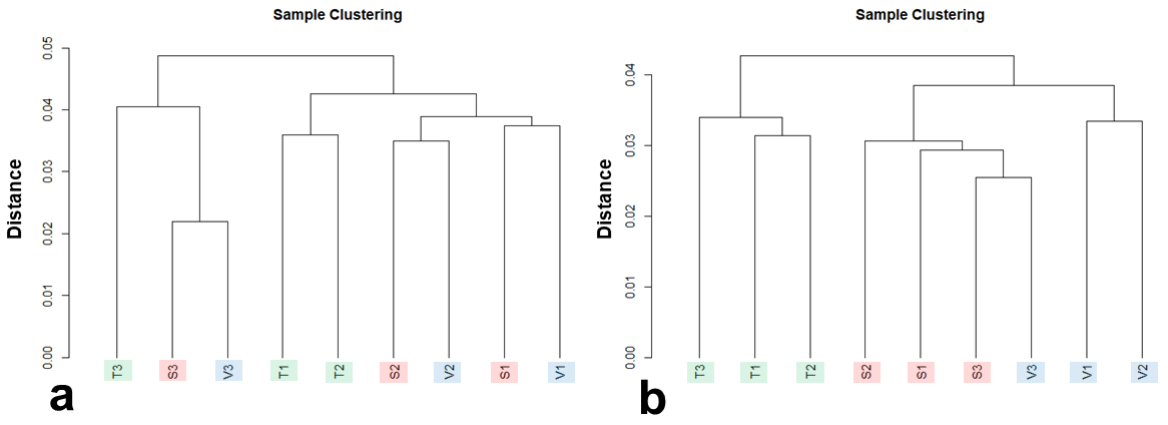

Figure 4.1 Hierarchical clustering analysis of RNA-seq samples a) before and b) after batch effect correction with ComBat-seq. Distance calculated based on Spearman rank correlation. Before batch effect correction, samples cluster based on experimental repeat. After batch correction, samples (except for V3) cluster together by treatment. S – control, V – nanovibration, T – TGFβ1.

4.3 Results

4.3.1 LC-MS metabolomics analysis

To investigate how nanovibrational stimulation affects the fibroblast metabolome, fibroblasts were stimulated in 2D and 3D cultures for 7 and 14 days, and metabolites were extracted for LC-MS analysis. In 2D extractions, a total of 470 metabolites were identified. Principal component analysis (PCA) of the 2D culture metabolites showed that samples treated for 14 days shifted in a positive direction along PC1 compared to 7 days, and nanovibration-treated samples were shifted in a negative direction along PC2 compared to control samples (Figure 4.2 a). This indicated that both nano-vibrational treatment and the time in culture influenced fibroblast metabolome in 2D. Nanovibration-treated samples appeared to be more affected by the treatment on day 7 than on day 14. However, two samples in the day 7 treatment group clustered close to the control group, suggesting that the effects were slightly inconsistent at this timepoint (Figure 4.2 a).

Out of 470 metabolites identified in 2D, levels of 115 and 75 were significantly affected (p adjusted < 0.2) by nanovibrational stimulation on day 7 and on day 14 respectively. The effects of nanovibrational treatment were subtle, as the majority of significantly affected metabolites showed less than two-fold change at both timepoints (Figure 4.2 c and d). Among the significantly changed

metabolites, the most affected was glutathione (GSH), which showed nearly 9-fold increase in nanovibration-treated group after 7 days of treatment (Figure 4.2 b).

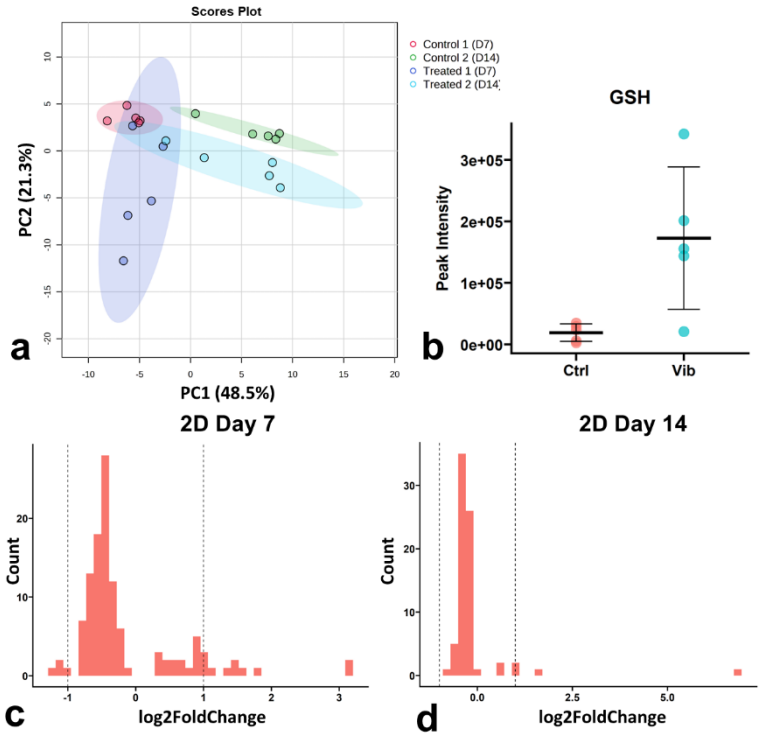

Figure 4.2 a) PCA plot with 95% confidence ellipses showing PC1 and PC2 of metabolite samples collected from 2D cultures.

b) Glutathione levels in fibroblasts treated with nanovibration for 7 days in 2D cultures (vib) and controls (ctrl). Bars indicate mean with SD.

c) Histogram of log2 fold change values of differentially expressed metabolites in 2D cultures on day 7. Dashed lines indicate 1 and -1 equal to two-fold change.

d) Histogram of log2 fold change values of differentially expressed metabolites on day 14.

Significantly affected metabolites were selected for over-representation analysis (ORA) using KEGG pathway database. ORA evaluates if features mapped to certain biological pathways occur more frequently than expected by chance. On day 7, the top 12 enriched pathways were related to amino acid metabolism, t-RNA synthesis, glycerophospholipid and glycerolipid metabolism, glyoxylate and dicarboxylate metabolism and vitamin B6 (Figure 4.3 a). Many of the significantly affected metabolites were lipids which were not mapped to any KEGG pathways and excluded from ORA. Therefore, lipids, including those which were not significantly altered, were plotted in a heatmap to get additional insights into how they might have been affected by nanovibrational stimulation (Figure 4.3 b). Among lipids showing a trend towards downregulation fatty acyls (FA) were the most common, while trending towards upregulation were mostly phospholipids (PC, PE).

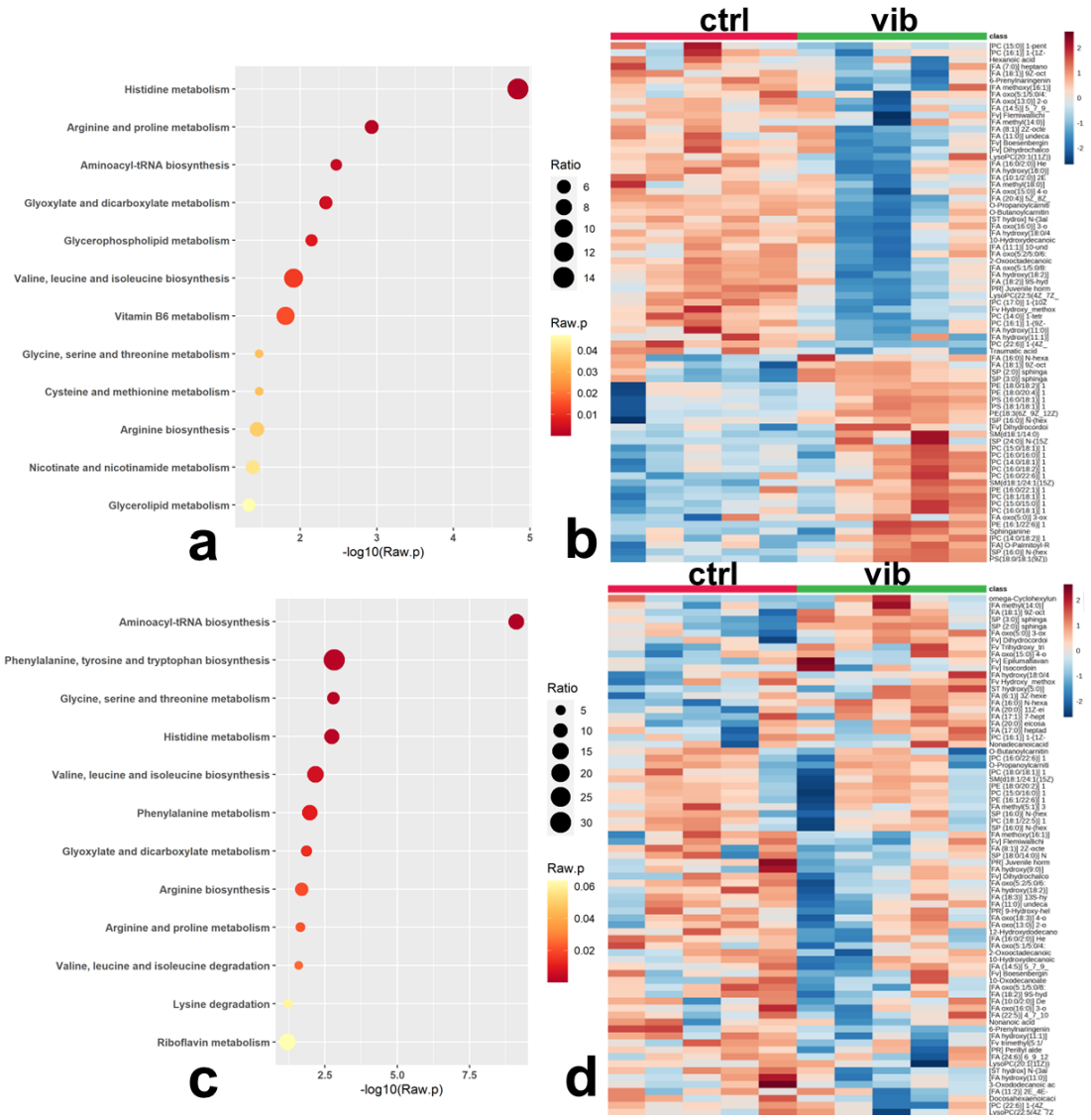

Figure 4.3 a) Overrepresentation analysis of differentially expressed metabolites in 2D on day 7 and c) on day 14. On day 7, amino acid and lipid metabolic pathways were found to be affected by nanovibrational treatment. On day 14 amino acid metabolic pathways were affected by nanovibrational treatment, but not lipid metabolism. T-RNA synthesis pathway was affected at both time points. Ratio is calculated as metabolites detected/ metabolites expected. Metabolic pathways from KEGG database. b) Heatmap of top 70 lipids (by t-test p-value) on day 7 and d) day 14. Patterns of lipid up- and downregulation can be observed on day 7, however they are no longer apparent on day 14. Heatmap colours indicate z-score calculated individually for every feature.

Similarly, on day 14 over-represented pathways were mostly related to amino acid metabolism, however, lipid metabolism was not as affected (Figure 4.3 c). This was further confirmed by a lipid heatmap, which did not show any clear trends in lipid regulation (4.3 d).

In 3D samples, a total of 773 metabolites were identified. Metabolite levels were much more affected by the time in culture than nanovibrational stimulation

(Figure 4.4 a) as samples from the same timepoint clustered close together on the PCA plot independent of treatment. Only one metabolite was significantly affected (p adjusted < 0.2) on day 7 and none on day 14. Since in 2D, lipid levels were influenced by nanovibration, lipid heatmap was generated for 3D samples treated for 7 days (Figure 4.4 b). The heatmap showed a group of lipids that trended towards downregulation and small group, which trended towards upregulation in nanovibration-treated samples, indicating that nanovibration may affect lipid metabolism in 3D but not to the same extent as in 2D.

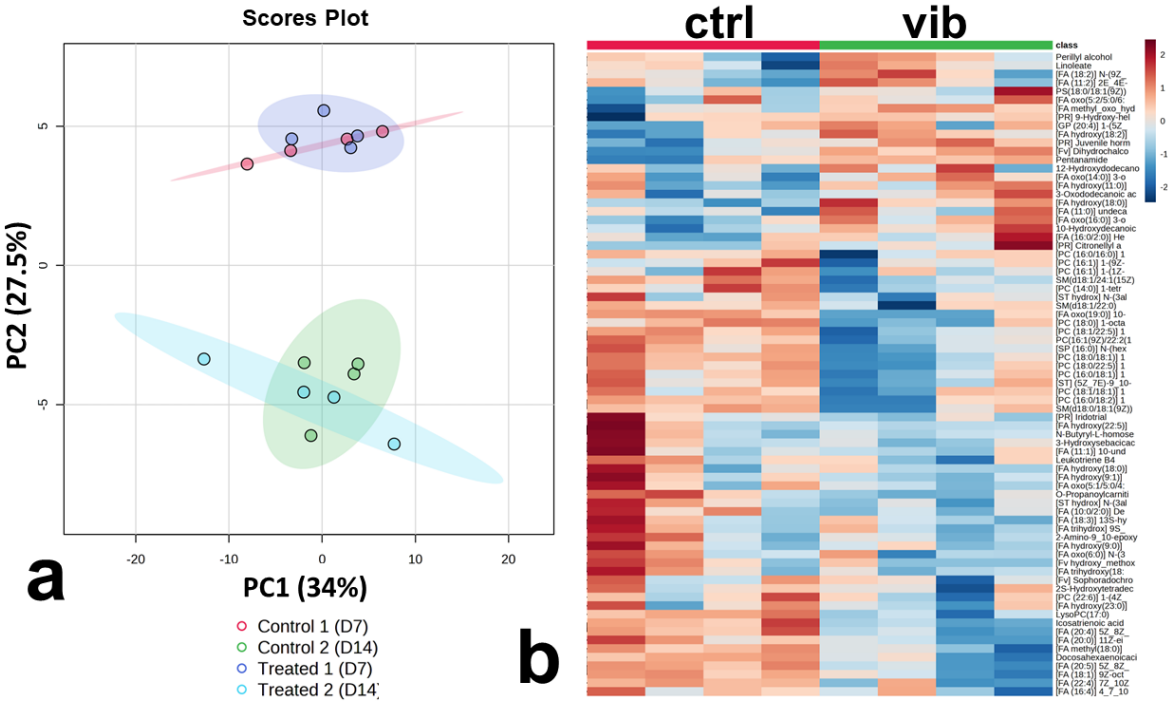

Figure 4.4 a) PCA plot with 95% confidence ellipses showing PC1 and PC2 of samples treated with nanovibration in 3D cultures for 7 and 14 days and controls. A clear separation by time point can be seen, while vibration-treated samples cluster close to untreated controls. b) heatmap of top 70 lipids (by t-test p-value) in 3D day 7 samples. A pattern of up- and downregulation of lipids can be seen in the heatmap. Heatmap colours indicate z-score calculated individually for every feature.

4.3.2 Molecular activity prediction and validation

IPA Molecular Activity Predictor (MAP) tool was used to predict the activation states of signalling molecules based on the fold change values of all identified metabolites in 2D samples. The MAP tool predicted changes in the activity of several key signalling kinases – extracellular signal related kinase 1/2 (ERK1/2, Figure 4.5 a and b), c-Jun N-terminal kinase (Jnk, Figure 4.5 c and d) and protein

kinase B, also known as Akt (Figure 4.5 e and f). ERK1/2 was predicted to be downregulated in nanovibration-treated samples on day 7 and unaffected on day 14, based on reduced levels of glutamine, phenylalanine, and several organic acids (Figure 4.5 b). Jnk was predicted to be activated by nanovibration on day 7 (Figure 4.5 c) and downregulated on day 14 (Figure 4.5 d). Akt activity was predicted to be reduced on both time points (Figure 4.5 e and f).

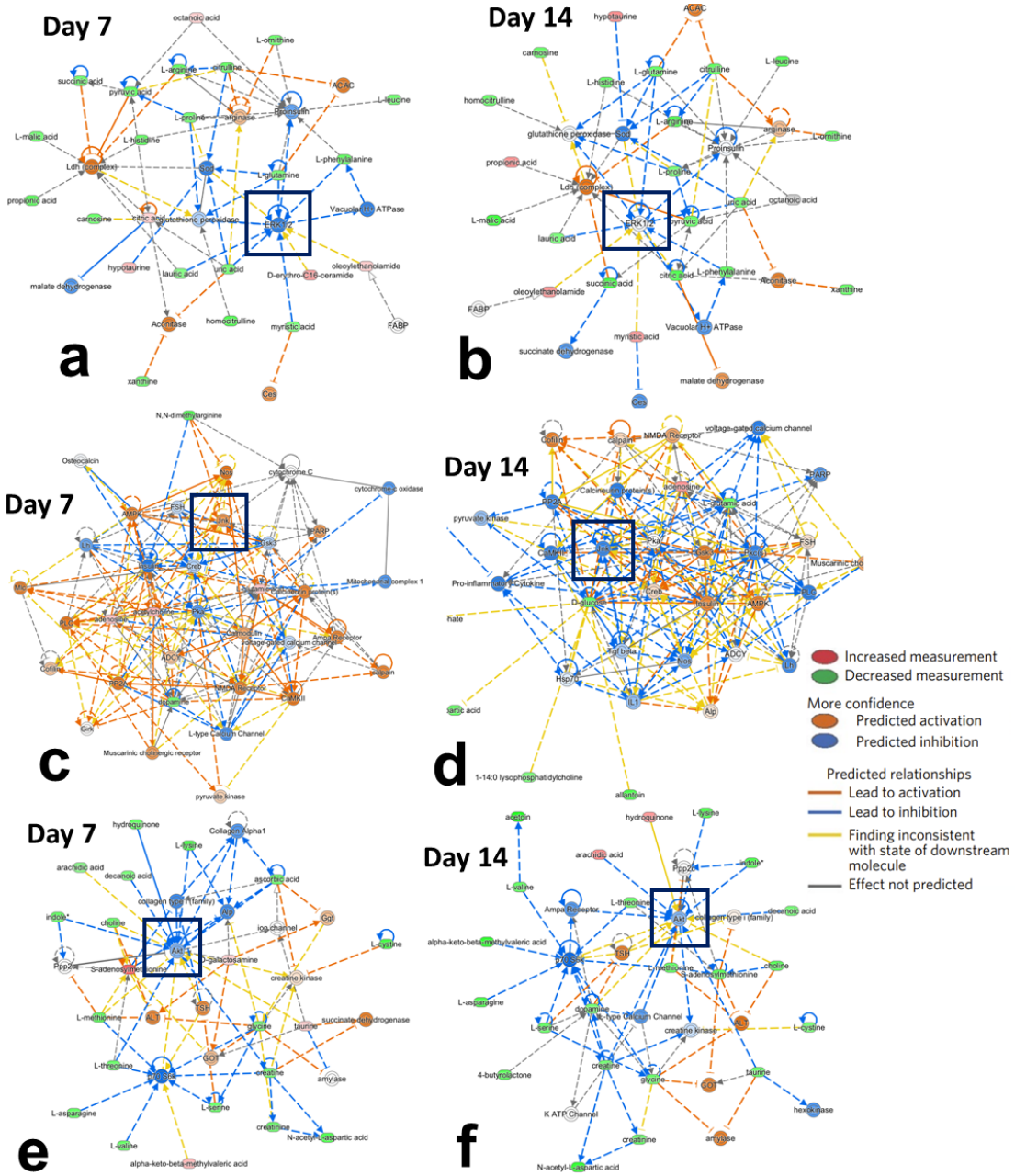

Figure 4.5 Metabolic network diagrams generated in IPA showing molecular activity predictions based on metabolite levels in 2D nanovibration-treated samples. ERK1/2 activity is predicted to be reduced on day 7 (a) and unaffected by treatment on day 14 (b). Jnk is predicted to be upregulated on day 7 (c) and downregulated on day 14 (d). Akt activity is predicted to be downregulated on both day 7 (e) and day 14 (f).

The activity of signalling kinases, such as ERK1/2, Jnk and Akt depends on their phosphorylation status. Therefore, to confirm the MAP predictions, the ratios of active phospho-proteins to total proteins were assessed using in-cell western. In contrast to MAP results, phosho-ERK1/2 was found to be upregulated in response to nanovibrational stimulation on day 7 (Figure 4.6 a), which is in agreement with the results presented in the previous chapter (chapter 3 Figure 3.3 b). On day 14, nanovibration led to a significant downregulation of phospho-ERK1/2, both on its own and in combination with TGFß1 (Figure 4.6 b). Akt and Jnk activity appeared to be regulated by TGFß1 but unaffected by nanovibrational treatment, with phospho-Akt being upregulated to a similar level in both TGFß1-treated groups on day 7 (Figure 4.6 e) and phosho-Jnk downregulated in both TGFß1 groups on day 14 (Figure 4.6 d).

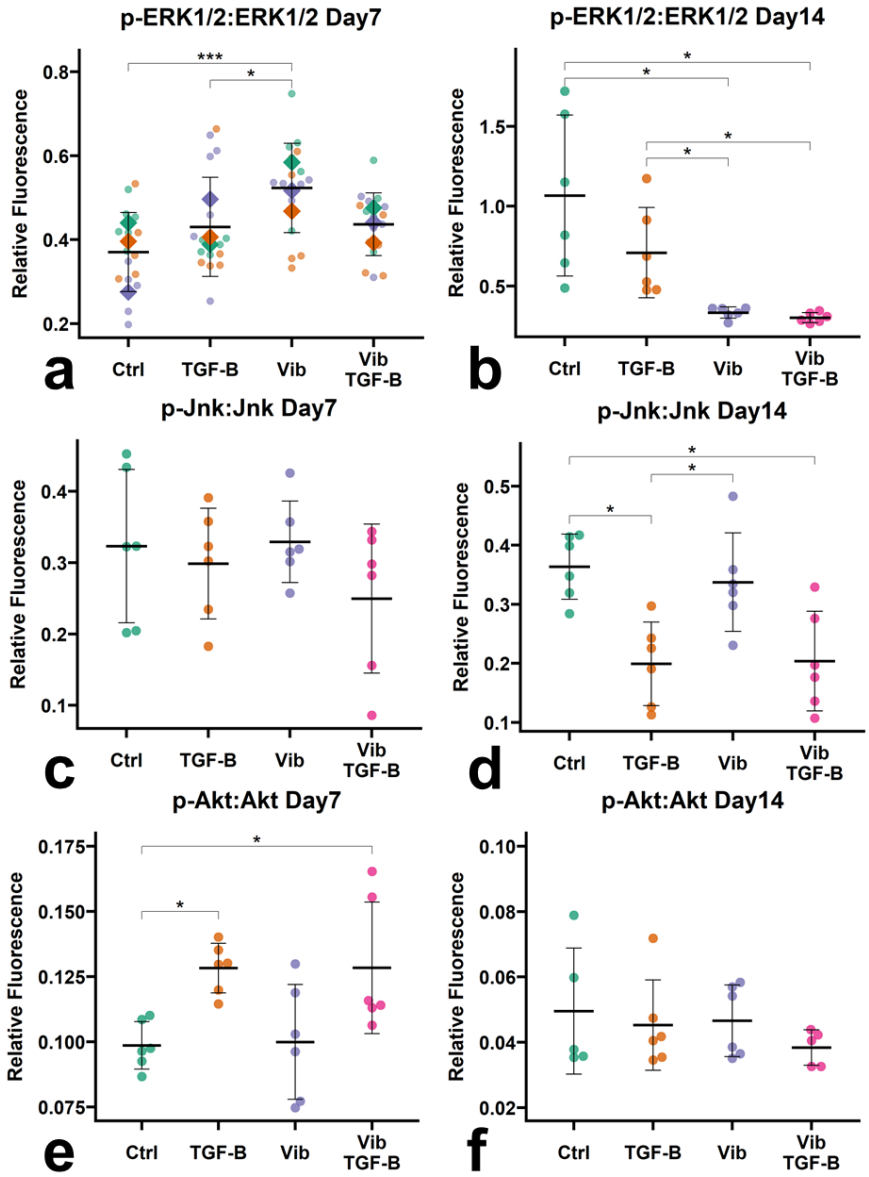

Figure 4.6 In-cell western analysis of the ratio of phospho-protein to total protein. a) ERK1/2 on day 7 and b) on day 14. c) Jnk on day 7 and d) on day 14. e) Akt on day 7 and f) day 14.

Bars show median with SD. In (a) data from three experimental repeats is shown, indicated by different colours. Rectangles mark mean of each repeat. Statistical analysis by two-factor ANOVA followed by Tukey post-hoc test. The rest of the panels show data from one experimental repeat. Statistical analysis by Kruskall-Wallis test followed by Wilcoxon pairwise rank sum test. In (a) n = 18 in each group, in the rest of the panels n = 6. * = p < 0.05, ** = p < 0.01, *** = p < 0.001.

4.3.3 RNA-Seq analysis

Samples treated with nanovibration in 2D for 7 days showed the most altered metabolic profile, therefore these conditions were selected for RNA sequencing experiment, to determine how nanovibrational stimulation affects gene transcription. TGFβ1-treated samples were included in this experiment as a positive control of pro-fibrotic phenotype. Genes with a p-value, adjusted for multiple comparisons, below 0.1 were considered differentially expressed. Out of 25 791 genes detected in the samples, 2 975 were differentially expressed (DE) in the TGFβ1 group and 136 in the nanovibration-stimulated group, indicating that TGFβ1 had a much stronger effect on the fibroblast transcriptome. This was illustrated by PCA analysis, as TGFβ1-treated samples shifted much further from the controls compared to the nanovibration-treated samples (Figure 4.7 a). In addition, similarly to metabolites, the majority of DE genes in the nanovibration-treated group showed less than a two-fold change in either direction, suggesting that the effects of nanovibrational treatment on gene transcript levels were subtle (Figure 4.7 b).

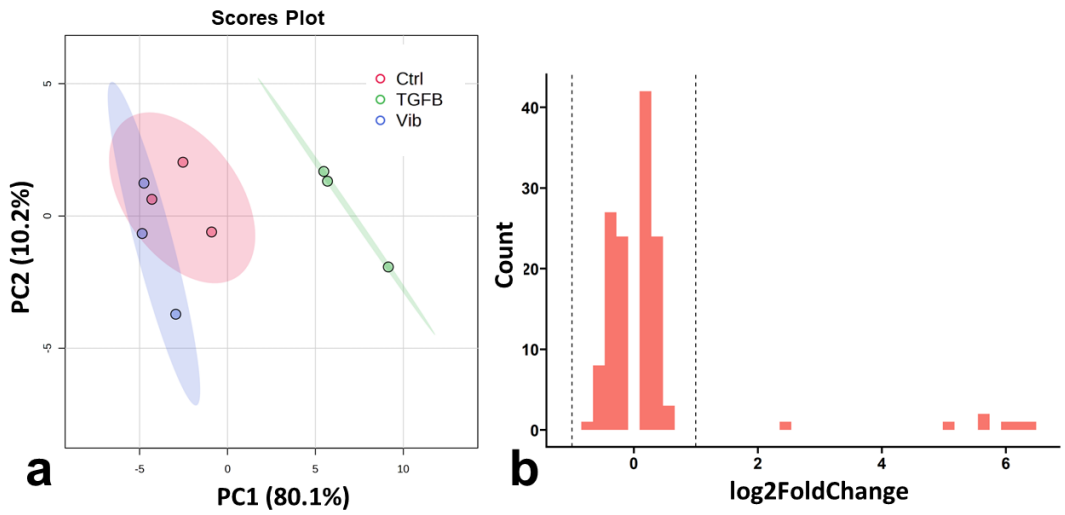

Figure 4.7 a) PCA plot with 95% confidence ellipses of transcript counts in control (ctrl), nanovibration-treated (vib) and TGFβ1-treated samples. b) Histogram of log2 fold change values of genes differentially expressed in nanovibraition-treated group. Dashed lines indicate -1 and 1, equivalent to two-fold change compared to control group.

There were 48 genes that appeared in DE gene lists in both nanovibration and TGFβ1-treated groups. Interestingly, the two treatments appeared to have

opposite effects on nearly all of these genes (Figure 4.8a). Among the genes which were differentially regulated by both treatments were genes encoding collagens COL1A1, COL5A1 and COL7A1, cytoskeletal proteins, such as alpha-actinin 4 (ACTN4), myosin heavy chain 9 (MYH9), filamins (FLNA, FLNC) and cell adhesion proteins integrin-α5 (ITGA5), talin (TLN1), periostin (POSTN), all of which were upregulated by TGFβ1 but downregulated by nanovibrational treatment (Figure 4.8a).

ORA was performed on the genes differentially regulated by nanovibrational stimulation to identify enriched biological process terms listed in gene ontology database (GO:BP) (Figure 4.8 b). The analysis revealed that among DE genes, a large number were involved in cytoplasmic translation, and several were associated with ribosomal large unit biogenesis. Other enriched biological processes were cell-substrate adhesion, mitotic cell cycle phase, a couple of pathways related to ATP synthesis and wound healing (Figure 4.8 b).

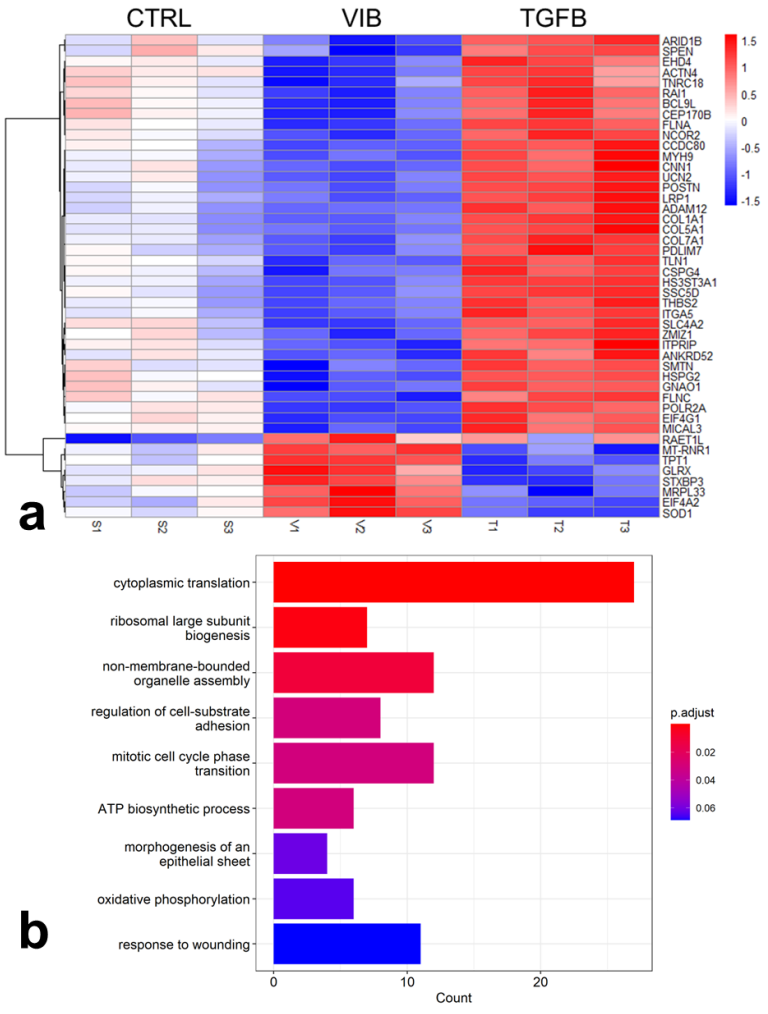

Figure 4.8

a) Heatmap of 48 genes that were differentially expressed in both nanovibration and TGFβ1 treated groups. Colours indicate z-score.

b) Enrichment analysis of genes differentially expressed in nanovibration treated samples, showing enriched GO: biological

Network diagram of the genes in the GO:BP enriched terms (Figure 4.9) showed that genes belonging to the cytoplasmic translation pathway, most of which encode ribosomal proteins (RPs), were all upregulated to a small degree. Genes related to the cell cycle showed both upregulation and downregulation. Among the downregulated genes were transcription factor FOXM1, which is a key regulator of cell cycle progression (Penke et al., 2018), claspin (CLSPN), which is required for DNA replication (Masai et al., 2017) and inner centromere protein INCENP important for regulation of mitosis (Figure 4.9) (Papini et al., 2019). This could indicate that in nanovibration-treated fibroblasts cell proliferation was slowing down. On the other hand, gene encoding RB1, which prevents cell cycle progression from G1 to S phase (Zhou et al.,2022) was also downregulated and CDC26, which is a part of anaphase promoting complex (Barford, 2010) was increased (Figure 4.9). However, activity of many cell-cycle proteins is largely regulated by post-translational modification and interaction with other factors and therefore small variation in the transcript levels may not be meaningful.

Nearly all genes mapped to the pathways associated with cell adhesion, morphogenesis of the epithelial sheet and response to wounding were downregulated by nanovibrational stimulation. Among them were genes encoding collagens, cytoskeletal proteins and adhesion proteins (Figure 4.9), which were positively TGFß1 (Figure 4.8). In addition, nanovibration downregulated the gene encoding NOTCH2, which is a transcriptional regulator with many downstream targets and has been implicated in fibrotic diseases (Condorelli et al., 2021). Transcript of an anti-apoptotic protein BCL-2 was also downregulated (Figure 4.9), indicating that nanovibration-treated fibroblasts may be more prone to apoptosis. However, BCL-2 can also be involved in mitochondrial metabolism and calcium homeostasis (Gross and Katz, 2017), both of which are potentially impacted by nanovibrational stimulation.

DE genes involved in ATP synthesis and oxidative phosphorylation (OXPHOS) were all upregulated (Figure 4.9). Genes associated with these processes, except for TMSB4X, encode subunits of electron transport chain complexes. This indicates that nanovibration might promote OXPHOS in fibroblasts cultured in 2D.

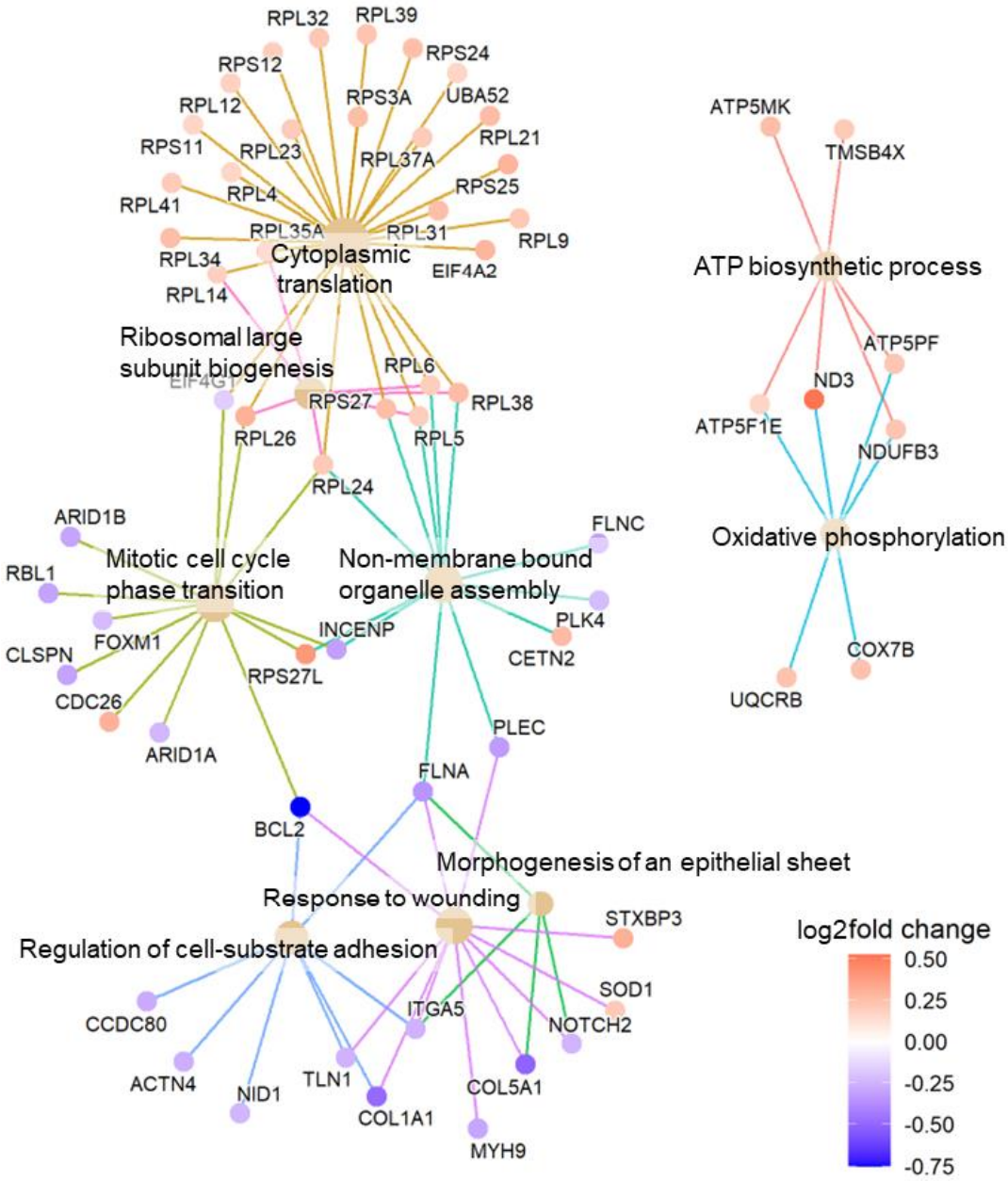

Figure 4.9 Network plot of enriched GO: biological process terms and associated genes, differentially expressed in fibroblasts treated with nanovibration for 7 days in 2D cultures.

TGFβ1 has been shown to induce a metabolic shift in fibroblasts, suppressing OXPHOS and promoting glycolysis (Wang et al., 2020). To compare the effects on the OXPHOS gene transcription between nanovibrational stimulation and TGFβ1, genes that encode subunits of the electron transport chain and appear in either one of the DE gene lists were plotted in a heatmap (Figure 4.10 a). While none of the genes were significantly affected by both treatments, nearly all of them showed a pattern of downregulation in TGFβ1-treated group and upregulation in nanovibration-treated group. This indicated that TGFβ1 suppressed OXPHOS and nanovibration had the opposite effect.

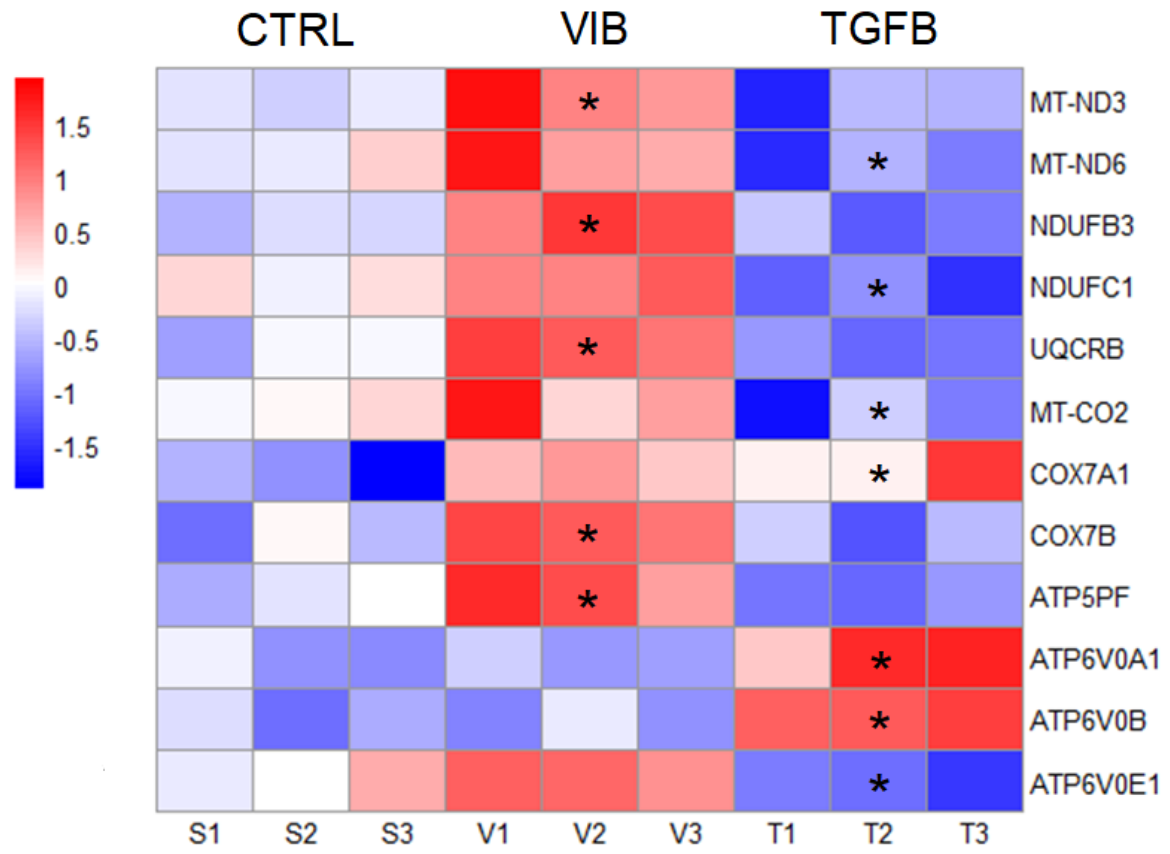

Figure 4.10 Heatmap of genes encoding subunits of the electron transport chain complexes, which were differentially expressed in either nanovibration or TGFβ1-treated samples. Asterix in the middle column indicates in which group (TGFβ1 or nanovibration) a particular gene was found to be differentially expressed compared to control group. Colour indicates Z-score.

In contrast, the transcript levels of a key glycolytic enzyme PFKFB3 were upregulated after TGFβ1 treatment, but unaffected by nanovibrational stimulation (Figure 4.11 a). Gene encoding LDHA, which converts pyruvate to lactate, was not affected by TGFβ1 (Figure 4.11 b), but LDHB, which facilitates lactate conversion into pyruvate was significantly downregulated (Figure 4.11 c). This suggests that TGFβ1 promoted glycolysis and potentially increased lactate production in fibroblasts.

Two genes encoding proteins with antioxidant function SOD1 and GLRX were also upregulated by nanovibrational stimulation, and both were downregulated by TGFβ1 (Figure 4.11 d and e). The gene encoding ROS generating enzyme NOX4 was increased in the TGFβ1 but not in the nanovibration-treated group (Figure 4.11 c).

Combined with increased GSH concentration observed in the nanovibration-treated samples (Figure 4.2 b) in the metabolomics experiment, this suggests that nanovibrational stimulation might improve ROS scavenging in dermal fibroblasts and potentially have anti-fibrotic effects, as ROS signalling is required for TGFβ1 induced fibroblast activation (Dosoki et al., 2017).

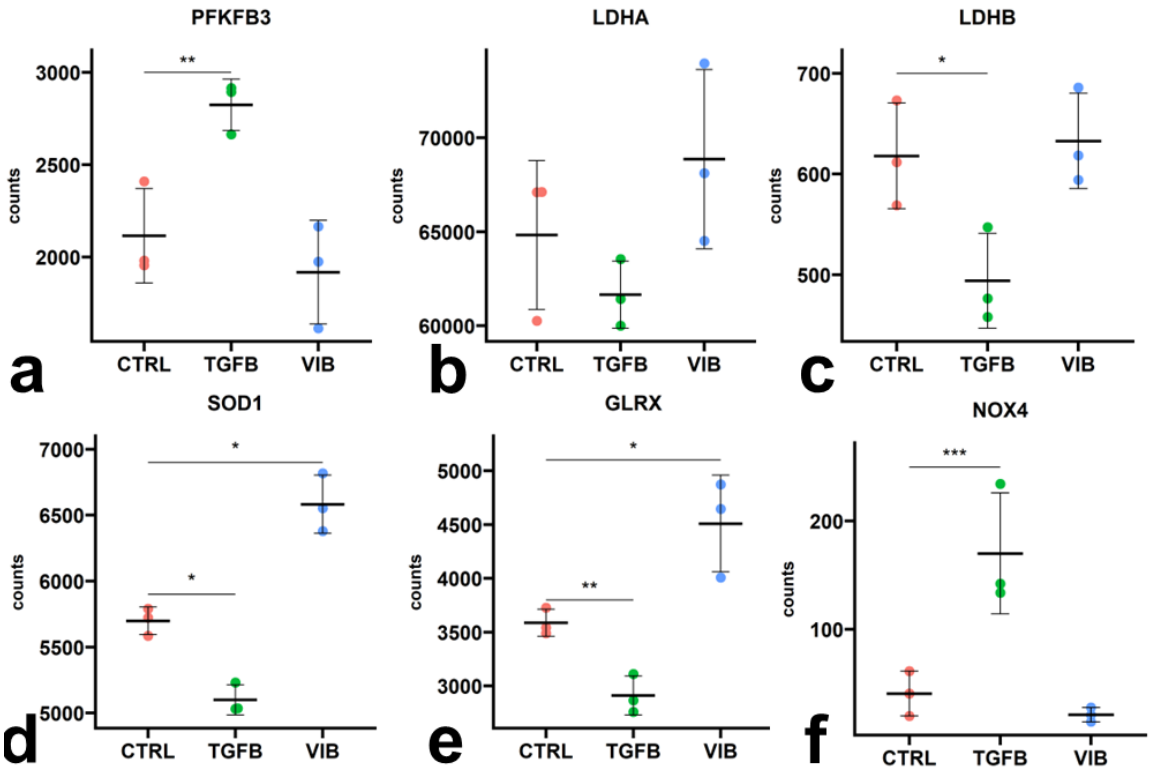

Figure 4.11 Counts of gene transcripts obtained by RNA-Seq. Glycolytic enzymes: a) PFKFB3, b) LDHA, c) LDHB, ROS scavengers: d) SOD1 and e) GLRX, and ROS generating enzyme f) NOX4. Each dot represents a single sample, bars indicate mean with SD. Statistical significance determined by Wald test with Benjamini-Hochberg adjustment for multiple testing. * = p.adj < 0.1, ** = p.adj < 0.01, *** = p.adj < 0.001. N = 3 in every group.

4.4 Discussion

In this chapter, metabolite and transcriptome analyses of nanovibration-treated fibroblasts were presented. The data from the metabolomics experiment, comparing 2D and 3D cultures at two different timepoints, suggested that

fibroblasts are more sensitive to nanovibrational stimulation in 2D than in 3D. Previous studies investigating the effects of nanovibration on MSC phenotype demonstrated that in 2D, focal adhesion signalling and cytoskeleton dynamics play a key role in the response to nanovibrational treatment (Nikukar et al., 2013). Similarly, fibroblasts treated with nanovibration in 2D cultures showed changes to cell adhesion and cytoskeleton protein gene transcription. However, while in MSCs the treatment increased the adhesion size and cytoskeleton tension (Nikukar et al., 2013), in fibroblasts it seemed to have the opposite effect. ITGA5 and TLN1 transcripts, which encode focal adhesion components, and MYH9, which encodes the heavy chain of contractile protein non-muscle myosin II, were downregulated in fibroblasts after 7 days of treatment in 2D culture. In MSCs treated in 3D collagen cultures, adhesion and cytoskeleton dynamics were less important, with mechanosensitive ion channels being the key mediators of nanovibration-induced change in cell phenotype (Tsimbouri et al., 2017). Perhaps the same occurs in fibroblasts but they are less sensitive to fluctuations in intracellular ion concentration than MSCs, leading to few detectable outcomes.

Based on the metabolite levels in nanovibration-treated 2D fibroblast cultures, MAP tool predicted changes to activity of ERK1/2, Jnk and Akt, which are signalling kinases regulating proliferation, cell survival, migration, and other biological processes crucial for fibroblast wound healing function (Nikoloudaki et al., 2020, Teng et al., 2021). On the protein level, only ERK1/2 phosphorylation was affected by nanovibrational stimulation, with other two responding only to TGFß1. Interestingly, reduced ERK1/2 activity was predicted on day 7 but more activated phosho-ERK1/2 was detected at this timepoint. However, by day 14 phospho-ERK levels were significantly reduced in the groups which received nanovibrational stimulation. As seen in the previous chapter, consistently with ERK1/2 activation, cell proliferation was also increased on day 7 (Chapter 3 Figure 3.2 a). However, at the same time point, genes FOXM1 and INCENP, CLSPN which are required for cell cycle progression were downregulated (Penke et al., 2018, Masai et al., 2017, Papini et al., 2019). Together, these results suggest that, when delivered continuously, nanovibration promoted ERK1/2 activation and cell proliferation early in the treatment but perhaps started suppressing it at some point between 7 and 14 days and the metabolome and transcriptome potentially reflect this

transition. A proliferation experiment after 10 or 14 days of treatment would help to clarify how the effects on proliferation change over time.

A number of metabolites that were significantly affected by nanovibration were involved in t-RNA synthesis on both day 7 and day 14. In addition, day 7 transcriptome data also showed upregulation of genes involved in cytoplasmic translation and ribosome biogenesis. This suggests that even though in nanovibration stimulated fibroblasts proliferation may be slowing down at this time point, protein translation is still highly active. Certain ribosomal proteins may also preferentially bind specific transcripts thus enhancing their transcription efficiency and adding another layer of complexity to the regulation of protein expression (Li and Wang, 2020). For example, RLP26 has been shown to enhance translation of a tumour suppressor gene p53 (Guimaraes and Zavolan, 2016). In addition, several RPs have functions, outside of ribosome, such as RPL5, which can translocate to nucleoplasm and stabilise p53, promoting cell cycle arrest (Guimaraes and Zavolan, 2016). On the opposite, RPL32 can induce p53 degradation and promote cell proliferation (Xie et al., 2020). Considering a large number of RPs differentially regulated in response to nanovibrational stimulation, and that their specific functions are largely unknown, it is difficult to predict what kinds of effects the upregulation of these RPs may have on fibroblast phenotype beyond protein translation.

Nanovibrational stimulation influenced lipid metabolism in fibroblasts, but only on day 7, as glycerophospholipid and glycerolipid metabolism pathways were found to be enriched. In addition, the lipid heatmap revealed that many lipids showed trends towards upregulation or downregulation in nanovibration-treated group, even if they were not statistically significantly altered. This was no longer the case on day 14, where no lipid associated pathways were found to be enriched and no trends were apparent on the heatmap. Even though there were no significantly altered lipids observed in fibroblasts treated in 3D, similarly to 2D, the lipid heatmap indicated some trends in their regulation. This could indicate that lipid metabolism was also influenced by nanovibrational stimulation in 3D, but the effect was too small to detect with the current experimental design.

Phospholipids are key components of cellular membranes, which define cell boundaries and separate cellular compartments. The phospholipid composition of the cell membrane can influence cellular adhesion (Lietha and Izard, 2020). It is a possibility that changes in phospholipid levels in response to nanovibrational treatment reflect changes in cell adhesion, as genes encoding several adhesion components were downregulated in 2D fibroblast cultures after vibrational treatment. In addition, changes in cellular lipid composition might be associated with energy metabolism, as fatty acids can serve as substrates in mitochondrial ATP synthesis (Wang et al., 2022). Previous studies of the effects of nanovibration on MSCs found changes in lipid metabolism, which reflect increased energy demand in stimulated cells undergoing differentiation (Kennedy et al., 2021).

Several metabolic pathways associated with energy metabolism were found to be altered in response to nanovibrational stimulation, including vitamin B6 metabolism (Parra et al., 2018), nicotinate and nicotinamide metabolism (Ström et al., 2018) and valine, leucine and isoleucine metabolism (Ye et al., 2020). Furthermore, several genes involved in OXPHOS and ATP biosynthesis were found to be upregulated by nanovibrational treatment after 7 days. In contrast, TGFβ1 downregulated OXPHOS gene transcripts and upregulated the glycolytic enzyme PFKFB3. This is consistent with the previous observations that TGFβ1 induces a metabolic shift in fibroblasts, favouring glycolysis over OXPHOS for energy production (Wang et al., 2020). LDHA transcript levels in TGFβ1-treated fibroblasts were comparable to those in control samples, however LDHB was significantly reduced. LDHA is an enzyme, which converts pyruvate into lactate, while LDHB catalyses the opposite reaction (Lin et al., 2022). This indicates that lactate production was upregulated in fibroblasts treated with TGFβ1, which has been shown to induce latent TGFβ1 activation and sustain activated phenotype in fibrotic diseases (Kottman et al., 2015). Nanovibration did not significantly influence glycolytic enzyme gene levels.

OXPHOS is an efficient method of ATP production but also results in increased ROS generation (Ung et al., 2021). ROS generation through NOX4 is also important for TGFβ1-induced fibroblast activation (Dosoki et al., 2017), and NOX4 mRNA was found to be upregulated in TGFβ1-treated cells. Nanovibration did not have an

effect on NOX4, but increased transcript levels of antioxidant proteins SOD1 and GLRX, while TGFß1 suppressed their transcription. GSH, which is an important antioxidant compound, was also highly upregulated in nanovibration-treated fibroblasts. Together these results suggest that even though OXPHOS is potentially increased in response to nanovibrational stimulation, stimulated fibroblasts may also be more resistant to ROS damage than untreated or TGFß1-stimulated cells.

Considering that TGFß1 and nanovibration had opposing effects on nearly all overlapping DE genes, including those involved in wound healing and fibrosis, and energy metabolism pathways, it is possible that it might have an anti-fibrotic effect. However, the effects on both transcriptome and metabolome were quite subtle and it is unclear if they could counteract the effects of a strong biochemical fibroblast activator, such as TGFß1. In addition, it seems these effects do not appear in 3D cultures to the same extent and therefore might not translate to *in vivo* application. However, this further confirms that when applied as bone anabolic mechanotherapy, nanovibration should not have any negative effects on the surrounding soft tissues as it did not induce a any major responses in 3D.

4.5 Conclusions

In this chapter, the results from two high-throughput experiments were presented. LC-MS based metabolomics study explored the differences in fibroblast response to nanovibrational stimulation in 2D and 3D cultures and 7-day and 14-day treatment periods. It was discovered that fibroblasts are much more sensitive to nanovibrational treatment when cultured in 2D and that the effects are more pronounced after a shorter stimulation period. Fibroblasts showed the highest number of significantly affected metabolites in 2D and on day 7 and these metabolites were involved in t-RNA synthesis, lipid metabolism, amino acid metabolism, and energy pathways.

A bulk RNA-Seq experiment was carried out to further investigate fibroblast response to nanovibrational stimulation in 2D after 7 days of treatment and compare it to TGFß1. Nanovibration downregulated genes involved in cell-substate adhesion, wound healing, and cell cycle progression, while genes involved in

cytoplasmic translation and ribosome assembly, as well as ATP synthesis and oxidative phosphorylation were found upregulated. Nearly all genes that were differentially regulated by both nanovibration and TGFß1 showed opposing responses to the two treatments, which could indicate that nanovibration has anti-fibrotic effects in 2D cultures. However, samples which received both treatments at the same time were not included in the analysis, due to high costs associated with RNA-seq, therefore it is unclear if these effects would be strong enough to counteract a biochemical activator, such as TGFß1.

Combined results from both experiments indicated that nanovibration influences protein translation and energy metabolism in 2D cultures after 7 days of continuous treatment. Even though higher metabolic activity may lead to increased ROS generation, nanovibration also upregulated transcription of ROS scavenging proteins and a key antioxidant compound GSH. It would be interesting to determine if the increase in these ROS scavengers can not only compensate for higher ROS generation due to OXPHOS, but also confer further resistance to ROS induced damage.

Chapter 5: Reactive oxygen species in nanovibrationally stimulated fibroblasts

5.1 Introduction

Reactive oxygen species (ROS) are unstable, highly reactive molecules containing oxygen, such as hydrogen peroxide, superoxide anion and hydroxyl radical (Shield et al., 2021). In the cells they are mainly generated as by-products of mitochondrial respiration, but can also be produced during peroxisomal fatty acid oxidation or by enzymes, such as NADPH oxidases (NOX) (Shield et al., 2021). Basal levels of ROS are important for many biological functions, including wound healing (Janda et al., 2016). However, when elevated beyond normal levels, ROS cause damage to DNA and proteins and can lead to cell death (Shield et al., 2021). To protect against ROS induced damage, cells produce ROS scavenging enzymes, such as superoxide dismuthase (SOD) or catalase (CAT), and small antioxidant molecules, such as glutathione (GSH) (Liu and Pravia, 2010). These antioxidant systems work together to maintain cellular redox homeostasis and prevent oxidative stress-induced damage.

During normal wound healing process, ROS contribute to regulation of fibroblast proliferation (Murell et el., 1990), migration (Hurd et al., 2012) and intracellular signalling pathways (Nakano et al., 2006). However, chronically elevated ROS levels have been observed in fibrotic diseases (Lu et al., 2021, Richter and Kietzmann, 2016) and are associated with sustained fibroblast activation (Spadoni et al., 2015). TGFß1, a major regulator of fibroblast activation, has been shown to upregulate ROS by several mechanisms. It promotes the expression of a membrane protein NOX4 (Bai et al., 2014), which generates ROS by oxidising NADPH, producing NADP+ and hydrogen peroxide. Inhibition of NOX4 has been shown to prevent TGFß1-induced ECM synthesis and cell contractility (Dosoki et al., 2017, Murphy-Marshman et al., 2017), which are characteristic features of the activated fibroblast phenotype. In addition, TGß1 downregulates the expression of ROS scavengers SOD and CAT (Liu and Desai, 2015) and depletes GSH (Liu et al., 2004). It has been shown that reversing GSH depletion abrogated TGFß1-induced collagen synthesis in fibroblasts (Michaeloudes et al., 2011).

Increased ROS generation is not only essential for TGFβ1-induced fibroblast activation, but can promote endogenous TGFβ1 expression (Montorfano et al., 2014), latent TGFβ1 activation (Jobling et al., 2006) and potentiate TGFβ1 signalling (Amara et al., 2010). While it was demonstrated that TGFβ1 induces NOX4 upregulation through SMAD2/SMAD3 activation (Bai et al., 2014), inhibition of NOX4 also reduced active SMAD2/SMAD3 levels in lung fibroblasts (Amara et al., 2010). These observations indicate that ROS and TGFβ1 signalling are tightly interlinked and regulate each other reciprocally. The positive feedback loop between ROS and TGFβ1 has been implicated in the development of systemic sclerosis (Spadoni et al., 2015), idiopathic pulmonary fibrosis (Estronut et al., 2022) and other fibrotic diseases (Richter and Kietzmann, 2016). Use of antioxidants has been proposed as a potential treatment strategy for these diseases (Richter and Kietzmann, 2016, Estronut et al., 2022).

In the previous chapter, it was shown that TGFβ1 increased the mRNA levels of NOX4 and downregulated mRNA of ROS scavengers SOD1 and glutaredoxin (GLRX) in fibroblasts (Chapter 4 Figure 4.11 d, e and f). Nanovibrational stimulation upregulated the transcription of SOD1 and GLRX and showed increased levels of GSH after 7 days of treatment (Chapter 4 Figure 4.2 b), indicating a stronger presence of the antioxidant defence system in these cells. In addition, nanovibration and TGFβ1 had an opposite effect on common differentially expressed genes, including collagen I and myosin heavy chain, which are important for activated fibroblast function (Chapter 4 Figure 4.8 a). This chapter aims to determine if these effects could be related to differential modulation of ROS by the two treatments. Nanovibration, TGFβ1 or both treatments were applied to fibroblasts for 7 days in 2D or 3D cultures and the levels of oxidative stress were assessed by measuring ROS with flow cytometry, and DNA damage by the alkaline comet assay. In addition, since excessive oxidative stress can lead to apoptosis (Feng et al., 2020), the percentage of apoptotic cells was also measured in these samples using flow cytometry.

5.2 Materials and Methods

5.2.1 Glutathione assay

Reduced glutathione (GSH) to oxidised glutathione (GSSG) ratio was determined using GSH/GSSG ratio detection assay kit (Abcam, #ab205811). The cells were detached from sample wells using trypsin solution and centrifuged for 5 min at 400 g. Then the pellets were lysed using 0.5% Triton-X (Thermo Fischer Scientific, #A16046.AE). Lysates were centrifuged for 15 min at 4°C at top speed. Supernatant was transferred into fresh tubes and kept on ice.

To remove proteins from the samples, 100 % TCA (trichloroacetic acid) was added to each sample, in ratio 1:5 to sample volume. The samples were incubated for 7 min on ice. After the incubation, samples were centrifuged for 5 min at 12 000 g and 4°C. TCA was neutralized by adding small volumes of $NaHCO_3$ until pH reached 5-7, as shown by pH indicator strip. The remaining procedure was completed following the protocol provided in the assay kit.

The fluorescence was recorded using Modulus™ II microplate reader (Turner BioSystems) at Ex/Em = 490/520 nm. The concentration of GSH and total glutathione was calculated from the standard curve. GSSG concentration was calculated as:

$$GSSG = \frac{Total\ glutathione - GSH}{2}$$

5.2.2 Flow cytometry

Cells grown in 2D cultures were detached from multi-well plates by incubation with trypsin solution for 5 min at 37°C, transferred to 1.5 ml microcentrifuge tubes, and centrifuged at 400 g for 5 min. 3D collagen gels were digested by incubating with 2.5 mg/ml collagenase D (Merck Life Science, #COLLD-RO) at 37°C for 1.5 h. Once gels were fully liquid, they were filtered and transferred to microcentrifuge tubes and centrifuged at 400 g for 5 min to form cell pellet. The

pellets then were resuspended in PBS or 50 µM TBHP (tert-butyl hydroperoxide) and incubated at 37°C for 30 min. After this incubation, the samples were centrifuged at 400 g for 5 min and supernatant was removed. The samples were then resuspended in 50 µl 1X ROS deep red stain solution (Abcam, #ab186029) and incubated at 37°C for 40 min. After 45 min 10 µl of apoptotic cell staining solution, containing 3 µl Alexa Fluor™ 488 annexin V and 0.6 µl 100 µg/ml propidium iodide (Thermo Fisher, #V13245) were added to each sample and samples were incubated for 15 min at room temperature, protected from light. After 15 min incubation, 200 µl 1X annexin staining buffer (Thermo Fisher, # V13245) was added to each sample and samples were placed on ice.

Flow cytometry was performed using Attune™ NxT Flow Cytometer (Thermo Fisher). Compensation was calculated and median fluorescence intensity was obtained for each sample using FlowJo software (BD).

5.2.3 Alkaline comet assay

Clear glass microscope slides were coated with 1% normal melting point agarose (Bio-Rad, #1613100) and allowed to dry at room temperature overnight.

Cells pellets from samples cultured in 2D and 3D were collected as detailed in 5.2.2. The pellets were resuspended in PBS or 100 µM hydrogen peroxide (H_2O_2) and incubated at 37°C for 30 min. After the incubation, the samples were centrifuged at 400 g for 5 min and the supernatant was removed from sample tubes. The pellets were then resuspended in 40 µl 1% ultra-low melting point agarose (Sigma-Aldrich, #A5030), the suspension was spotted onto the agarose-coated microscope slides and covered with 22 x 22 mm coverslips. The slides were placed in 4°C for 15 min to allow agarose to harden. After 15 min the coverslips were gently removed.

The slides with samples were submerged in lysis solution (2.5 M NaCl, 0.1 M EDTA Na2, 10 mM Tris-HCl, 1% Triton-X) and incubated for 1.5 h at 4°C. After the lysis, the slides were transferred into evolving solution (0.3 M NaOH, 1mM EDTA) and incubated for 20 min at 4°C. After the incubation they were placed in Sub-Cell

Model 96 electrophoresis tank (Bio-Rad) with pre-cooled electrophoresis buffer (0.03 M NaOH, 10 mM EDTA). The electrophoresis was run at 29 V constant voltage and approximately 30 mA for 15 min. The slides were washed with water 3 times and allowed to dry at room temperature.

DNA was stained right before imaging using 20 µl mounting medium with DAPI (Vector Laboratories, #H-1200-10). Images were taken with EVOS M7000 imaging system (Thermo Fisher), collecting images of 50 nuclei from each sample. The images were analysed using CometScore 2.0 (TriTek Corp). The percentage of tail DNA was used as a measure of DNA damage and the median tail DNA was calculated for each sample for statistical analysis.

5.3 Results

5.3.1 GSH/GSSG ratio in fibroblasts treated with nanovibration

GSH is a tripeptide with potent antioxidant properties, key to maintaining redox homeostasis in the cells (Zitka et al., 2012). When GSH reacts with ROS, it is converted into its oxidised form GSSG (Vairetti et al., 2021). Therefore, GSH to GSSG ratio is an indicator of oxidative stress in the cells (Vairetti et al., 2021, Zitka et al., 2012). Results from the metabolomics experiment, presented in chapter 4, indicated that GSH was highly increased in fibroblasts treated with nanovibration. To compare the effects of nanovibration on the GSH levels to those of TGFß1, GSH/GSSG ratio was measured in fibroblasts treated for 7 days, using a commercially available kit (Thermo Fischer Scientific, #A16046.AE). The results showed a slightly increased GSH/GSSG ratio in all groups compared to control but no significant differences (Figure 5.1).

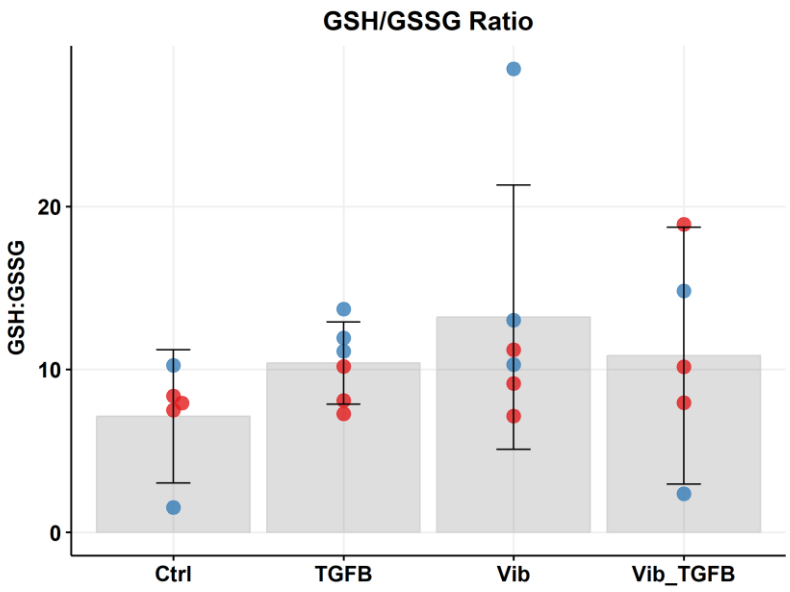

Figure 5.1 GSH/GSSG ratio in fibroblasts after 7 days of stimulation with TGFβ1, nanovibration or both. Statistical analysis by two-factor ANOVA. Bars indicate SD. Data from two independent experiments, indicated by colour, each dot represents a single sample. N = 6.

5.3.2 Measurement of ROS levels in fibroblasts by flow cytometry

To determine if nanovibration or TGFβ1 influence the levels of ROS in fibroblasts, these treatments were applied for 7 days in 2D and 3D cultures and the amount of ROS was measured by flow cytometry using a fluorescent ROS indicator. An oxidising agent tert-butyl hydroperoxide (TBHP) was added to samples to upregulate ROS and determine if any of the treatments altered fibroblast sensitivity to oxidative stress. In the 2D samples, both nanovibration and TGFβ1 slightly reduced ROS levels but these results were not statistically significant (Figure 5.2 a). However, a combination of the two treatments caused a significant reduction in intracellular ROS (Figure 5.2 a). In addition, TGFβ1-treated groups showed higher average ROS levels in response to TBHP, compared to those untreated or stimulated with nanovibration only, however not to a statistically significant degree (Figure 5.2 a). In 3D, nanovibration or TGFβ1 did not affect ROS levels in fibroblasts, neither on their own nor in combination (Figure 5.2 b). TBHP also induced similar levels of ROS in all groups.

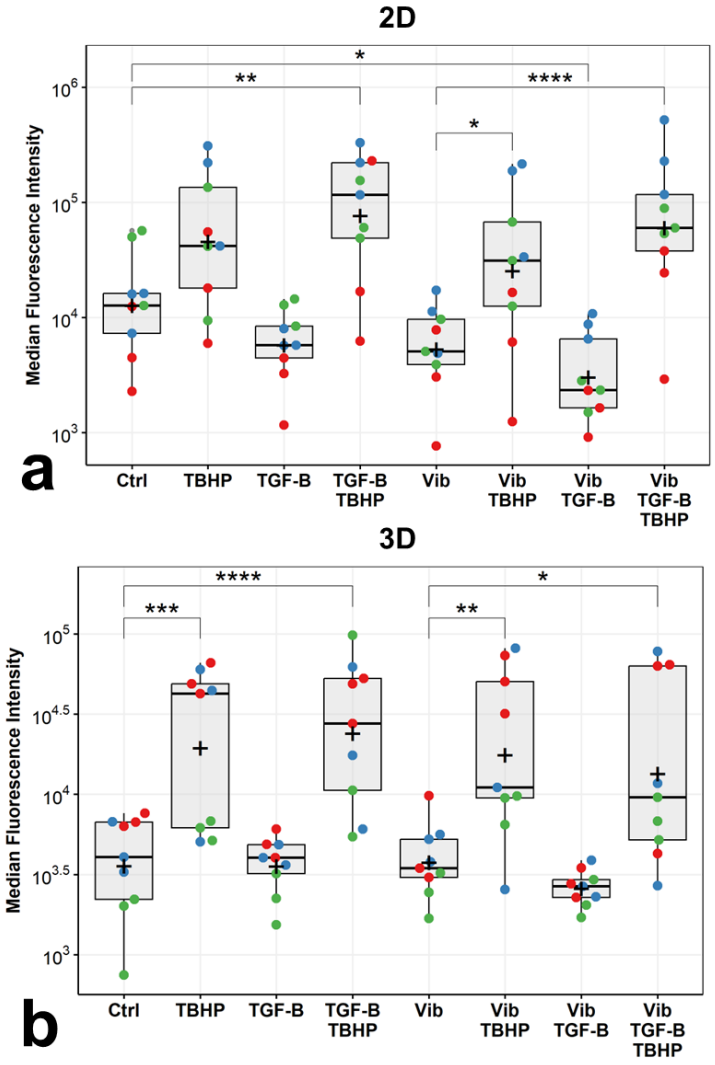

Figure 5.2. ROS levels in fibroblasts after 7 days of stimulation with nanovibration, TGFβ1 or both in a) 2D monolayrers and b) 3D collagen gels.

To induce ROS generation, samples were incubated with 50μM TBHP for 30 min before adding fluorescent ROS indicator. ROS was measured using flow cytometry.

Points represent median fluorescence intensity from a single sample and samples from three independent experiments are indicated by colour. Statistical analysis by two-factor ANOVA followed by Tukey post-hoc test, performed on log10 transformed values. Horizontal bar indicates the median, plus sign indicates the mean. * = $p < 0.05$, ** = $p < 0.01$, *** = $p < 0.001$, **** = $p < 0.0001$. N = 9 in every group.

Strangely, even though transcription of NOX4 was upregulated and ROS scavengers SOD1 and GLRX were downregulated after 7 days of TGFβ1 treatment (Chapter 4 Figure 4.11 d, e and f), the same treatment group did not show higher intracellular ROS levels than the untreated controls. Perhaps during this treatment period, the TGFβ1-stimulated fibroblasts employed other ROS scavenging mechanisms to prevent oxidative damage (Schwörer et al., 2020). To determine if TGFβ1 or nanovibration could induce short term changes in the cellular ROS levels, a trial experiment was carried out. Treatments were applied to one sample from each test group for only 2 h before measuring ROS with flow cytometry. It was observed that the TGFβ1-treated sample showed higher levels of ROS compared to the untreated but not as high as the TBHP-treated sample (Figure 5.3). Nanovibrational stimulation reduced the levels of ROS both on its own and when applied in combination with TGFβ1 (Figure 5.3). TBHP also induced less ROS generation in the sample which received both TGFβ1 and nanovibration for 2 h

(Figure 5.3). This could suggest that nanovibrational stimulation upregulates antioxidant activities and potentially prevents TGFß1-induced ROS upregulation early in the treatment period. However, further analysis on a larger set of samples is required to validate this observation.

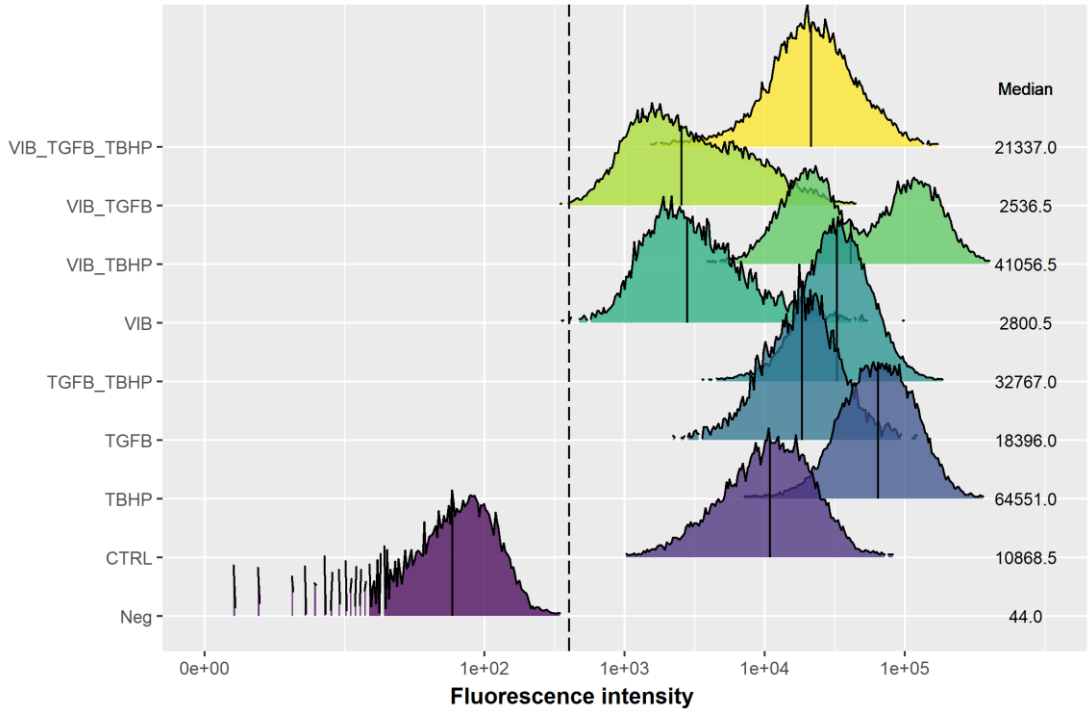

Figure 5.3. Density plot showing distribution of fluorescence intensity values in samples treated with nanovibration, TGFβ1 or both for 2h. ROS accumulation was induced by incubating samples with 50uM TBHP for 30 min. Fluorescence values were recorded for 10 000 cells from each sample. Dashed line indicates the maximum fluorescence intensity detected in unstained controls. Vertical lines on the distribution curves show the median.

5.3.3 Apoptosis in fibroblasts

Overwhelming the ROS scavenging systems can lead to cell death by apoptosis (Dong et al., 2022). To investigate if fibroblasts are more susceptible to apoptosis after nanovibration or TGFß1 treatment, the samples were stained with annexin V and propidium iodide (PI) and analysed by flow cytometry (Figure 5.4). Annexin V is a protein that specifically binds phosphatidylserine molecules, which are components of the inner cell membrane (Vermes et al., 1995). In early apoptosis some of these molecules are exposed to the cell exterior allowing annexin V binding. As apoptosis progresses, membrane integrity is lost, causing PI to enter the cells and become highly fluorescent upon interaction with the DNA (Vermes et

al., 1995). This allows detection and quantification of cells that are in early or late apoptosis by measuring fluorescence.

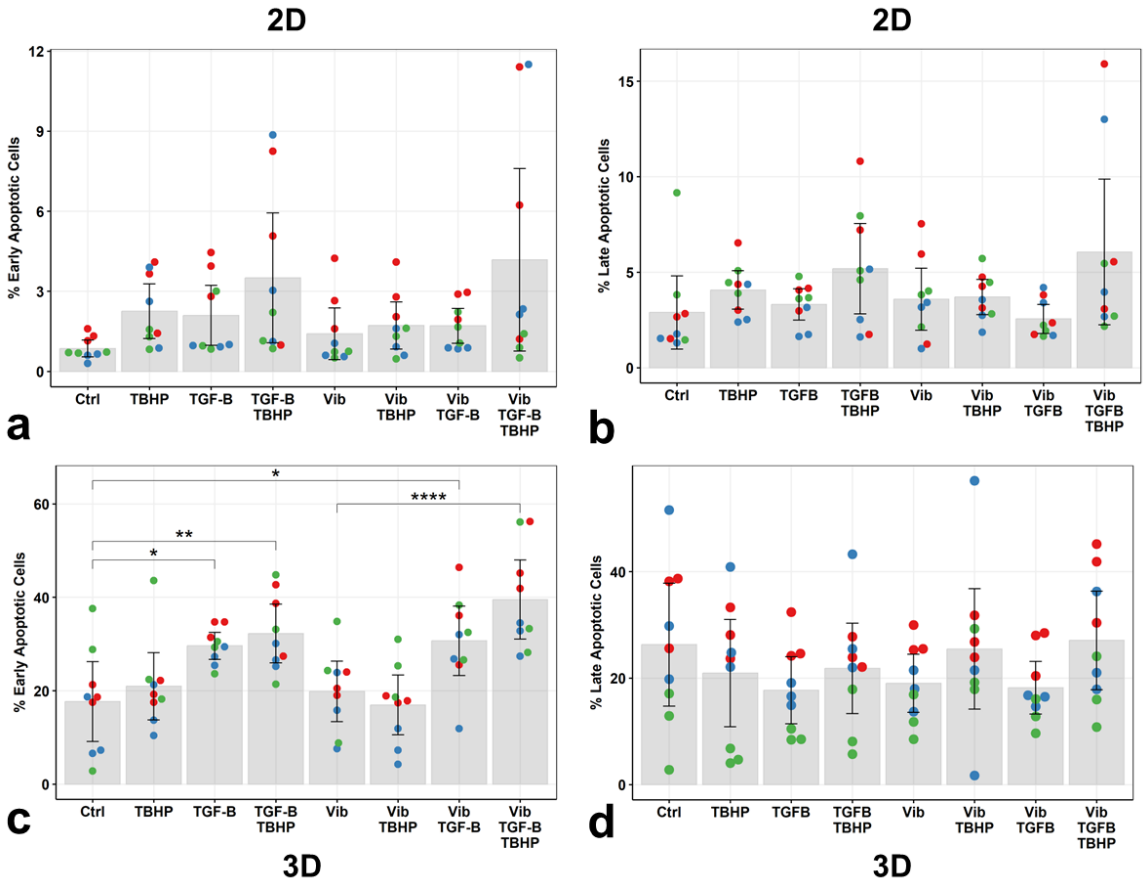

Figure 5.4 Percentage of cells in early and late apoptosis: 2D a) early apoptotic cells, b) late apoptotic cells and 3D c) early apoptotic cells, d) late apoptotic cells. Samples were treated with nanovibration, TGFβ1 or both for 7 days in 2D monolayers and 3D collagen gels. TBHP (50uM for 30min) was added to induce ROS generation. Fibroblasts were stained with annexin V and propidium iodide (PI) and fluorescence was measured using flow cytometry. Statistical analysis by two-factor ANOVA, followed by Tukey post-hoc test. Data from three independent experiments represented by different colour, each dot representing a single sample . Bars indicate SD. * = p < 0.05, ** = p < 0.01, *** = p < 0.001, **** = p < 0.0001. N = 9 in every group.

In the 2D samples, none of the treatments significantly increased the numbers of apoptotic cells. There was a small increase in the percentage of both early and late apoptotic cells in the groups, which received both TGFß1 and TBHP, but it was not statistically significant (Figure 5.4 a and b). In 3D however, every TGFß1 treated group showed a significantly higher percentage of early apoptotic cells (Figure 5.4 c). This was not reflected in the percentage of late apoptotic cells, as there were no statistically significant changes between the groups (Figure 5.4 d). Fibroblasts stimulated with TGFß1 have been shown to undergo apoptosis when

mechanical tension is lost in 3D collagen matrices (Kobayashi et al., 2005). Therefore, collagen digestion during the sample processing may be the factor underlying the increase in apoptosis observed in TGFß1-treated groups.

5.3.4 DNA damage in fibroblasts treated with nanovibration or TGFβ1

Another outcome of increased oxidative stress is DNA damage (Fang et al., 2015, Svegliati et al., 2014). DNA strand breaks can be detected using alkaline comet assay, in which DNA fragments are separated using electrophoresis (Fang et al., 2015). Intact DNA molecules are bulky and do not migrate easily, forming the head of the 'comet', while smaller fragments migrate further and form a 'tail'. When stained with fluorescent DNA dye, brightness of the head and tail represent relative amounts of intact and fragmented DNA respectively.

To determine if any of the treatments increased DNA damage in fibroblasts, they were treated with nanovibration or TGFß1 for 7 days and alkaline comet assay was performed. H_2O_2 was used to induce oxidative stress and to determine if any of the groups were more resistant or sensitive to DNA damage caused by H_2O_2. In 2D, none of the groups showed significant changes in the percentage of tail DNA, except when treated with H_2O_2 (Figure 5.5 a). When applied to the group, which received both TGFß1 and nanovibration, H_2O_2 led to less DNA damage than in other groups, as in these samples the average percentage of tail DNA was not significantly higher than in the untreated controls.

Similar results were observed in 3D, where H_2O_2 but not nanovibration or TGFß1 increased DNA breaks on their own (Figure 5.5 b). However, in the samples which received both treatments, percentage of tail DNA was on average 12% higher than in the untreated controls (Figure 5.5 b). These samples did not show increased ROS levels when assessed by flow cytometry, indicating that the observed increase in DNA damage may not be due to oxidative stress but other unknown factors.

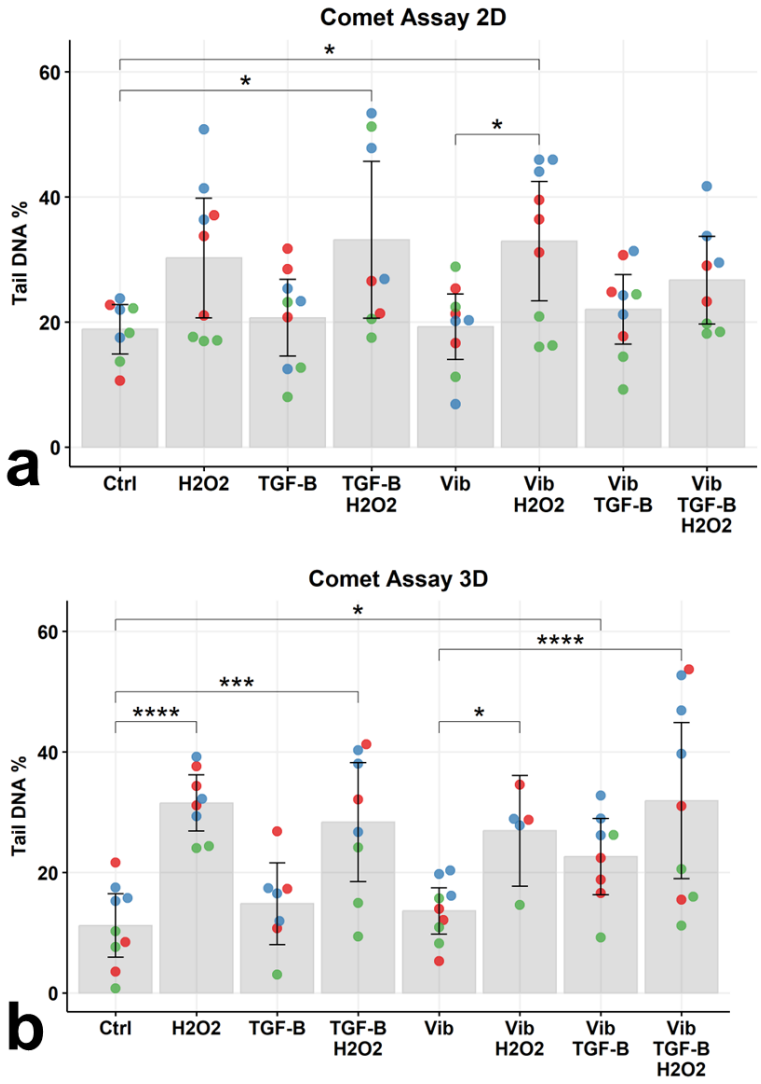

Figure 5.5 DNA damage in fibroblasts after 7 days of stimulation with nanovibration, TGFβ1 or both in a) 2D monolayrers and b) 3D collagen gels.

To induce DNA damage, samples were incubated with 100uM H_2O_2 for 30 min and DNA damage was assessed by alkaline comet assay.

Data collected from three independent experiments, indicated by colour, each dot represents median tail DNA percentage in a single sample. Statistical analysis by two-factor ANOVA followed by Tukey post-hoc test. Bars indicate SD.

*** = p < 0.05, ** = p < 0.01, *** = p < 0.001, **** = p < 0.0001. N = 9 in every group.**

5.4 Discussion

This chapter investigated the levels of ROS and the outcomes of increased oxidative stress, such as apoptosis and DNA damage, in fibroblasts following TGFβ1 and nanovibrational stimulation.

In the previous chapter, it was shown that more GSH was detected in fibroblasts after nanovibrational treatment (chapter 4 Figure 4.2 b), as well as higher transcript levels of GSH binding antioxidant enzyme GLRX (chapter 4 Figure 4.11 e). However, GSH/GSSG ratio was found unchanged in the samples stimulated with nanovibration. GSH is required to prevent oxidative damage from ROS generated

during aerobic respiration (Franco and Cidlowski, 2009). Nanovibration upregulated the transcription of several proteins involved in oxidative phosphorylation, therefore it is possible more GSH is required to neutralise mitochondrial ROS in these cells rate and therefore GSH/GSSG ratio is unchanged. GSH is also sensitive to pH changes and undergoes oxidation when pH exceeds 6.5 (Gnaiger et al., 1999). Since the sample processing protocol involved adjusting the pH, perhaps GSH in the samples was partially oxidised. Future experiments could be performed employing a more gentle processing protocol or focusing on other factors, such as glutathione reductase activity.

In fibroblasts cultured in 2D, nanovibration led to a small, not significant reduction in ROS. TBHP treatment also induced lower levels of ROS in nanovibration-treated group compared to others, but not significantly. This could be an indication that nanovibration potentially increased fibroblast antioxidant capacity, but the effect was too small and inconsistent to be significant. Further experiments, perhaps with a more optimised dose of TBHP, are needed to clarify this result. Surprisingly, TGFβ1 did not upregulate ROS in fibroblasts, despite increased NOX4 transcription, observed previously (chapter 4 Figure 4.11 f). A number of studies documented the positive effect of TGFβ1 on ROS generation, through downregulation of antioxidants and induction of NOX4 (Richter and Kietzmann, 2016, Michaeloudes et al., 2011). However, Schwörer et al. (2020) reported that TGFβ1 increased intracellular ROS in lung fibroblasts early after treatment, but this effect was no longer present after 48 h, even after further stimulation with TGFβ1. They suggested that the cells adapted their metabolism to prevent oxidative damage by rerouting respiration metabolites into the proline biosynthesis pathway. This could explain why ROS was not upregulated after 7 days of TGFβ1 treatment. In addition, combination of TGFβ1 and nanovibration significantly reduced levels of ROS compared to the untreated controls. The reason for this is unclear but perhaps there is a synergistic effect between different oxidative stress defence mechanisms induced by TGFβ1 and nanovibration.

To determine if nanovibration or TGFβ1 influenced ROS levels after a short treatment period, a preliminary experiment was conducted, where ROS was

investigated after 2 h of stimulation. During this period, TGFβ1 upregulated ROS and nanovibration suppressed it. A combination of treatments also downregulated ROS, to a level comparable to the group which received nanovibration only. This could suggest that the effects of nanovibrational stimulation on ROS scavenging appear as early as 2 h after stimulation and are strong enough to prevent TGFβ1 induced ROS generation during this time. However, further experiments with this treatment duration are needed to determine if these effects are consistent.

When ROS generation exceeds the antioxidant capacity in the cells, it can lead to DNA damage and apoptosis (Kreger and Zhang, 2007). While these effects were not statistically significant, TBHP seemed to induce slightly more ROS in the sample groups that were treated with TGFβ1 in 2D cultures, and these samples also showed higher percentage of both early and late apoptotic cells. This could suggest that TGFβ1 reduced the fibroblast ability to defend against TBHP-induced oxidative stress and that nanovibration does not substantially influence this effect. However, TGFβ1 did not increase fibroblast sensitivity to H_2O_2, at least in terms of DNA damage. Interestingly, the group which received both TGFβ1 and nanovibration showed lower levels of DNA damage than others after application of H_2O_2. While TBHP and H_2O_2 both cause oxidative stress, they do so through different mechanisms. TBHP depletes glutathione by regulating the activity of glutathione peroxidase-1 and increases lipid peroxidation but has little direct effect on DNA damage or mitochondrial dynamics (Spector et al., 2005). H_2O_2 on the other hand, has broader effects, and has been shown to impair mitochondrial membrane transport, mitochondrial viability and interact with DNA repair enzymes, leading to increased DNA damage (Spector et al., 2005). Combination of nanovibration and TGFβ1 reduced basal levels of ROS and potentially improved fibroblast defence against H_2O_2-induced DNA damage but did not affect ROS upregulated by TBHP or apoptosis. This suggests that if there is a synergistic activity between ROS defence mechanisms induced by nanovibration and TGFβ1, they are specific to certain sources of ROS, perhaps protecting against mitochondrial stress but not lipid peroxidation. In addition, H_2O_2 but not TBHP can be broken down by antioxidant enzyme CAT (Spector et al., 2005), so the protective effect against H_2O_2-induced DNA damage might be associated with the activity of this enzyme.

In 3D, the percentage of apoptotic cells was higher across all groups compared to 2D, which could indicate that fibroblasts were undergoing apoptosis at a higher rate when cultured in 3D. Sample groups which were stimulated with TGFβ1, on its own or in combination with other treatments, showed a significantly higher number of cells in early apoptosis than the untreated controls. It has been shown that fibroblasts activated with TGFβ1 undergo apoptosis when mechanical tension in the matrix is reduced (Kobayashi et al., 2005) or cell contact with collagen I through integrins is lost (Agarwal et al., 2020). Considering that no increase in ROS levels was observed in TGFβ1-treated groups, it is unlikely that cell death observed in this experiment was associated with oxidative stress. Perhaps methods which do not involve collagen digestion should be used to study fibroblast apoptosis in 3D cultures if TGFβ1 is used as a treatment.

TGFβ1 did not increase the levels of DNA damage in fibroblasts in 3D gels and neither did nanovibration. However, in samples which received both treatments simultaneously, more DNA strand breaks were present when assessed with the alkaline comet assay. Since ROS was not found upregulated in this group and even slightly reduced, it is unclear what might have caused this result. In the chapter 3, it was observed that TGFβ1 and nanovibration in concert increased transcript levels of inflammatory cytokines osteopontin (OPN) and interleukin-6 (IL-6), thought the later result was not significant (chapter 3 figure 3.8 b). Expression of OPN has been associated with mitochondrial DNA damage in cardiac fibroblasts (Du et al., 2022). However, both OPN and IL-6 were also shown to be upregulated in response to DNA damage (Kato et al., 2014, Squarzoni et al., 2021). It would be interesting to investigate if increased inflammatory signalling is the cause or the consequence of DNA damage in fibroblasts treated with TGFβ1 and nanovibration in 3D cultures. It is also worth noting that with the current experimental procedure only DNA strand breaks could be detected. ROS also causes DNA damage by oxidising DNA bases (Collins 2014). Modified DNA bases can be cleaved using bacterial endonucleases, allowing this type of damage to be detected with the comet assay (Collins, 2014). Including endonuclease digestion step in future experiments would help to more accurately assess DNA damage caused specifically by ROS.

5.5 Conclusions

In this chapter, the effects of nanovibration and TGFß1 on ROS balance, apoptosis and DNA damage were investigated. While previous experiments showed that nanovibration increased the amount of GSH in fibroblasts, GSH/GSSG ratio was not significantly altered, suggesting that nanovibration does not increase the ROS scavenging capacity through GSH. ROS levels were found slightly but not significantly downregulated in nanovibration-treated fibroblasts and similar was observed in TGFß1-treated fibroblasts. This could indicate that both treatments can slightly decrease the accumulation of ROS in fibroblasts when applied for 7 days, with nanovibration potentially upregulating expression of antioxidant enzymes, and TGFß1 perhaps altering the metabolic pathways. However, further studies are needed to confirm these claims. Combination of TGFß1 and nanovibration also caused a significant downregulation of ROS in 2D, which suggests that there might be a degree of synergy between ROS defence mechanisms induced by these treatments. TGFß1 and nanovibration applied simultaneously did not improve the fibroblast resistance to ROS induced by TBHP, but potentially had a protective effect against H_2O_2-induced DNA damage in 2D cultures. Interestingly, the opposite was observed in 3D, where combination of TGFß1 and nanovibration resulted in a significant increase in DNA damage. This suggests that increased levels of OPN mRNA, previously observed in this treatment group, might be due to DNA damage response in fibroblasts.

Together, these results indicate that nanovibration or TGFß1 did not significantly alter the intracellular levels of ROS after 7 days of treatment and it is unclear if differential regulation of gene expression by these two treatments could be associated with modulation of ROS levels. There were indications that they might influence ROS levels in the cells at earlier time points, but this requires further investigation. When applied together to 2D monolayers, these treatments significantly reduced ROS levels in fibroblasts and potentially had a protective effect against DNA damage. However, in 3D this combination of treatments upregulated DNA damage through currently unclear mechanisms, which is another indication that nanovibrational mechanotherapy may not be appropriate to patients with fibrotic diseases or healing wounds.

Chapter 6: General discussion and conclusions

6.1 Discussion

Nanovibrational stimulation was demonstrated to be a potent inducer of osteogenic phenotype in MSCs (Tsimbouri et al., 2017) and therefore shows promise for therapeutic *in vivo* applications. However, it is a novel type of treatment, with largely unknown effects on cell types other than MSCs. Fibroblasts are the key mediators of wound healing and tissue repair, and their activation is regulated by a myriad of biochemical and biomechanical factors. Upsetting the balance among these factors with an external stimulus can potentially lead to undesirable outcomes, such as aberrant wound healing and tissue fibrosis. On the other hand, a moderate effect on fibroblast features associated with the activated phenotype might indicate therapeutic potential of nanovibration in improving wound healing or treating fibrotic conditions.

To gain insights into the potential effects of nanovibrational treatment on the soft connective tissues, this work examined fibroblast responses to nanovibration in regular and pro-fibrotic conditions, simulated by addition of TGFβ1. The treatment was applied to 2D fibroblast monolayers and 3D collagen hydrogel cultures, to determine whether the culture conditions influence the effects of the stimulation. It was observed that nanovibration did not dramatically alter the fibroblast phenotype under basal conditions, especially in 3D, where the only significant effect observed was a slight reduction in proliferation. It is well documented that fibroblasts proliferate less in 3D collagen hydrogels compared to 2D monolayer cultures (Woodley et al., 2022). This is thought to be associated with altered activity of ERK signalling pathway, influenced by the mechanical environment, as well as specific interactions between fibroblast cells and collagen (Woodley et al., 2022). While the ERK pathway activation in 3D was not examined in this work, it was found to be affected by nanovibrational stimulation in MSCs cultured in soft collagen hydrogels, suggesting that mechanotransduction pathways stimulated by nanovibration can modulate ERK signalling in 3D (Tsimbouri et al., 2017). However, in MSCs, nanovibration promoted ERK activation, which is usually associated with increased proliferation. It would be

interesting to investigate if the reduced proliferation rate observed in the 3D fibroblast culture in response to nanovibrational treatment was associated with cell type specific effects on the ERK pathway. However, this effect was subtle and perhaps unlikely to have negative consequences *in vivo*, where fibroblast proliferation rate is low under homeostatic conditions (Kirk et al., 2021).

In contrast to 3D, nanovibration applied to 2D monolayer cultures had a positive effect on fibroblast proliferation and showed increased levels of active ERK1/2. Previous studies demonstrated that vibrational stimulation can both promote and reduce fibroblast proliferation depending on the vibration parameters (Judex and Pongkitwitoon, 2018, Jiang et al., 2015, Kutty and Webb, 2010). Interestingly, positive effects were observed when vibration displacements were under 300 µm, with 12 µm inducing the strongest proliferative response (Jiang et al., 2015), while higher displacements lead to reduction (Judex and Pongkitwitoon, 2018, Kutty and Webb, 2010). Considering that there was an overlap between the frequency and acceleration ranges used in the different experiments, this could indicate that lower displacements, including those on the nanoscale, are favourable to fibroblast proliferation in 2D. However, studies investigating the influence of topography on cell behaviour suggest that nano- and microscale features may lead to the same functional outcomes but through different mechanisms. For example, both nano- and microtopographies can enhance cell adhesion, but nanoscale features promote integrin clustering, while microscale features influence orientation and arrangement of focal adhesions (Nguyen et al., 2016). Therefore, until more is known about the mechanisms through which different vibration parameters affect cell proliferation, direct parallels between treatments employing largely different parameters should not be drawn.

Except for a short-term upregulation in α-SMA production and a modest increase in proliferation observed in 2D, there were no indications that nanovibration may promote fibroblast activation in the absence of other factors. On the contrary, transcriptome changes in nanovibration-treated 2D cultures indicated downregulation in genes associated with wound healing and upregulation in genes involved in oxidative phosphorylation and ROS scavenging. Fibroblast activation involves increased ROS generation and a metabolic shift towards glycolysis (Janda

et al., 2016, Ung et al., 2021). This suggests that by opposing these activities, nanovibration could have an anti-fibrotic effect but also potentially slow down wound healing. However, nanovibration did not influence basal or TGFβ1-stimulated expression of collagens I and III. It also downregulated the expression of OPN, which is associated with increased inflammation and impaired wound healing (Mori et al., 2008). Maintenance of the ECM protein synthesis indicates that nanovibrational stimulation is unlikely to impair wound healing and the effects on OPN suggests that it may even benefit it, by suppresing OPN-mediated inflammatory signalling (Mori et al., 2008).

However, when applied to fibroblasts in the presence of pro-fibrotic factor TGFβ1, nanovibration did not reduce the expression of inflammatory factors and even increased it. In 2D, IL-6 production was found to be upregulated after nanovibrational treatment under pro-fibrotic conditions. And while in 2D TGFβ1-induced OPN expression was partially abrogated by nanovibration, in 3D it was significantly higher than after TGFβ1 treatment alone. While inflammation is a necessary part of wound healing process, amplified inflammatory signalling is associated with slower wound closure and increased scarring (Moretti et al., 2022). In addition, fibroblasts treated with TGFβ1 and nanovibration in 3D showed higher levels of DNA damage but not increased apoptosis, compared to those treated with TGFβ1 alone. When not accompanied by cell death, accumulation of DNA damage can result in altered epigenetic states and gene mutations, leading to the development of fibrotic disorders (Zhu et al., 2022, Vlachogiannis et al., 2020). Therefore, the effects of nanovibration in a pro-fibrotic 3D environment are concerning and may indicate that nanovibrational treatment should not be applied to patients with fibrotic diseases or to the tissues with healing wounds.

Interestingly, in 2D nanovibration and TGFβ1 applied together did not induce DNA damage and appeared to have a protective effect on DNA when H_2O_2 was applied. In addition, the combination of these treatments significantly reduced ROS levels. Since nanovibration promoted the expression of the antioxidant enzymes SOD1 and GLRX in basal conditions, perhaps it could increase ROS scavenging capabilities in TGFβ1-stimulated fibroblasts as well, but further studies are needed to clarify this. Downregulation of ROS accumulation could have

therapeutic benefit, as the positive feedback loop between ROS and TGFβ1 has been implicated in the development of fibrotic diseases (Liu and Desai, 2015). Unfortunately, these effects were not observed in the 3D cultures, which more accurately represent cell microenvironment *in vivo* (Woodley et al., 2022). A better understanding of how exactly the culture conditions influence the fibroblast response to nanovibration could perhaps help to develop treatment strategies which harness the positives, while avoiding the negative outcomes of nanovibrational treatment.

The major difference between 2D tissue culture plastic and 3D collagen hydrogel cultures is the substrate stiffness, which itself is a mechanical stimulus regulating fibroblast behaviour (Woodley et al., 2022). Fibroblasts cultured on plastic proliferate faster and show α-SMA positive stress fibres, indicative of activated phenotype (Woodley et al., 2022). In 3D collagen gels, not only their proliferation but also sensitivity to growth factor stimulation is reduced (Woodley et al., 2022). These differences are associated with the activity of mechanotransduction pathways, such as ERK activation through FAK signalling or YAP/TAZ nuclear localisation due to increased cytoskeleton tension in 2D (Woodley et al., 2022, Smithmyer et al., 2019). In nanovibrational stimulation experiments presented in this work, it was observed that fibroblasts cultured in 2D were more sensitive to the treatment in the absence of TGFβ1 that those in 3D, showing increased proliferation, ERK1/2 activation, changes in metabolic pathways and gene transcription, while 3D responses were limited to slight reduction in proliferation. This might indicate that nanovibration interacts with mechanotransduction pathways activated by a stiff substrate but does not strongly induce their activation on a softer matrix, such as collagen. On the other hand, in 3D, nanovibration sensitised fibroblasts to TGFβ1, significantly increasing endogenous TGFβ1 and OPN gene expression, and showing a trend, although insignificant, in IL-6, α-SMA and COL1A mRNA upregulation while most of these responses were not observed in 2D. This suggests that there might be an interplay between the substrate stiffness, TGFβ1 and nanovibrational stimuli. However, differences in the cell morphology between 2D and 3D as well as the bioactive properties of collagen may also contribute to the inconsistent fibroblast response to nanovibration between the two types of cultures.

6.2 Summary of the key findings

This thesis presents the first investigation of the effects of nanovibrational stimulation on human dermal fibroblasts. While further studies are needed to gain a comprehensive understanding of fibroblast response to nanovibration in health and disease, several key observations were made:

- Fibroblasts are sensitive to nanovibrational stimulation, however their sensitivity is affected by the culture conditions, with 2D cultures showing a stronger response.
- Nanovibration does not strongly affect collagen synthesis, neither in presence nor in absence of TGFβ1.
- Nanovibration can regulate the expression of inflammatory factors and endogenous TGFβ1 with specific effects dependent on culture conditions and TGFβ1 presence.
- Nanovibration affects metabolic pathways and gene transcription in fibroblasts cultured in 2D. Its effects on gene expression appear to be the opposite of those induced by TGFβ1.
- In 2D, nanovibration and TGFβ1 synergistically downregulate ROS accumulation and have a protective effect against ROS-induced DNA damage. In contrast, application of the two treatments simultaneously in 3D collagen gels can lead to increased DNA damage.

6.3 Recommendations for future work

Regulation of fibroblast behaviour is complex and involves integration of mechanical and biochemical stimuli. Results presented in this thesis indicate that nanovibrational stimulation differentially affects fibroblast proliferation, inflammatory factor synthesis and DNA susceptibility to damage when applied to 2D tissue culture plastic and 3D collagen cultures. The 2D and 3D cultures utilised throughout this work present vastly different mechanical environments, which makes it difficult to infer the reasons between the observed differences in the fibroblast responses to nanovibration. While some of the observed outcomes of nanovibrational treatment, such as downregulation of OPN or ROS, may suggest a

therapeutic benefit of nanovibration in fibrotic diseases, others, such as increased DNA damage, indicate that it may be detrimental *in vivo*. Therefore, a better understanding of how exactly the mechanical properties of the matrix influence the sensation and the response to nanovibrational stimulation is highly desirable. This could be achieved by employing hydrogels with tunable stiffness for 3D fibroblast cultures in the future studies. Poly(ethylene glycol) (PEG)-based hydrogels functionalised with MMP degradable peptides can be prepared in a stiffness range which can mimic both healthy and fibrotic tissues (Marby et al., 2015). Growth factors can also be incorporated into PEG hydrogel formulations for more accurate modelling of wound microenvironment in 3D (Sokic and Papavasiliou, 2012).

Previous studies demonstrated that vibration could affect fibroblast migration, which is another characteristic of the activated phenotype, important for successful wound repair (Mohammed et al., 2016, Enomoto et al., 2020). Mohammed et al. (2016) reported that application of vibration with 1600 Hz and sub-micrometer displacement reduced fibroblast migration. This is the only study to date that employed vibration parameters in a similar range to nanovibration, suggesting that nanovibration may influence fibroblast motility as well. Fibroblast gap closure assay would allow to determine if and how fibroblast migration is affected by nanovibrational stimulation.

While collagens are the major ECM proteins synthesised by fibroblasts, they also produce fibronectin, laminin, elastin and other ECM components (Pfisterer et al., 2021). ECM composition can affect the course of wound healing and the quality of repair (Pfisterer et al., 2021). Therefore, future studies should investigate the effects of nanovibration on a wider range of ECM component synthesis. Similarly, studies of inflammatory and growth factor production in response to nanovibration could be expanded to include PDGF, CTGF, FGF, VEGF, IL-11, IL-4 and other factors involved in the regulation of fibroblast phenotype during wound healing and fibrosis. Current data suggests that nanovibration modulates IL-6, OPN and TGFß1 gene expression but the full extent of the effects on the signalling factor synthesis remains unclear. Furthermore, secretion of these signalling molecules could be

investigated using ELISA, to determine if the observed changes in gene expression are reflected in secretory activity of nanovibrationally stimulated fibroblasts.

Finally, the high-throughput experiments investigating metabolomic and transcriptomic changes in response to nanovibrational stimulation yielded some interesting results in 2D cultures, suggesting that it could have an anti-fibrotic effect. However, nanovibration-induced transcriptomic and metabolomic alterations were not examined in the presence of TGFß1, therefore it is unclear how pro-fibrotic environment might influence these effects. Future 'omics' studies should incorporate a sample group simultaneously stimulated with both treatments to better understand the interaction between nanovibration-induced effects and TGFß1 signalling. In addition, the effects of nanovibration on the fibroblast transcriptome in 3D were not investigated in this work. Perhaps this experiment could provide insights into the reasons underlying different fibroblast responses to nanovibration in 2D and 3D.

6.4 Conclusion

Overall, this work demonstrates that dermal fibroblasts are sensitive to nanovibrational stimulation. The specific responses vary based on the culture conditions and the presence of biochemical signalling factors, such as TGFß1. In the absence of biochemical stimulation, the effects are subtle, indicating that nanovibrational stimulation can be safely applied as mechanotherapy for bone regeneration to patients without soft tissue injuries or fibrotic diseases. However, it is less clear how it influences the fibroblast phenotype under pro-fibrotic conditions, with different effects observed in 2D and 3D cultures. Future studies exploring the interactions between matrix mechanics, signalling factors and nanovibration could help to determine if nanovibrational stimulation may offer therapeutic benefits in treatment of fibrotic diseases or aberrant wound healing.

List of References

Adami, E., Viswanathan, S., Widjaja, A. A., Ng, B., Chothani, S., Zhihao, N., Tan, J., Lio, P. M., George, B. L., Altunoglu, U., Ghosh, K., Paleja, B. S., Schafer, S., Reversade, B., Albani, S., Ling, A. L. H., O'Reilly, S., & Cook, S. A. (2021). IL11 is elevated in systemic sclerosis and IL11-dependent ERK signalling underlies TGFß-mediated activation of dermal fibroblasts. Rheumatology (Oxford, England), 60(12), 5820–5826.

Agarwal, M., Goheen, M., Jia, S., Ling, S., White, E. S., & Kim, K. K. (2020). Type I Collagen Signaling Regulates Opposing Fibrotic Pathways through α2ß1 Integrin. American journal of respiratory cell and molecular biology, 63(5), 613–622.

Akasaka, Y., Ono, I., Kamiya, T., Ishikawa, Y., Kinoshita, T., Ishiguro, S., Yokoo, T., Imaizumi, R., Inomata, N., Fujita, K., Akishima-Fukasawa, Y., Uzuki, M., Ito, K. and Ishii, T. (2010), The mechanisms underlying fibroblast apoptosis regulated by growth factors during wound healing. J. Pathol., 221: 285-299.

Akhmanova, M., Osidak, E., Domogatsky, S., Rodin, S., & Domogatskaya, A. (2015). Physical, Spatial, and Molecular Aspects of Extracellular Matrix of In Vivo Niches and Artificial Scaffolds Relevant to Stem Cells Research. Stem Cells International, 2015, 167025.

Albert J. Banes, Mari Tsuzaki, Juro Yamamoto, Brian Brigman, Thomas Fischer, Thomas Brown, and Larry Miller. (1995). Mechanoreception at the cellular level: the detection, interpretation, and diversity of responses to mechanical signals. Biochemistry and Cell Biology. 73(7-8): 349-365.

Amara, N., Goven, D., Prost, F., Muloway, R., Crestani, B., & Boczkowski, J. (2010). NOX4/NADPH oxidase expression is increased in pulmonary fibroblasts from patients with idiopathic pulmonary fibrosis and mediates TGFbeta1-induced fibroblast differentiation into myofibroblasts. Thorax, 65(8), 733–738.

Arif, S., Attiogbe, E., & Moulin, V. J. (2021). Granulation tissue myofibroblasts during normal and pathological skin healing: The interaction between their secretome and the microenvironment. Wound repair and regeneration: official publication of the Wound Healing Society [and] the European Tissue Repair Society, 29(4), 563–572.

Asensio, G., Vázquez-Lasa, B., & Rojo, L. (2019). Achievements in the Topographic Design of Commercial Titanium Dental Implants: Towards Anti-Peri-Implantitis Surfaces. Journal of Clinical Medicine, 8(11), 1982.

Bai, G., Hock, T. D., Logsdon, N., Zhou, Y., & Thannickal, V. J. (2014). A far-upstream AP-1/Smad binding box regulates human NOX4 promoter activation by transforming growth factor-ß. Gene, 540(1), 62-67.

Baker, Brendon M, and Christopher S Chen. “Deconstructing the third dimension: how 3D culture microenvironments alter cellular cues.” Journal of cell science vol. 125, Pt 13 (2012): 3015-24.

Barford, D. (2011). Structure, function and mechanism of the anaphase promoting complex (APC/C). Quarterly Reviews of Biophysics, 44(2), 153-190.

Bartel, L., & Mosabbir, A. (2021). Possible Mechanisms for the Effects of Sound Vibration on Human Health. Healthcare (Basel, Switzerland), 9(5), 597.

Bentov, I., Damodarasamy, M., Plymate, S., & Reed, M. J. (2014). Decreased proliferative capacity of aged dermal fibroblasts in a three dimensional matrix is associated with reduced IGF1R expression and activation. Biogerontology, 15(4), 329–337.

Berry, C. C., Dalby, M. J., McCloy, D., & Affrossman, S. (2005). The fibroblast response to tubes exhibiting internal nanotopography. Biomaterials, 26(24), 4985–4992.

Bhattacharjee, P., Cavanagh, B. L., & Ahearne, M. (2020). Effect of substrate topography on the regulation of human corneal stromal cells. Colloids and Surfaces B: Biointerfaces, 190, 110971.

Biggs, M. J. P., Curtis, A. S. G., Salmerón-Sánchez, M., Reid, S., & Dalby, M. J. (2017). Stimulation of 3D osteogenesis by mesenchymal stem cells using a nanovibrational bioreactor. Nature biomedical engineering, 1(9), 758–770.

Borthwick, L. A., Wynn, T. A., & Fisher, A. J. (2013). Cytokine mediated tissue fibrosis. Biochimica et Biophysica Acta (BBA) - Molecular Basis of Disease, 1832(7), 1049-1060.

Bryan, N., Ahswin, H., Smart, N., Bayon, Y., Wohlert, S., & Hunt, J. A. (2012). Reactive oxygen species (ROS) – A family of fate deciding molecules pivotal in constructive inflammation and wound healing. European Cells and Materials, 24, 249-265.

Buscemi, L., Ramonet, D., Klingberg, F., Formey, A., Smith-Clerc, J., Meister, J. J., & Hinz, B. (2011). The single-molecule mechanics of the latent TGF-β1 complex. Current biology : CB, 21(24), 2046–2054.

van Caam, A., Vonk, M., van den Hoogen, F., van Lent, P., & van der Kraan, P. (2018). Unraveling SSc Pathophysiology; The Myofibroblast. Frontiers in immunology, 9, 2452.

Campos, M. S., Volpon, J. B., Ximenez, J. P. B., Franttini, A. P., Dalloul, C. E., Sousa-Neto, M. D., Silva, R. A., Kacena, M. A., & Zamarioli, A. (2022). Vibration therapy as an effective approach to improve bone healing in diabetic rats. Frontiers in endocrinology, 13, 909317.

Cao, Z., Liao, Q., Su, M., Huang, K., Jin, J., & Cao, D. (2019). AKT and ERK dual inhibitors: The way forward? Cancer Letters, 459, 30-40.

Carthy, J. M., Sundqvist, A., Heldin, A., van Dam, H., Kletsas, D., Heldin, C. H., & Moustakas, A. (2015). Tamoxifen Inhibits TGF-β-Mediated Activation of Myofibroblasts by Blocking Non-Smad Signaling Through ERK1/2. Journal of cellular physiology, 230(12), 3084–3092.

Cerciello, S., Rossi, S., Visonà, E., Corona, K., & Oliva, F. (2016). Clinical applications of vibration therapy in orthopaedic practice. Muscles, ligaments and tendons journal, 6(1), 147–156.

Chen B., Lin T., Yang X., Li Y., Xie D., Zheng W., Cui H., Deng W. and Tan X. (2016). Low-magnitude, high-frequency vibration promotes the adhesion and the osteogenic differentiation of bone marrow-derived mesenchymal stem cells cultured on a hydroxyapatite-coated surface: The direct role of Wnt/ß-catenin signaling pathway activation. International Journal of Molecular Medicine, 38, 1531-1540.

Chen Z., Zhang N., Chu H.Y., Yu Y., Zhang Z-K., Zhang G. and Zhang B-T. (2020) Connective Tissue Growth Factor: From Molecular Understandings to Drug Discovery. Front. Cell Dev. Biol. 8:593269.

Cheung, W. H., Wong, R. M. Y., Choy, V. M. H., Li, M. C. M., Cheng, K. Y. K., & Chow, S. K. H. (2021). Enhancement of osteoporotic fracture healing by vibration treatment: The role of osteocytes. Injury, 52(Supplement 2), S97-S100.

Chi, Y.-H., Wang, W.-P., Hung, M.-C., Liou, G.-G., Wang, J.-Y., & Chao, P.-H. G. (2022). Deformation of the nucleus by TGFß1 via the remodeling of nuclear envelope and histone isoforms. Epigenetics & Chromatin, 15(1), 1.

Cialdai, F., Risaliti, C., & Monici, M. (2022). Role of fibroblasts in wound healing and tissue remodeling on Earth and in space. Frontiers in bioengineering and biotechnology, 10, 958381.

Collins, A.R. (2014). Measuring oxidative damage to DNA and its repair with the comet assay. Biochimica et Biophysica Acta (BBA), 1840(2), 794-800.

Condorelli, A. G., El Hachem, M., Zambruno, G., & Castiglia, D. (2021). Notch-ing up knowledge on molecular mechanisms of skin fibrosis: focus on the multifaceted Notch signalling pathway. Journal of Biomedical Science, 28(1), 36.

Cox, T. R., & Erler, J. T. (2011). Remodeling and homeostasis of the extracellular matrix: implications for fibrotic diseases and cancer. Disease models & mechanisms, 4(2), 165–178.

Creek, D. J., Jankevics, A., Burgess, K. E. V., Breitling, R., & Barrett, M. P. (2012). IDEOM: An Excel interface for analysis of LC-MS-based metabolomics data. Bioinformatics, 28(7), 1048-1049.

Cui, Y., Hameed, F. M., Yang, B., Lee, K., Pan, C. Q., Park, S., & Sheetz, M. (2015). Cyclic stretching of soft substrates induces spreading and growth. Nature Communications, 6, 6333.

Dadrich, M., Nicolay, N. H., Flechsig, P., Bickelhaupt, S., Hoeltgen, L., Roeder, F., Hauser, K., Tietz, A., Jenne, J., Lopez, R., Roehrich, M., Wirkner, U., Lahn, M., & Huber, P. E. (2016). Combined inhibition of TGFß and PDGF signaling attenuates radiation-induced pulmonary fibrosis. OncoImmunology, 5(5).

Dai, Z-X., Shih, P-J., Yen, J-Y., & Wang, I-J. (2022). Effect of Static and Dynamic Stretching on Corneal Fibroblast Cell Processes. Processes, 10(3), 605.

Daniels, J. T., Schultz, G. S., Blalock, T. D., Garrett, Q., Grotendorst, G. R., Dean, N. M., & Khaw, P. T. (2003). Mediation of transforming growth factor-beta(1)-stimulated matrix contraction by fibroblasts: a role for connective tissue growth factor in contractile scarring. The American journal of pathology, 163(5), 2043–2052.

Darby, I. A., Laverdet, B., Bonté, F., & Desmoulière, A. (2014). Fibroblasts and myofibroblasts in wound healing. Clinical, cosmetic and investigational dermatology, 7, 301–311.

Datta, N., Pham, Q. P., Sharma, U., et al. (2006). In vitro generated extracellular matrix and fluid shear stress synergistically enhance 3D osteoblastic differentiation. Proceedings of the National Academy of Sciences, 103(8), 2488-2493.

Davies, S.L., Gibbons, C.E., Vizard, T., & Ward, D.T. (2006). Ca2+-sensing receptor induces Rho kinase-mediated actin stress fiber assembly and altered cell morphology, but not in response to aromatic amino acids. American Journal of Physiology-Cell Physiology, 290(6), C1543-C1550.

Davis, J., Burr, A. R., Davis, G. F., Birnbaumer, L., & Molkentin, J. D. (2012). A TRPC6-dependent pathway for myofibroblast transdifferentiation and wound healing in vivo. Developmental cell, 23(4), 705–715.

Diller, R. B., & Tabor, A. J. (2022). The Role of the Extracellular Matrix (ECM) in Wound Healing: A Review. Biomimetics (Basel, Switzerland), 7(3), 87.

Dolivo, D. M., Larson, S. A., & Dominko, T. (2017). FGF2-mediated attenuation of myofibroblast activation is modulated by distinct MAPK signaling pathways in human dermal fibroblasts. Journal of dermatological science, 88(3), 339–348.

Dong, Y., Lv, D., Zhao, Z., Xu, Z., Hu, Z., & Tang, B. (2022). Lycorine inhibits hypertrophic scar formation by inducing ROS-mediated apoptosis. Frontiers in Bioengineering and Biotechnology, 10, 826093.

Donovan, J., Shiwen, X., Norman, J., & Abraham, D. (2013). Platelet-derived growth factor alpha and beta receptors have overlapping functional activities towards fibroblasts. Fibrogenesis & Tissue Repair, 6, 10.

Dosoki, H., Stegemann, A., Taha, M., Schnittler, H., Luger, T. A., Schröder, K., Distler, J. H., Kerkhoff, C., & Böhm, M. (2017). Targeting of NADPH oxidase in vitro and in vivo suppresses fibroblast activation and experimental skin fibrosis. Experimental dermatology, 26(1), 73–81.

Du, X., Liu, T., Shen, C., He, B., Feng, M., Liu, J., Zhuo, W., Fu, G., Wang, B., Xu, Y., & Chu, H. (2022). Anti-fibrotic mechanism of SPP1 knockdown in atrial fibrosis associates with inhibited mitochondrial DNA damage and TGF-β/SREBP2/PCSK9 signaling. Cell Death Discovery, 8, 246.

Dunnill, C., Patton, T., Brennan, J., Barrett, J., Dryden, M., Cooke, J., Leaper, D., & Georgopoulos, N. T. (2017). Reactive oxygen species (ROS) and wound

healing: The functional role of ROS and emerging ROS-modulating technologies for augmentation of the healing process. Volume 14, Issue 1, 89-96.

D'Urso, M., & Kurniawan, N. A. (2020). Mechanical and Physical Regulation of Fibroblast-Myofibroblast Transition: From Cellular Mechanoresponse to Tissue Pathology. Frontiers in bioengineering and biotechnology, 8, 609653.

El-Mohri, H., Wu, Y., Mohanty, S., & Ghosh, G. (2017). Impact of matrix stiffness on fibroblast function. Materials science & engineering. C, Materials for biological applications, 74, 146–151.

Elosegui-Artola, A., Andreu, I., Beedle, A. E. M., Lezamiz, A., Uroz, M., Kosmalska, A. J., Oria, R., Kechagia, J. Z., Rico-Lastres, P., Le Roux, A. L., Shanahan, C. M., Trepat, X., Navajas, D., Garcia-Manyes, S., & Roca-Cusachs, P. (2017). Force Triggers YAP Nuclear Entry by Regulating Transport across Nuclear Pores. Cell, 171(6), 1397–1410.e14.

Enomoto, U, Imashiro, C, Takemura, K. (2020) Collective cell migration of fibroblasts is affected by horizontal vibration of the cell culture dish. Eng Life Sci. 20: 402– 411.

Estornut, C., Milara, J., Bayarri, M. A., Belhadj, N., & Cortijo, J. (2021). Targeting Oxidative Stress as a Therapeutic Approach for Idiopathic Pulmonary Fibrosis. Frontiers in Pharmacology, 12, 794997.

Everaert, C., Luypaert, M., Maag, J. L. V., Cheng, Q. X., Dinger, M. E., Hellemans, J., & Mestdagh, P. (2017). Benchmarking of RNA-sequencing analysis workflows using whole-transcriptome RT-qPCR expression data. Scientific reports, 7(1), 1-13.

Fang, B., Liu, Y., Zheng, D., et al. (2019). The effects of mechanical stretch on the biological characteristics of human adipose-derived stem cells. Journal of Cellular and Molecular Medicine, 23, 4244-4255.

Fang, L., Neutzner, A., Turtschi, S., Flammer, J., & Mozaffarieh, M. (2015). Comet assay as an indirect measure of systemic oxidative stress. Journal of visualized experiments : JoVE, (99), e52763.

Feng, Y., Wu, J. J., Sun, Z. L., Liu, S. Y., Zou, M. L., Yuan, Z. D., Yu, S., Lv, G. Z., & Yuan, F. L. (2020). Targeted apoptosis of myofibroblasts by elesclomol inhibits hypertrophic scar formation. eBio Medicine, 54, 102715.

Farooq, M., Khan, A. W., Kim, M. S., & Choi, S. (2021). The Role of Fibroblast Growth Factor (FGF) Signaling in Tissue Repair and Regeneration. Cells, 10(11), 3242.

Finnson, K. W., Almadani, Y., & Philip, A. (2020). Non-canonical (non-SMAD2/3) TGF-β signaling in fibrosis: Mechanisms and targets. Seminars in Cell & Developmental Biology, 101, 115-122.

Fortier, S. M., Penke, L. R., King, D., Pham, T. X., Ligresti, G., & Peters-Golden, M. (2021). Myofibroblast dedifferentiation proceeds via distinct transcriptomic and phenotypic transitions. JCI Insight, 6(6), e144799.

Franco, R., & Cidlowski, J. (2009). Apoptosis and glutathione: beyond an antioxidant. Cell Death & Differentiation, 16(10), 1303–1314.

Frangogiannis N. (2020). Transforming growth factor-ß in tissue fibrosis. The Journal of experimental medicine, 217(3), e20190103.

Franklin, RA. (2021). Fibroblasts and macrophages: Collaborators in tissue homeostasis. Immunol Rev, 302, 86–103.

Fratini, A., Bonci, T., & Bull, A. M. J. (2016). Whole Body Vibration Treatments in Postmenopausal Women Can Improve Bone Mineral Density: Results of a Stimulus Focussed Meta-Analysis. PLOS ONE, 11(12), e0166774.

Frost, J., Estivill, X., Ramsay, M., & Tikly, M. (2019). Dysregulation of the Wnt signaling pathway in South African patients with diffuse systemic sclerosis. Clinical rheumatology, 38(3), 933–938.

Fujisawa, Y., Matsuda, K., & Uehara, T. (2020). Osteopontin enhances the migration of lung fibroblasts via upregulation of interleukin-6 through the extracellular signal-regulated kinase (ERK) pathway. Biological Chemistry, 401(9), 1071-1080.

Ghosh, A. K., & Vaughan, D. E. (2012). PAI-1 in tissue fibrosis. Journal of cellular physiology, 227(2), 493–507.

Gnaiger, E., Kuznetsov, A. V., Königsrainer, A., & Margreiter, R. (1999). Autooxidation and stabilization of reduced glutathione in organ preservation solutions. Transplantation, 67(9), S653.

Goffin, J. M., Pittet, P., Csucs, G., Lussi, J. W., Meister, J. J., & Hinz, B. (2006). Focal adhesion size controls tension-dependent recruitment of alpha-smooth muscle actin to stress fibers. The Journal of cell biology, 172(2), 259–268.

Gonzalez, A. C., Costa, T. F., Andrade, Z. A., & Medrado, A. R. (2016). Wound healing - A literature review. Anais brasileiros de dermatologia, 91(5), 614–620.

Goodman, M. B., Haswell, E. S., Vásquez, V. (2023). Mechanosensitive membrane proteins: Usual and unusual suspects in mediating mechanotransduction. J Gen Physiol, 155(3), e202213248.

Goult, B. T., Yan, J., & Schwartz, M. A. (2018). Talin as a mechanosensitive signaling hub. The Journal of cell biology, 217(11), 3776–3784.

Grosche, J., Meißner, J., & Eble, J. A. (2018). More than a syllable in fib-ROS-is: The role of ROS on the fibrotic extracellular matrix and on cellular contacts. Molecular Aspects of Medicine, 63, 30-46.

Gross, A., & Katz, S. G. (2017). Non-apoptotic functions of BCL-2 family proteins. Cell death and differentiation, 24(8), 1348–1358.

Guimaraes, J. C., & Zavolan, M. (2016). Patterns of ribosomal protein expression specify normal and malignant human cells. Genome biology, 17(1), 236.

Gupta, S., Patel, L., Mitra, K., & Bit, A. (2022). Fibroblast Derived Skin Wound Healing Modeling on Chip under the Influence of Micro-Capillary Shear Stress. Micromachines, 13(2), 305.

Gutiérrez, J., Droppelmann, C. A., Contreras, O., Takahashi, C., & Brandan, E. (2015). RECK-Mediated ß1-Integrin Regulation by TGF-ß1 Is Critical for Wound Contraction in Mice. PloS one, 10(8), e0135005.

Han, S. B., Kim, J. K., Lee, G.,Kim, D.-H. (2020). Mechanical Properties of Materials for Stem Cell Differentiation. Advanced Biosystems, 4, 2000247.

He, J., Fang, B., Shan, S., Xie, Y., Wang, C., Zhang, Y., Zhang, X., & Li, Q. (2021). Mechanical stretch promotes hypertrophic scar formation through mechanically activated cation channel Piezo1. Cell death & disease, 12(3), 226.

van Heuvelen, M. J. G., Rittweger, J., Judex, S., Sañudo, B., Seixas, A., Fuermaier, A. B. M., Tucha, O., Nyakas, C., Marín, P. J., Taiar, R., Stark, C., Schoenau, E., Sá-Caputo, D. C., Bernardo-Filho, M., & van der Zee, E. A. (2021). Reporting Guidelines for Whole-Body Vibration Studies in Humans, Animals and Cell Cultures: A Consensus Statement from an International Group of Experts. Biology, 10(10), 965.

Hewitson, T. D., & Smith, E. R. (2021). A metabolic reprogramming of glycolysis and glutamine metabolism is a requisite for renal fibrogenesis-why and how?. Frontiers in Physiology, 12, 645857.

Hinz, B. (2007). Formation and Function of the Myofibroblast during Tissue Repair. Journal of Investigative Dermatology, 127(3), 526-537.

Hinz B. (2015). The extracellular matrix and transforming growth factor-ß1: Tale of a strained relationship. Matrix biology : journal of the International Society for Matrix Biology, 47, 54–65.

Holmes, H.R., Vlaisavljevich, E., Tan, E.L., Snyder, K.L., Ong, K.G., & Rajachar, R.M. (2018). Control of cellular adhesion and myofibroblastic character with sub-micrometer magnetoelastic vibrations. Journal of Biomechanics, 71, 199-207.

Holt, J. R., Zeng, W. Z., Evans, E. L., Woo, S. H., Ma, S., Abuwarda, H., Loud, M., Patapoutian, A., & Pathak, M. M. (2021). Spatiotemporal dynamics of PIEZO1 localization controls keratinocyte migration during wound healing. eLife, 10, e65415.

Hortobagyi, D., Grossmann, T., Tschernitz, M., Grill, M., Kirsch, A., Gerstenberger, C., & Gugatschka, M. (2020). In vitro mechanical vibration down-regulates pro-inflammatory and pro-fibrotic signaling in human vocal fold fibroblasts. PloS one, 15(11), e0241901.

Huang, C., Holfeld, J., Schaden, W., Orgill, D., & Ogawa, R. (2013). Mechanotherapy: Revisiting physical therapy and recruiting mechanobiology for a new era in medicine. Trends in Molecular Medicine, 19(9), 555-564.

Huang, C., & Ogawa, R. (2012). Fibroproliferative disorders and their mechanobiology. Connective Tissue Research, 53(3), 187-196.

Huang, X., Yang, N., Fiore, V. F., Barker, T. H., Sun, Y., Morris, S. W., Ding, Q., Thannickal, V. J., & Zhou, Y. (2012). Matrix stiffness-induced myofibroblast differentiation is mediated by intrinsic mechanotransduction. American journal of respiratory cell and molecular biology, 47(3), 340–348.

Huang, Y., Qian, J. Y., Cheng, H., & Li, X. M. (2021). Effects of shear stress on differentiation of stem cells into endothelial cells. World journal of stem cells, 13(7), 894–913.

Hunter, C., Bond, J., Kuo, P. C., Selim, M. A., & Levinson, H. (2012). The role of osteopontin and osteopontin aptamer (OPN-R3) in fibroblast activity. Journal of Surgical Research, 176(1), 348-358.

Hurd, T. R., DeGennaro, M., & Lehmann, R. (2012). Redox regulation of cell migration and adhesion. Trends in cell biology, 22(2), 107–115.

Igbokwe, E. O., Taube, W., & Beinert, K. (2022). A Comparison of the Effects of Stochastic Resonance Therapy, Whole-Body Vibration, and Balance Training on Pain Perception and Sensorimotor Function in Patients With Chronic Nonspecific Neck Pain: Protocol for a Randomized Controlled Trial. JMIR research protocols, 11(6), e34430.

Iturriaga, L., Van Gordon, K.D., Larrañaga-Jaurrieta, G. and Camarero-Espinosa, S. (2021), Strategies to Introduce Topographical and Structural Cues in 3D-Printed Scaffolds and Implications in Tissue Regeneration. Adv. NanoBiomed Res., 1: 2100068.

Iwanicki, M. P., Vomastek, T., Tilghman, R. W., Martin, K. H., Banerjee, J., Wedegaertner, P. B., & Parsons, J. T. (2008). FAK, PDZ-RhoGEF and ROCKII cooperate to regulate adhesion movement and trailing-edge retraction in fibroblasts. Journal of Cell Science, 121(6).

Jain, M., Rivera, S., Monclus, E. A., Synenki, L., Zirk, A., Eisenbart, J., Feghali-Bostwick, C., Mutlu, G. M., Budinger, G. R., & Chandel, N. S. (2013). Mitochondrial reactive oxygen species regulate transforming growth factor-ß signaling. The Journal of biological chemistry, 288(2), 770–777.

Janda, J., Nfonsam, V., Calienes, F., Sligh, J. E., & Jandova, J. (2016). Modulation of ROS levels in fibroblasts by altering mitochondria regulates the process of wound healing. Archives of Dermatological Research, 308(4), 239-248.

Jiang, Y. Y., Park, J. K., Yoon, H. H., Choi, H., Kim, C. W., & Seo, Y. K. (2015). Enhancing proliferation and ECM expression of human ACL fibroblasts by sonic vibration. Preparative biochemistry & biotechnology, 45(5), 476–490.

Joannes, A., Brayer, S., Besnard, V., Marchal-Sommé, J., Jaillet, M., Mordant, P., Mal, H., Borie, R., Crestani, B., & Mailleux, A. A. (2016). FGF9 and FGF18 in idiopathic pulmonary fibrosis promote survival and migration and inhibit myofibroblast differentiation of human lung fibroblasts in vitro. American Journal of Physiology-Lung Cellular and Molecular Physiology, 310(7).

Jobling, M. F., Mott, J. D., Finnegan, M. T., Jurukovski, V., Erickson, A. C., Walian, P. J., Taylor, S. E., Ledbetter, S., Lawrence, C. M., Rifkin, D. B., & Barcellos-Hoff, M. H. (2006). Isoform-specific activation of latent transforming growth factor ß (LTGF-ß) by reactive oxygen species. Radiation Research, 166(6), 839-848.

Johnson, B. Z., Stevenson, A. W., Prêle, C. M., Fear, M. W., & Wood, F. M. (2020). The Role of IL-6 in Skin Fibrosis and Cutaneous Wound Healing. Biomedicines, 8(5), 101.

Jones, H., Feth, L., Rumpf, D., Hefti, A., & Mariotti, A. (2000). Acoustic energy affects human gingival fibroblast proliferation but leaves protein production unchanged. Journal of clinical periodontology, 27(11), 832–838.

Juhl, P., Bondesen, S., Hawkins, C.L., Karsdal, M.A., & Siebuhr, A.S. (2020). Dermal fibroblasts have different extracellular matrix profiles induced by TGF-ß, PDGF and IL-6 in a model for skin fibrosis. Scientific Reports, 10(1), 17300.

Jungbauer, S., Gao, H., Spatz, J. P., & Kemkemer, R. (2008). Two Characteristic Regimes in Frequency-Dependent Dynamic Reorientation of Fibroblasts on Cyclically Stretched Substrates. Biophysical Journal, 95(7), 3470-3478.

Kanta J. (2015). Collagen matrix as a tool in studying fibroblastic cell behavior. Cell adhesion & migration, 9(4), 308–316.

Karamanos, N.K., Theocharis, A.D., Piperigkou, Z., Manou, D., Passi, A., Skandalis, S.S., Vynios, D.H., Orian-Rousseau, V., Ricard-Blum, S., Schmelzer, C.E.H., Duca, L., Durbeej, M., Afratis, N.A., Troeberg, L., Franchi, M., Masola, V. and Onisto, M. (2021), A guide to the composition and functions of the extracellular matrix. FEBS J, 288: 6850-6912.

Karska, J., Kowalski, S., Saczko, J., Moisescu, M. G., & Kulbacka, J. (2023). Mechanosensitive Ion Channels and Their Role in Cancer Cells. Membranes, 13(2), 167.

Kato, A., Okura, T., Hamada, C., Miyoshi, S., Katayama, H., Higaki, J., & Ito, R. (2014). Cell stress induces upregulation of osteopontin via the ERK pathway in type II alveolar epithelial cells. PloS One, 9(6), e100106.

Kendall, R. T., & Feghali-Bostwick, C. A. (2014). Fibroblasts in fibrosis: novel roles and mediators. Frontiers in pharmacology, 5, 123.

Kennedy, J.W., Tsimbouri, P.M., Campsie, P., Sood, S., Childs, P.G., Reid, S., Young, P.S., Meek, D.R.M., Goodyear, C.S., & Dalby, M.J. (2021). Nanovibrational stimulation inhibits osteoclastogenesis and enhances osteogenesis in co-cultures. Scientific Reports, 11, 22741.

Kennedy, J.W., Tsimbouri, P.M., Campsie, P., Sammons, R.L., García-Gareta, E., Oreffo, R.O., Dalby, M.J. (2021). Nanovibrational stimulation inhibits osteoclastogenesis and enhances osteogenesis in co-cultures. Scientific Reports, 11(1), 22741.

Khorsandi, K., Hosseinzadeh, R., Esfahani, H. S., Zandsalimi, K., Shahidi, F. K., & Abrahamse, H. (2022). Accelerating skin regeneration and wound healing by controlled ROS from photodynamic treatment. Inflammation and Regeneration, 42, 40.

Kilebrant, S., Braathen, G., Emilsson, R., Glansén, U., Söderpalm, A. C., Zetterlund, B., Westerberg, B., Magnusson, P., & Swolin-Eide, D. (2015). Whole-body vibration therapy in children with severe motor disabilities. Journal of rehabilitation medicine, 47(3), 223–228.

Kim, D., Paggi, J. M., Park, C., et al. (2019). Graph-based genome alignment and genotyping with HISAT2 and HISAT-genotype. Nature biotechnology, 37(8), 907-915.

Kim, I. S., Song, Y. M., Lee, B., & Hwang, S. J. (2012). Human Mesenchymal Stromal Cells are Mechanosensitive to Vibration Stimuli. Journal of Dental Research, 91(12), 1135-1140.

Kim, M. H., Sawada, Y., Taya, M., et al. (2014). Influence of surface topography on the human epithelial cell response to micropatterned substrates with convex and concave architectures. Journal of Biological Engineering, 8, 13.

Kim, M. S., Baek, A. R., Lee, J. H., Jang, A. S., Kim, D. J., Chin, S. S., & Park, S. W. (2019). IL-37 attenuates lung fibrosis by inducing autophagy and regulating TGF-β1 production in mice. Journal of Immunology, 203(8), 2265-2275.

Kim, N. G., & Gumbiner, B. M. (2015). Adhesion to fibronectin regulates Hippo signaling via the FAK-Src-PI3K pathway. The Journal of cell biology, 210(3), 503–515.

Kimura, S. and Tsuji, T. (2021). Mechanical and Immunological Regulation in Wound Healing and Skin Reconstruction. International Journal of Molecular Sciences, 22(11), 5474.

Kirk, T., Ahmed, A., & Rognoni, E. (2021). Fibroblast Memory in Development, Homeostasis and Disease. Cells, 10(11), 2840.

Klingberg, F., Hinz, B., & White, E. S. (2013). The myofibroblast matrix: implications for tissue repair and fibrosis. The Journal of pathology, 229(2), 298–309.

Kobayashi, T., Liu, X., Kim, H. J., Kohyama, T., Wen, F.-Q., Abe, S., Fang, Q., Zhu, Y. K., Spurzem, J. R., Bitterman, P., & Rennard, S. I. (2005). TGF-β1 and serum both stimulate contraction but differentially affect apoptosis in 3D collagen gels. Respiratory Research, 6(1), 141.

Kollmannsberger, P., Bidan, C. M., Dunlop, J. W. C., & Fratzl, P. (2018). Tensile forces drive a reversible fibroblast-to-myofibroblast transition during tissue growth in engineered clefts. Science Advances, 4(3), eaao4881.

Kong, X., Ma, L., Ji, Z., Dong, Z., Zhang, Z., Hou, J., Zhang, S., Ma, L., & Jiang, L. (2018). Pro-fibrotic effect of IL-6 via aortic adventitial fibroblasts indicates IL-

6 as a treatment target in Takayasu arteritis. Clinical and experimental rheumatology, 36(1), 62–72.

Kottmann, R. M., Trawick, E., Judge, J. L., Wahl, L. A., Epa, A. P., Owens, K. M., Thatcher, T. H., Phipps, R. P., & Sime, P. J. (2015). Pharmacologic inhibition of lactate production prevents myofibroblast differentiation. American journal of physiology. Lung cellular and molecular physiology, 309(11), L1305–L1312.

Kregel, K. C., & Zhang, H. J. (2007). An integrated view of oxidative stress in aging: basic mechanisms, functional effects, and pathological considerations. American Journal of Physiology-Regulatory, Integrative and Comparative Physiology, 292(1), R18-R36.

Kubiczkova, L., Sedlarikova, L., Hajek, R., & Sevcikova, S. (2012). TGF-β – an excellent servant but a bad master. Journal of Translational Medicine, 10, 183.

Kulasekaran, P., Scavone, C. A., Rogers, D. S., Arenberg, D. A., Thannickal, V. J., & Horowitz, J. C. (2009). Endothelin-1 and transforming growth factor-beta1 independently induce fibroblast resistance to apoptosis via AKT activation. American journal of respiratory cell and molecular biology, 41(4), 484–493.

Küppers, M., Faust, D., Linz, B., & Dietrich, C. (2011). Regulation of ERK1/2 activity upon contact inhibition in fibroblasts. Biochemical and Biophysical Research Communications, 406(3), 483-487.

Kutty, J. K., & Webb, K. (2010). Vibration stimulates vocal mucosa-like matrix expression by hydrogel-encapsulated fibroblasts. Journal of Tissue Engineering and Regenerative Medicine, 4(1), 62-72.

Lafyatis R. (2014). Transforming growth factor β--at the centre of systemic sclerosis. Nature reviews. Rheumatology, 10(12), 706–719.

Lau, E., Lee, W. D., Li, J., Xiao, A., Davies, J. E., Wu, Q., Wang, L., & You, L. (2011). Effect of low-magnitude, high-frequency vibration on osteogenic differentiation of rat mesenchymal stromal cells. Journal of orthopaedic research : official publication of the Orthopaedic Research Society, 29(7), 1075–1080.

Lau, R. W., Liao, L. R., Yu, F., Teo, T., Chung, R. C., & Pang, M. Y. (2011). The effects of whole body vibration therapy on bone mineral density and leg muscle strength in older adults: A systematic review and meta-analysis. Clinical Rehabilitation, 25(11), 975-988.

Lei, X., Liu, B., Wu, H., Wu, X., Wang, X. L., Song, Y., Zhang, S. S., Li, J. Q., Bi, L., & Pei, G. X. (2020). The effect of fluid shear stress on fibroblasts and stem cells on plane and groove topographies. Cell adhesion & migration, 14(1), 12–23.

Lenga, Y., Koh, A., Perera, A. S., McCulloch, C. A., Sodek, J., & Zohar, R. (2008). Osteopontin expression is required for myofibroblast differentiation. Circulation Research, 102, 319-327.

Li, B., & Wang, J. H. (2011). Fibroblasts and myofibroblasts in wound healing: force generation and measurement. Journal of tissue viability, 20(4), 108–120.

Li, D., & Wang, J. (2020). Ribosome heterogeneity in stem cells and development. Journal of Cell Biology, 219(6), e202001108.

Li, J., Liu, X., Zuo, B., & Zhang, L. (2015). The Role of Bone Marrow Microenvironment in Governing the Balance between Osteoblastogenesis and Adipogenesis. Aging and disease, 7(4), 514–525.

Li, S. S., He, S. H., Xie, P.-Y., Li, W., Zhang, X.X., Li, T.-F., & Li, D.-F. (2021). Recent Progresses in the Treatment of Osteoporosis. Frontiers in Pharmacology, 12.

Liao, Y., Smyth, G. K., & Shi, W. (2013). The Subread aligner: fast, accurate and scalable read mapping by seed-and-vote. Nucleic acids research, 41(10), e108.

Lietha, D., & Izard, T. (2020). Roles of Membrane Domains in Integrin-Mediated Cell Adhesion. International journal of molecular sciences, 21(15), 5531.

Lin, Y., Wang, Y., & Li, P. (2022). Mutual regulation of lactate dehydrogenase and redox robustness. Frontiers in Physiology, 13, 1038421.

Lipson, K. E., Wong, C., Teng, Y., & Spong, S. (2012). CTGF is a central mediator of tissue remodeling and fibrosis and its inhibition can reverse the process of fibrosis. Fibrogenesis & Tissue Repair, 5(1), S24.

Liu, F., Lagares, D., Choi, K. M., Stopfer, L., Marinković, A., Vrbanac, V., Probst, C. K., Hiemer, S. E., Sisson, T. H., Horowitz, J. C., Rosas, I. O., Fredenburgh, L. E., Feghali-Bostwick, C., Varelas, X., Tager, A. M., & Tschumperlin, D. J. (2015). Mechanosignaling through YAP and TAZ drives fibroblast activation and fibrosis. Science Translational Medicine, 7(367), 367ra166.

Liu, R. M., & Desai, L. P. (2015). Reciprocal regulation of TGF-ß and reactive oxygen species: A perverse cycle for fibrosis. Redox Biology, 6, 565-577.

Liu, R. M., & Gaston Pravia, K. A. (2010). Oxidative stress and glutathione in TGF-beta-mediated fibrogenesis. Free radical biology & medicine, 48(1), 1–15.

Liu, S., Shi-wen, X., Kennedy, L., Pala, D., Chen, Y., Eastwood, M., Carter, D. E., Black, C. M., Abraham, D. J., & Leask, A. (2007). FAK is required for TGFß-induced JNK phosphorylation in fibroblasts: Implications for acquisition of a matrix-remodeling phenotype. Molecular Biology of the Cell, 18(6), 2169-2178.

Liu, Y., Rath, B., Tingart, M., & Eschweiler, J. (2020). Role of implants surface modification in osseointegration: A systematic review. Journal of biomedical materials research. Part A, 108(3), 470–484.

Lopes-Souza, P., Dionello, C. F., Sá-Caputo, D. da C., Moreira-Marconi, E., Frederico, E. H. F., Marchon, R. M., Bergmann, A., Furness, T., Bernardo-Filho, M. (2018). Whole body vibration exercise in the management of cancer therapy-related morbidities: A systematic review. Drug Discoveries & Therapeutics, 12(4), 239-247.

Love, M. I., Huber, W., & Anders, S. (2014). Moderated estimation of fold change and dispersion for RNA-seq data with DESeq2. Genome Biology, 15(12), 550.

Lu, W., Su, X., Klein, M. S., Lewis, I. A., Fiehn, O., & Rabinowitz, J. D. (2017). Metabolite measurement: Pitfalls to avoid and practices to follow. Annual review of biochemistry, 86, 277-304.

Lu, Y., Zhao, Q., Liu, Y., Zhang, L., Li, D., Zhu, Z., Gan, X., & Yu, H. (2018). Vibration loading promotes osteogenic differentiation of bone marrow-derived mesenchymal stem cells via p38 MAPK signaling pathway. Journal of Biomechanics, 71, 67-75.

Lu, Y. Y., Wu, C. H., Hong, C. H., Chang, K. L., & Lee, C. H. (2021). GLUT-1 Enhances Glycolysis, Oxidative Stress, and Fibroblast Proliferation in Keloid. Life, 11(6), 505.

Lund, S. A., Giachelli, C. M., & Scatena, M. (2009). The role of osteopontin in inflammatory processes. Journal of cell communication and signaling, 3(3-4), 311–322.

Macarak, E. J., Wermuth, P. J., Rosenbloom, J., & Uitto, J. (2021). Keloid disorder: Fibroblast differentiation and gene expression profile in fibrotic skin diseases. Experimental Dermatology, 30, 132-145.

Maiworm, A. , Monteiro, M. , Santos-Filho, S. , Lopes, A. , Azeredo, L. , Missailidis, S. , Marín, P. and Bernardo-Filho, M. (2011) Cystic fibrosis and the relevance of the whole-body vibration exercises in oscillating platforms: a short review. Health, 3, 656-662.

Mabry, K. M., Lawrence, R. L., & Anseth, K. S. (2015). Dynamic stiffening of poly(ethylene glycol)-based hydrogels to direct valvular interstitial cell phenotype in a three-dimensional environment. Biomaterials, 49, 47–56.

Marín-Cascales, E., Alcaraz, P. E., Ramos-Campo, D. J., Martinez-Rodriguez, A., Chung, L. H., & Rubio-Arias, J. Á. (2018). Whole-body vibration training and bone health in postmenopausal women: A systematic review and meta-analysis. Medicine, 97(34), e11918.

Marin-Puyalto, J., Gomez-Cabello, A., Gonzalez-Agüero, A., Gomez-Bruton, A., Matute-Llorente, A., Casajús, J. A., & Vicente-Rodríguez, G. (2018). Is Vibration Training Good for Your Bones? BioMed Research International. Volume 2018, Article ID 5178284.

Masai, H., Yang, C. C., & Matsumoto, S. (2017). Mrc1/Claspin: A new role for regulation of origin firing. Current Genetics, 63(5), 813-818.

Mateu, R., Živicová, V., Krejčí, E.D., Grim, M., Strnad, H., Vlček, Č., Kolář, M., Lacina, L., Gál, P., Borský, J., Smetana Jr, K., & Dvořánková, B. (2016). Functional differences between neonatal and adult fibroblasts and keratinocytes: Donor age affects epithelial-mesenchymal crosstalk in vitro. International Journal of Molecular Medicine, 38, 1063-1074

Mathew-Steiner, S. S., Roy, S., & Sen, C. K. (2021). Collagen in Wound Healing. Bioengineering (Basel, Switzerland), 8(5), 63.

Mescher A. L. (2017). Macrophages and fibroblasts during inflammation and tissue repair in models of organ regeneration. Regeneration (Oxford, England), 4(2), 39–53.

Michaeloudes, C., Sukkar, M. B., Khorasani, N. M., Bhavsar, P. K., & Chung, K. F. (2011). TGF-β regulates Nox4, MnSOD and catalase expression, and IL-6 release in airway smooth muscle cells. American Journal of Physiology-Lung Cellular and Molecular Physiology, 300(2), L295-L304.

Micholt, L., Gärtner, A., Prodanov, D., Braeken, D., Dotti, C. G., & Bartic, C. (2013). Substrate Topography Determines Neuronal Polarization and Growth In Vitro. PLOS ONE, 8(6), e66170.

Mimura, Y., Ihn, H., Jinnin, M., Asano, Y., Yamane, K., & Tamaki, K. (2005). Constitutive Phosphorylation of Focal Adhesion Kinase Is Involved in the Myofibroblast Differentiation of Scleroderma Fibroblasts. Journal of Investigative Dermatology, 124(5), 886-892.

Mohammed, T., Murphy, M. F., Lilley, F., Burton, D. R., & Bezombes, F. (2016). The effects of acoustic vibration on fibroblast cell migration. Materials science & engineering. C, Materials for biological applications, 69, 1256–1262.

Moodley, Y. P., Misso, N. L., Scaffidi, A. K., Fogel-Petrovic, M., McAnulty, R. J., Laurent, G. J., Thompson, P. J., & Knight, D. A. (2003). Inverse effects of interleukin-6 on apoptosis of fibroblasts from pulmonary fibrosis and normal lungs. American journal of respiratory cell and molecular biology, 29(4), 490–498.

Moretti, L., Stalfort, J., Barker, T. H., & Abebayehu, D. (2022). The interplay of fibroblasts, the extracellular matrix, and inflammation in scar formation. JBC Reviews, 298(2), 101530.

Mori, R., Shaw, T. J., & Martin, P. (2008). Molecular mechanisms linking wound inflammation and fibrosis: knockdown of osteopontin leads to rapid repair and reduced scarring. The Journal of experimental medicine, 205(1), 43–51.

Mountford, S., Effenberger, M., Noll-Puchta, H., Griessmair, L., Ringleb, A., Haas, S., Denk, G., Reiter, F. P., Mayr, D., Dinarello, C. A., Tilg, H., & Bufler, P. (2021). Modulation of Liver Inflammation and Fibrosis by Interleukin-37. Frontiers in immunology, 12, 603649.

Murphy-Marshman, H., Quensel, K., Shi-Wen, X., Barnfield, R., Kelly, J., Peidl, A., Stratton, R. J., & Leask, A. (2017). Antioxidants and NOX1/NOX4 inhibition blocks TGFβ1-induced CCN2 and α-SMA expression in dermal and gingival fibroblasts. PloS one, 12(10), e0186740.

Murphy-Marshman, H., Quensel, K., Shi-wen, X., Barnfield, R., Kelly, J., Peidl, A., Stratton, R. J., & Leask, A. (2017). Antioxidants and NOX1/NOX4 inhibition blocks TGFβ1-induced CCN2 and α-SMA expression in dermal and gingival fibroblasts. Radical Biology and Medicine, 112, 44-47.

Murrell, G. A., Francis, M. J., & Bromley, L. (1990). Modulation of fibroblast proliferation by oxygen free radicals. The Biochemical journal, 265(3), 659–665.

Nakamura, R., Hiwatashi, N., Bing, R., Doyle, C. P., & Branski, R. C. (2021). Concurrent YAP/TAZ and SMAD signaling mediate vocal fold fibrosis. Scientific reports, 11(1), 13484.

Nakano, H., Nakajima, A., Sakon-Komazawa, S., Piao, J. H., Xue, X., Okumura, K., & Reactive, O. Species (2006). mediate crosstalk between NF-κB and JNK. Cell Death and Differentiation, 13(5), 730-737.

Nardone, G., Oliver-De La Cruz, J., Vrbsky, J., Martini, C., Pribyl, J., Skládal, P., Pešl, M., Caluori, G., Pagliari, S., Martino, F., Maceckova, Z., Hajduch, M., Sanz-Garcia, A., Pugno, N. M., Stokin, G. B., & Forte, G. (2017). YAP regulates cell mechanics by controlling focal adhesion assembly. Nature communications, 8, 15321.

Nguyen, J. K., Austin, E., Huang, A., Mamalis, A., & Jagdeo, J. (2020). The IL-4/IL-13 axis in skin fibrosis and scarring: mechanistic concepts and therapeutic targets. Archives of dermatological research, 312(2), 81–92.

Nguyen, A. T., Sathe, S. R., & Yim, E. K. (2016). From nano to micro: topographical scale and its impact on cell adhesion, morphology and contact guidance. Journal of physics. Condensed matter : an Institute of Physics journal, 28(18), 183001.

Nigdelioglu, R., Hamanaka, R. B., Meliton, A. Y., O'Leary, E., Witt, L. J., Cho, T., Sun, K., Bonham, C., Wu, D., Woods, P. S., Husain, A. N., Wolfgeher, D., Dulin, N. O., Chandel, N. S., & Mutlu, G. M. (2016). Transforming Growth Factor TGF-β Promotes de Novo Serine Synthesis for Collagen Production. The Journal of biological chemistry, 291(53), 27239–27251.

Nikoloudaki, G., Brooks, S., Peidl, A. P., Tinney, D., & Hamilton, D. W. (2020). JNK Signaling as a Key Modulator of Soft Connective Tissue Physiology, Pathology, and Healing. International journal of molecular sciences, 21(3), 1015.

Nikukar, H., Reid, S., Tsimbouri, P. M., Riehle, M. O., Curtis, A. S. G., & Dalby, M. J. (2013). Osteogenesis of Mesenchymal Stem Cells by Nanoscale Mechanotransduction. ACS Nano, 7(3), 2758-2767.

Nishimura, K., Blume, P., Ohgi, S., & Sumpio, B. E. (2009). The Effect of Different Frequencies of Stretch on Human Dermal Keratinocyte Proliferation and Survival. Journal of Surgical Research, 155(1), 125-131.

Noguchi, S., Saito, A., & Nagase, T. (2018). YAP/TAZ Signaling as a Molecular Link between Fibrosis and Cancer. International journal of molecular sciences, 19(11), 3674.

Oh, S., Shida, T., Sawai, A., Maruyama, T., Eguchi, K., Isobe, T., Okamoto, Y., Someya, N., Tanaka, K., Arai, E., Tozawa, A., & Shoda, J. (2014). Acceleration training for managing nonalcoholic fatty liver disease: a pilot study. Therapeutics and clinical risk management, 10, 925–936.

Paluch, E. K., Nelson, C. M., Biais, N., Fabry, B., Moeller, J., Pruitt, B. L., Wollnik, C., Kudryasheva, G., Rehfeldt, F., & Federle, W. (2015). Mechanotransduction: use the force(s). BMC biology, 13, 47.

Pan, Y., Wen, X., Hao, D., Wang, Y., Wang, L., He, G., & Jiang, X. (2020). The role of IL-37 in skin and connective tissue diseases. Biomedicine & Pharmacotherapy, 122, 109705.

Paolini, C., Agarbati, S., Benfaremo, D., Mozzicafreddo, M., Svegliati, S., & Moroncini, G. (2022). PDGF/PDGFR: A Possible Molecular Target in Scleroderma Fibrosis. International Journal of Molecular Sciences, 23(7), 3904.

Papini, D., Fant, X., Ogawa, H., Desban, N., Samejima, K., Feizbakhsh, O., Askin, B., Ly, T., Earnshaw, W. C., & Ruchaud, S. (2019). Cell cycle-independent furrowing triggered by phosphomimetic mutations of the INCENP STD motif requires Plk1. Journal of cell science, 132(21), jcs234401.

Pardo, A., Gibson, K., Cisneros, J., Richards, T. J., Yang, Y., Becerril, C., Yousem, S., Herrera, I., Ruiz, V., Selman, M., & Kaminski, N. (2005). Up-regulation and profibrotic role of osteopontin in human idiopathic pulmonary fibrosis. PLoS One, 5(9).

Park, J. S., Chu, J. S., Cheng, C., Chen, F., Chen, D., & Li, S. (2004). Differential effects of equiaxial and uniaxial strain on mesenchymal stem cells. Biotechnology and bioengineering, 88(3), 359–368.

Parra, M., Stahl, S., & Hellmann, H. (2018). Vitamin B_6 and Its Role in Cell Metabolism and Physiology. Cells, 7(7), 84.

Penke, L. R., Speth, J. M., Dommeti, V. L., White, E. S., Bergin, I. L., & Peters-Golden, M. (2018). FOXM1 is a critical driver of lung fibroblast activation and fibrogenesis. The Journal of clinical investigation, 128(6), 2389–2405.

Pfisterer, K., Shaw, L. E., Symmank, D., & Weninger, W. (2021). The Extracellular Matrix in Skin Inflammation and Infection. Frontiers in cell and developmental biology, 9, 682414.

Plikus, M. V., Wang, X., Sinha, S., Forte, E., Thompson, S. M., Herzog, E. L., Driskell, R. R., Rosenthal, N., Biernaskie, J., & Horsley, V. (2021). Fibroblasts: Origins, definitions, and functions in health and disease. Cell, 184(15), 3852-3872.

Qadir, A., Liang, S., Wu, Z., Chen, Z., Hu, L., Qian, A. (2020). Senile Osteoporosis: The Involvement of Differentiation and Senescence of Bone Marrow Stromal Cells. International Journal of Molecular Sciences, 21(1), 349

Rahaman, S. O., Grove, L. M., Paruchuri, S., Southern, B. D., Abraham, S., Niese, K. A., Scheraga, R. G., Ghosh, S., Thodeti, C. K., Zhang, D. X., Moran, M. M., Schilling, W. P., Tschumperlin, D. J., & Olman, M. A. (2014). TRPV4 mediates myofibroblast differentiation and pulmonary fibrosis in mice. The Journal of clinical investigation, 124(12), 5225–5238.

Richter, K., & Kietzmann, T. (2016). Reactive oxygen species and fibrosis: further evidence of a significant liaison. Cell and Tissue Research, 365, 591-605.

Richter, K., & Kietzmann, T. (2016). Reactive oxygen species and fibrosis: further evidence of a significant liaison. Cell and Tissue Research, 365(3), 591-605.

Rnjak-Kovacina, J., Wise, S. G., Li, Z., Maitz, P. K., Young, C. J., Wang, Y., & Weiss, A. S. (2011). Tailoring the porosity and pore size of electrospun synthetic human elastin scaffolds for dermal tissue engineering. Biomaterials, 32(28), 6729–6736.

Roberts, R. E., Bilgen, O., Kineman, R. D., & Koh, T. J. (2021). Parameter-Dependency of Low-Intensity Vibration for Wound Healing in Diabetic Mice. Frontiers in Bioengineering and Biotechnology, 9, 654920.

Robertson, S. N., Campsie, P., Childs, P. G., Madsen, F., Donnelly, H., Henriquez, F. L., Mackay, W. G., Salmerón-Sánchez, M., Tsimbouri, M. P., Williams, C., Dalby, M. J., & Reid, S. (2018). Control of cell behaviour through nanovibrational stimulation: nanokicking. Philosophical Transactions of the Royal Society A: Mathematical, Physical and Engineering Sciences, 376(2017), 20170290.

Robertson, S. N., Campsie, P., Childs, P. G., Madsen, F., Donnelly, H., Henriquez, F. L., Mackay, W. G., Salmerón-Sánchez, M., Tsimbouri, M. P., Williams, C., Dalby, M. J., & Reid, S. (2018). Control of cell behaviour through nanovibrational stimulation: nanokicking. Philosophical transactions. Series A, Mathematical, physical, and engineering sciences, 376(2120), 20170290.

Rogan, S., Hilfiker, R., Herren, K., Radlinger, L., & de Bruin, E. D. (2011). Effects of whole-body vibration on postural control in elderly: a systematic review and meta-analysis. BMC geriatrics, 11, 72.

Sabra, H., Brunner, M., Mandati, V., Wehrle-Haller, B., Lallemand, D., Ribba, A. S., Chevalier, G., Guardiola, P., Block, M. R., & Bouvard, D. (2017). β1 integrin-dependent Rac/group I PAK signaling mediates YAP activation of Yes-associated protein 1 (YAP1) via NF2/merlin. The Journal of biological chemistry, 292(47), 19179–19197.

Salinas, E. Y., Aryaei, A., Paschos, N., Berson, E., Kwon, H., Hu, J. C., & Athanasiou, K. A. (2020). Shear stress induced by fluid flow produces improvements in tissue-engineered cartilage. Biofabrication, 12(4), 045010.

Sawant, M., Hinz, B., Schönborn, K., Tiwari, N., Wolters, V., Müller, C., & Schneider, R. K. (2021). A story of fibers and stress: Matrix-embedded signals for fibroblast activation in the skin. Wound Repair and Regeneration, 29(3), 515-530.

Schieber, M., & Chandel, N. S. (2014). ROS function in redox signaling and oxidative stress. Current biology: CB, 24(10), R453–R462.

Schwörer, S., Berisa, M., Violante, S., Qin, W., Zhu, J., Hendrickson, R. C., Cross, J. R., & Thompson, C. B. (2020). Proline biosynthesis is a vent for TGFβ-induced mitochondrial redox stress. The EMBO Journal, 39(8), e103334.

Scott, K. E., Fraley, S. I., & Rangamani, P. (2021). A spatial model of YAP/TAZ signaling reveals how stiffness, dimensionality, and shape contribute to emergent outcomes. Proceedings of the National Academy of Sciences, 118(20), e2021571118.

Seitz, T., & Hellerbrand, C. (2021). Role of fibroblast growth factor signalling in hepatic fibrosis. Liver International, 41, 1201-1215.

Sen, C. K., & Roy, S. (2008). Redox signals in wound healing. Biochimica et Biophysica Acta (BBA) - General Subjects, 1780(11), 1348-1361.

Sharma, S., Goswami, R., Merth, M., Cohen, J., Lei, K. Y., Zhang, D. X., & Rahaman, S. O. (2017). TRPV4 ion channel is a novel regulator of dermal myofibroblast differentiation. American Journal of Physiology-Cell Physiology, 312(5), C562-C572.

She, Y. X., Yu, Q. Y., & Tang, X. X. (2021). Role of interleukins in the pathogenesis of pulmonary fibrosis. Cell Death Discovery, 7, 52.

Shi, X., Young, C. D., Zhou, H., & Wang, X. (2020). Transforming Growth Factor-ß Signaling in Fibrotic Diseases and Cancer-Associated Fibroblasts. Biomolecules, 10(12), 1666.

Shields, H. J., Traa, A., & Van Raamsdonk, J. M. (2021). Beneficial and Detrimental Effects of Reactive Oxygen Species on Lifespan: A Comprehensive Review of Comparative and Experimental Studies. Frontiers in Cell and Developmental Biology, 9, 628157.

Shih, B., Garside, E., McGrouther, D.A. and Bayat, A. (2010), Molecular dissection of abnormal wound healing processes resulting in keloid disease. Wound Repair and Regeneration, 18: 139-153.

Shimbori, C., Bellaye, P. S., Xia, J., Gauldie, J., Ask, K., Ramos, C., Becerril, C., Pardo, A., Selman, M., & Kolb, M. (2016). Fibroblast growth factor-1 attenuates TGF-β1-induced lung fibrosis. The Journal of pathology, 240(2), 197–210.

Singh, A., Varma, A. R. (2023). Whole-Body Vibration Therapy as a Modality for Treatment of Senile and Postmenopausal Osteoporosis: A Review Article. Cureus, 15(1), e33690.

Smithmyer, M. E., Sawicki, L. A., & Kloxin, A. M. (2014). Hydrogel scaffolds as in vitro models to study fibroblast activation in wound healing and disease. Biomaterials science, 2(5), 634–650.

Smithmyer, M. E., Cassel, S. E., & Kloxin, A. M. (2019). Bridging 2D and 3D culture: probing impact of extracellular environment on fibroblast activation in layered hydrogels. AIChE journal. American Institute of Chemical Engineers, 65(12), e16837.

Sokic, S., & Papavasiliou, G. (2012). FGF-1 and proteolytically mediated cleavage site presentation influence three-dimensional fibroblast invasion in biomimetic PEGDA hydrogels. Acta biomaterialia, 8(6), 2213–2222.

Song, Y. H., Zhu, Y. T., Ding, J., Zhou, F. Y., Xue, J. X., Jung, J. H., Li, Z. J., & Gao, W. Y. (2016). Distribution of fibroblast growth factors and their roles in skin fibroblast cell migration. Molecular medicine reports, 14(4), 3336–3342.

Spadoni, T., Svegliati Baroni, S., Amico, D., Albani, L., Moroncini, G., Avvedimento, E.V. and Gabrielli, A. (2015), A Reactive Oxygen Species–Mediated Loop Maintains Increased Expression of NADPH Oxidases 2 and 4 in Skin Fibroblasts From Patients With Systemic Sclerosis. Arthritis & Rheumatology, 67: 1611-1622.

Spector, A., Ma, W., Sun, F., Lian, D., & Kleiman, N. J. (2002). The effect of H2O2 and tertiary butyl hydroperoxide upon a murine immortal lens epithelial cell line. Experimental Eye Research, 75, 573-582.

Squarzoni, S., Schena, E., Sabatelli, P., Mattioli, E., Capanni, C., Cenni, V., D'Apice, M.R., Andrenacci, D., Sarli, G., Pellegrino, V., Festa, A., Baruffaldi, F., Storci, G., Bonafè, M., Barboni, C., Sanapo, M., Zaghini, A., & Lattanzi, G. (2021). Interleukin-6 neutralization ameliorates symptoms in prematurely aged mice. Aging Cell, 20, e13285.

Steppe, L., Liedert, A., Ignatius, A., & Haffner-Luntzer, M. (2020). Influence of Low-Magnitude High-Frequency Vibration on Bone Cells and Bone Regeneration. Frontiers in Bioengineering and Biotechnology, 8, 595139.

Ström, K., Morales-Alamo, D., Ottosson, F., Edlund, A., Hjort, L., Jörgensen, S. W., Almgren, P., Zhou, Y., Martin-Rincon, M., Ekman, C., Pérez-López, A., Ekström, O., Perez-Suarez, I., Mattiasson, M., de Pablos-Velasco, P., Oskolkov, N., Ahlqvist, E., Wierup, N., Eliasson, L., Vaag, A., … Hansson, O. (2018). N1-methylnicotinamide is a signalling molecule produced in skeletal muscle coordinating energy metabolism. Scientific reports, 8(1), 3016.

Svegliati, S., Marrone, G., Pezone, A., Spadoni, T., Grieco, A., Moroncini, G., Grieco, D., Vinciguerra, M., Agnese, S., Jüngel, A., Distler, O., Musti, A. M., Gabrielli, A., & Avvedimento, E. V. (2014). Oxidative DNA damage induces the ATM-mediated transcriptional suppression of the Wnt inhibitor WIF-1 in systemic sclerosis and fibrosis. Science Signaling, 7(341), ra84.

Syabariyah, S., Nurachmah, E., Widjojo, B. D., Prasetyo, S., Sanada, H., Irianto, Nakagami, G., Suriadi, Kardiatun, T., & Hisan, U. K. (2023). The Effect of Vibration on the Acceleration of Wound Healing of Diabetic Neuropathic Foot Ulcer: A Prospective Experimental Study on Human Patients. Healthcare (Basel, Switzerland), 11(2), 191.

Takahashi, F., Takahashi, K., Okazaki, T., Maeda, K., Ienaga, H., Maeda, M., Kon, S., Uede, T., & Fukuchi, Y. (2000). Role of osteopontin in the pathogenesis of bleomycin-induced pulmonary fibrosis. American Journal of Respiratory Cell and Molecular Biology, 24(3).

Takamura N, Renaud L, da Silveira WA and Feghali-Bostwick C (2021) PDGF Promotes Dermal Fibroblast Activation via a Novel Mechanism Mediated by Signaling Through MCHR1. Front. Immunol. 12:745308.

Tao, L., Huang, G., Song, H., Chen, Y., & Chen, L. (2017). Cancer associated fibroblasts: An essential role in the tumor microenvironment. Oncology letters, 14(3), 2611–2620.

Thompson, W. R., Yen, S. S., & Rubin, J. (2014). Vibration therapy: clinical applications in bone. Current opinion in endocrinology, diabetes, and obesity, 21(6), 447–453.

Tian, D., Jacobo, S. M., Billing, D., Rozkalne, A., Gage, S. D., Anagnostou, T., Pavenstädt, H., Hsu, H. H., Schlondorff, J., Ramos, A., & Greka, A. (2010). Antagonistic regulation of actin dynamics and cell motility by TRPC5 and TRPC6 channels. Science signaling, 3(145), ra77.

Tiffany, C. R., & Bäumler, A. J. (2019). omu, a Metabolomics Count Data Analysis Tool for Intuitive Figures and Convenient Metadata Collection. Microbiology Resource Announcements, 8(15).

Tomlins, S. A., Bollinger, N., Creim, J., & Rodland, K. D. (2005). Cross-talk between the calcium-sensing receptor and the epidermal growth factor receptor in Rat-1 fibroblasts. Experimental Cell Research, 308(2), 439-445.

Tracy, L. E., Minasian, R. A., & Caterson, E. J. (2016). Extracellular Matrix and Dermal Fibroblast Function in the Healing Wound. Advances in wound care, 5(3), 119–136.

Tsimbouri, P. M., Childs, P. G., Pemberton, G. D., Yang, J., Jayawarna, V., Orapiriyakul, W., Burgess, K., González-García, C., Blackburn, G., Thomas, D., Vallejo-Giraldo, C., Biggs, M. J. P., Curtis, A. S. G., Salmerón-Sánchez, M., Reid, S., & Dalby, M. J. (2017). Stimulation of 3D osteogenesis by mesenchymal stem cells using a nanovibrational bioreactor. Nature biomedical engineering, 1(9), 758–770.

Ung, C. Y., Onoufriadis, A., Parsons, M., McGrath, J. A., & Shaw, T. J. (2021). Metabolic perturbations in fibrosis disease. The International Journal of Biochemistry & Cell Biology, 139, 106073.

Vairetti, M., Di Pasqua, L. G., Cagna, M., Richelmi, P., Ferrigno, A., & Berardo, C. (2021). Changes in Glutathione Content in Liver Diseases: An Update. Antioxidants (Basel, Switzerland), 10(3), 364.

Velasquez, L. S., Sutherland, L. B., Liu, Z., Grinnell, F., Kamm, K. E., Schneider, J. W., Olson, E. N., & Small, E. M. (2013). Activation of MRTF-A-dependent gene expression with a small molecule promotes myofibroblast differentiation and wound healing. Proceedings of the National Academy of Sciences of the United States of America, 110(42), 16850–16855.

Vermes, I., Haanen, C., Steffens-Nakken, H., & Reutelingsperger, C. (1995). A novel assay for apoptosis. Flow cytometric detection of phosphatidylserine expression on early apoptotic cells using fluorescein labelled Annexin V. Journal of immunological methods, 184(1), 39–51.

Vlachogiannis, N. I., Pappa, M., Ntouros, P. A., Nezos, A., Mavragani, C. P., Souliotis, V. L., & Sfikakis, P. P. (2020). Association Between DNA Damage Response, Fibrosis and Type I Interferon Signature in Systemic Sclerosis. Frontiers in immunology, 11, 582401.

Walker, M., Godin, M., & Pelling, A. E. (2020). Mechanical stretch sustains myofibroblast phenotype and function in microtissues through latent TGF-β1 activation. Integrative biology: quantitative biosciences from nano to macro, 12(8), 199–210.

Walton, K. L., Johnson, K. E., & Harrison, C. A. (2017). Targeting TGF-β Mediated SMAD Signaling for the Prevention of Fibrosis. Frontiers in pharmacology, 8, 461.

Wang, S., Liang, Y., & Dai, C. (2022). Metabolic regulation of fibroblast activation and proliferation during organ fibrosis. Kidney Diseases, 8(2), 115-125.

Wei, K., Nguyen, H. N., & Brenner, M. B. (2021). Fibroblast pathology in inflammatory diseases. The Journal of clinical investigation, 131(20), e149538.

Weinheimer-Haus, E. M., Judex, S., Ennis, W. J., & Koh, T. J. (2014). Low-Intensity Vibration Improves Angiogenesis and Wound Healing in Diabetic Mice. PloS One, 9(3), e91355.

Weidinger, A., & Kozlov, A. V. (2015). Biological activities of reactive oxygen and nitrogen species: oxidative stress versus signal transduction. Biomolecules, 5(2), 472-484.

Wilson, S. E. (2021). TGF beta-1, -2 and -3 in the modulation of fibrosis in the cornea and other organs. Experimental Eye Research, 207, 108594.

Wishart, D. S. (2019). Metabolomics for investigating physiological and pathophysiological processes. Physiological Reviews, 99(4), 1819-1875.

Wolchok, J. C., & Tresco, P. A. (2013). Using vocally inspired mechanical conditioning to enhance the synthesis of a cell-derived biomaterial. Annals of biomedical engineering, 41(11), 2358–2366.

Wong, V. W., Rustad, K. C., Akaishi, S., Sorkin, M., Glotzbach, J. P., Januszyk, M., Nelson, E. R., Levi, K., Paterno, J., Vial, I. N., Kuang, A. A., Longaker, M. T., & Gurtner, G. C. (2011). Focal adhesion kinase links mechanical force to skin fibrosis via inflammatory signaling. Nature medicine, 18(1), 148–152.

Woodley, J. P., Lambert, D. W., & Asencio, I. O. (2022). Understanding Fibroblast Behavior in 3D Biomaterials. Tissue engineering. Part B, Reviews, 28(3), 569–578.

Wu, M., Schneider, D. J., Mayes, M. D., Assassi, S., Arnett, F. C., Tan, F. K., Blackburn, M. R., & Agarwal, S. K. (2012). Osteopontin in systemic sclerosis and its role in dermal fibrosis. Journal of Investigative Dermatology, 132(6), 1605-1614.

Wu, T., Hu, E., Xu, S., Chen, M., Guo, P., Dai, Z., Feng, T., Zhou, L., Tang, W., Zhan, L., Fu, X., Liu, S., Bo, X., & Yu, G. (2021). clusterProfiler 4.0: A universal enrichment tool for interpreting omics data. The Innovation, 2(3), 100141.

Xia, J., Psychogios, N., Young, N., & Wishart, D. S. (2009). MetaboAnalyst: a web server for metabolomic data analysis and interpretation. Nucleic acids research, 37(Web Server issue), W652–W660.

Xie, J., Zhang, W., Liang, X., Shuai, C., Zhou, Y., Pan, H., Yang, Y., & Han, W. (2020). RPL32 Promotes Lung Cancer Progression by Facilitating p53 Degradation. Molecular therapy. Nucleic acids, 21, 75–85.

Yamada, K., Hamashima, T., Ishii, Y., Yamamoto, S., Okuno, N., Yoshida, N., Yamada, M., Huang, T. T., Shioda, N., Tomihara, K., Fujimori, T., Mori, H., Fukunaga, K., Noguchi, M., & Sasahara, M. (2018). Different PDGF receptor dimers drive distinct migration modes of the mouse skin fibroblast. Cellular Physiology and Biochemistry, 51(3), 1461-1479.

Yang, S., & Plotnikov, S. V. (2021). Mechanosensitive Regulation of Fibrosis. Cells, 10(5), 994.

Ye, Z., Wang, S., Zhang, C., & Zhao, Y. (2020). Coordinated Modulation of Energy Metabolism and Inflammation by Branched-Chain Amino Acids and Fatty Acids. Frontiers in endocrinology, 11, 617.

Yeung, V., Sriram, S., Tran, J. A., Guo, X., Hutcheon, A. E. K., Zieske, J. D., Karamichos, D., & Ciolino, J. B. (2021). FAK Inhibition Attenuates Corneal Fibroblast Differentiation In Vitro. Biomolecules, 11(11), 1682.

Yin, L., An, Y., Chen, X., Yan, H., Zhang, T., Lu, X., & Yan, J. (2022). Local vibration therapy promotes the recovery of nerve function in rats with sciatic nerve injury. Journal of Integrative Medicine, 20(3), 265-273.

Yin, X., Choudhury, M., Kang, J.-H., Schaeferbauer, K.J., Jung, M.-Y., Andrianifahanana, M., Hernandez, D.M., & Leof, E.B. (2019). Hexokinase 2 couples glycolysis with the profibrotic actions of TGF-ß. Science Signaling, 12(612).

Zhai, K., Liskova, A., Kubatka, P., & Büsselberg, D. (2020). Calcium Entry through TRPV1: A Potential Target for the Regulation of Proliferation and Apoptosis in Cancerous and Healthy Cells. International journal of molecular sciences, 21(11), 4177.

Zhang, W., & Liu, H. (2002). MAPK signal pathways in the regulation of cell proliferation in mammalian cells. Cell Research, 12, 9-18.

Zhang, Y., Habibovic, P. (2022). Delivering Mechanical Stimulation to Cells: State of the Art in Materials and Devices Design. Advanced Materials, 34, 2110267.

Zhang, Y., Parmigiani, G., & Johnson, W. E. (2020). ComBat-seq: Batch effect adjustment for RNA-seq count data. NAR Genomics and Bioinformatics, 2(3), lqaa078.

Zhao, X.-K., Cheng, Y., Cheng, M. L., Yu, L., Mu, M., Li, H., Liu, Y., Zhang, B., Yao, Y., Guo, H., Wang, R., & Zhang, Q. (2016). Focal Adhesion Kinase Regulates Fibroblast Migration via Integrin ß-1 and Plays a Central Role in Fibrosis. Scientific Reports, 6, 19276.

Zhou, L., Ng, D. S. C., Yam, J. C., & Pang, C. P. (2022). Post-translational modifications on the retinoblastoma protein. Journal of Biomedical Science, 29(1), 33.

Zhu, J., Liu, L., Ma, X., Cao, X., Chen, Y., Qu, X., Ji, M., Liu, H., Liu, C., Qin, X., & Xiang, Y. (2022). The Role of DNA Damage and Repair in Idiopathic Pulmonary Fibrosis. Antioxidants (Basel, Switzerland), 11(11), 2292.

Zitka, O., Skalickova, S., Gumulec, J., Masarik, M., Adam, V., Hubalek, J. ... Kizek, R. (2012). Redox status expressed as GSH:GSSG ratio as a marker for oxidative stress in paediatric tumour patients. Oncology Letters, 4, 1247-1253.